From the DEPARTMENT OF CLINICAL NEUROSCIENCE
Karolinska Institutet, Stockholm, Sweden

MAGNETIC RESONANCE IMAGING TECHNIQUES FOR DIAGNOSTICS IN PARKINSON'S DISEASE AND ATYPICAL PARKINSONISM

Henrik Sjöström

Karolinska Institutet

Stockholm 2020

Published by Karolinska Institutet.
Printed by Eprint AB 2020

ISBN 978-91-7831-789-9

MAGNETIC RESONANCE IMAGING TECHNIQUES FOR DIAGNOSTICS IN PARKINSON'S DISEASE AND ATYPICAL PARKINSONISM

THESIS FOR DOCTORAL DEGREE (Ph.D.)

By

Henrik Sjöström

Principal Supervisor:
Professor Per Svenningsson
Karolinska Institutet
Department of Clinical Neuroscience
Division of Neuro

Co-supervisor(s):
Dr. Tobias Granberg
Karolinska Institutet
Department of Clinical Neuroscience
Division of Neuro

Professor Eric Westman
Karolinska Institutet
Department of Neurobiology, Care Sciences and Society
Division of Clinical Geriatrics

Opponent:
Professor Stéphane Lehéricy
Sorbonne Université
Institut du Cerveau et de la Moelle épinière - ICM
Center for NeuroImaging Research - CENIR

Examination Board:
Associate Professor Magnus Kaijser
Karolinska Institutet
Department of Medicine, Solna
Division of Clinical Epidemiology

Associate Professor Shala Berntsson
Uppsala University
Department of Neuroscience
Division of Neurology

Associate Professor Stefan Skare
Karolinska Institutet
Department of Clinical Neuroscience
Division of Neuro

To my dear wife Anna,

my daughters Astrid and Freja,

and my parents Ann-Christine and Birger

"All our knowledge begins with the senses, proceeds then to the understanding, and ends with reason. There is nothing higher than reason."

—Immanuel Kant (1724–1804)

ABSTRACT

Background: Parkinson's disease (PD) is a neurodegenerative disease characterized by rigidity, hypokinesia, tremor and postural instability. PD is a clinical diagnosis based on neurological examination, patient history and treatment response. Similar symptoms can be caused by other movement disorders such as progressive supranuclear palsy (PSP) and multiple system atrophy (MSA), making it difficult to clinically separate them in early stages. However, these diseases differ in underlying pathology, treatment and prognosis. PSP and MSA have more rapid deterioration and develop additional symptoms such as impaired eye movements or autonomic dysfunction. Magnetic resonance imaging (MRI) is commonly performed as part of the clinical work-up in patients presenting with parkinsonism. There are no overt changes on structural MRI in PD. In atypical parkinsonian syndromes there are typically no visible changes until later disease stages.

Purpose: The aim of this thesis is to evaluate novel MRI techniques for diagnostics and for investigation of disease processes in Parkinson's disease, PSP and MSA.

Paper I: A retrospective cohort from Karolinska University Hospital (102 participants; 62 PD, 15 PSP, 11 MSA, 14 controls) was assessed using susceptibility mapping processed from susceptibility weighted imaging. We show that there is elevated susceptibility in the red nucleus and the globus pallidus in PSP compared to PD, MSA and controls. Higher susceptibility levels were also seen in MSA compared to PD in the putamen, and in PD compared to controls in the substantia nigra. Using the red nucleus susceptibility as a diagnostic biomarker, PSP could be separated from PD with an accuracy of 97% (based on the area under the receiver operating characteristic curve, AUC), from MSA with AUC 75% and from controls with AUC 98%. We concluded that susceptibility changes, particularly in the red nucleus in PSP, could be potential biomarkers for differential diagnostics in parkinsonism.

Paper II: A prospective cohort from Lund, the BioFINDER study (199 participants; 134 PD, 11 PSP, 10 MSA, 44 controls), was investigated using the susceptibility mapping pipeline developed for Paper I. The finding from Paper I with elevated susceptibility in the red nucleus was validated for PSP compared to PD, MSA and controls. The elevated putaminal susceptibility was also confirmed in MSA compared to PD. The potential role of red nucleus susceptibility as a biomarker for separating PSP from PD and MSA was also similar to the results in Paper I, with AUC 98% for separating PSP from PD and AUC 96% for separating PSP from MSA. We concluded that we could confirm our previous findings from Paper I, with the red nucleus susceptibility being a potential biomarker for separating PSP from PD and MSA.

Paper III: A retrospective cohort from Karolinska University Hospital (196 participants; 140 PD, 29 PSP, 27 MSA) was evaluated to employ automated volumetric brainstem segmentation using FreeSurfer. The volumetric approach was compared to manual planimetric measurements: midbrain-pons ratio, magnetic resonance parkinsonism index 1.0 and 2.0. Intra- and inter-scanner as well as intra- and inter-rater reliability were calculated. We found good repeatability in both automated volumetric and manual planimetric measurements. Normalized midbrain volume performed better than the planimetric measurements for separating PSP from PD. We concluded that, if further developed and incorporated in a radiology workflow, automated brainstem volumetry could increase availability of brainstem metrics and possibly save time for radiologists conducting manual measurements.

Paper IV: Two cohorts, a retrospective from Karolinska University Hospital (184 participants; 129 PD, 28 PSP, 27 MSA) and a prospective from Lund (185 participants; 125 PD, 11 PSP, 8 MSA, 41 controls), were studied to investigate a new method of creating T_1-/T_2-weighted ratio images and its diagnostic capabilities in differentiating parkinsonian disorders. In the explorative retrospective cohort, differences in white matter normalized T_1-/T_2-weighted ratios were seen in the caudate nucleus, putamen, thalamus, subthalamic nucleus and red nucleus in PSP compared to PD; in the caudate nucleus and putamen in MSA compared to PD and in the subthalamic nucleus and the red nucleus in PSP compared to MSA. These differences were validated externally in the prospective cohort, where the changes could be confirmed in the subthalamic nucleus and the red nucleus in PSP compared to PD and MSA. We concluded that there are different patterns of white matter normalized T_1-/T_2-weighted ratio between the disorders and that this reflects differences in underlying pathophysiology. The T_1-/T_2-weighted ratio should be further investigated for better understanding of pathological processes in parkinsonian disorders and could possibly be utilized for diagnostic purposes if further developed.

LIST OF SCIENTIFIC PAPERS

This thesis is based on the following four papers, which will be referred to in the text by their roman numerals.

I. **Quantitative susceptibility mapping differentiates between parkinsonian disorders**
Sjöström H, Granberg T, Westman E, Svenningsson P
Parkinsonism & Related Disorders. 2017 Nov;44:51–57.

II. **Mapping of apparent susceptibility yields promising diagnostic separation of progressive supranuclear palsy from other causes of parkinsonism**
Sjöström H, Surova Y, Nilsson M, Granberg T, Westman E, van Westen D, Svenningsson P, Hansson O
Scientific Reports. 2019 Apr 15;9(1):6079.

III. **Automated brainstem volumetry can aid in the diagnostics of parkinsonian disorders**
Sjöström H, Granberg T, Hashim F, Westman E, Svenningsson P
Submitted manuscript

IV. **Differences in neurodegeneration in Parkinsonian syndromes revealed by T_1/T_2-weighted ratio imaging in two large cohorts**
Sjöström H, van Westen D, Hall S, Tjerkaski J, Westman E, Muehlboeck S, Hansson O, Svenningsson P, Granberg T
Submitted manuscript

CONTENTS

1 Introduction 1
1.1 Parkinson's disease 1
1.1.1 Background 1
1.1.2 Epidemiology 1
1.1.3 Etiology 4
1.1.4 Clinical manifestations 6
1.1.5 Diagnosis 6
1.1.6 Treatment 8
1.1.7 Clinical scales 9
1.2 Progressive supranuclear palsy 10
1.2.1 Background 10
1.2.2 Epidemiology 10
1.2.3 Etiology 10
1.2.4 Clinical manifestations 11
1.2.5 Diagnosis 11
1.2.6 Treatment 12
1.2.7 Clinical scales 12
1.3 Multiple system atrophy 13
1.3.1 Background 13
1.3.2 Epidemiology 13
1.3.3 Etiology 13
1.3.4 Clinical manifestations 14
1.3.5 Diagnosis 14
1.3.6 Treatment 15
1.3.7 Clinical scales 16
1.4 Other atypical parkinsonism 16
1.4.1 Corticobasal degeneration 16
1.4.2 Dementia with lewy bodies 16
1.5 Magnetic resonance imaging in parkinsonian disorders 17
1.5.1 Conventional MRI sequences 17
1.5.2 Advanced MRI sequences 19
1.6 Single-photon emission computed tomography and positron emission tomography in parkinsonian disorders 25
1.6.1 ^{123}I-ioflupane single-photon emission computed tomography 25
1.6.2 ^{18}F-fluorodeoxyglucose positron emission tomography 26
2 Aims 27
3 Material and methods 29
3.1 Ethical considerations 29
3.2 Procedures and participants 29
3.3 Clinical evaluations 31
3.4 Brain imaging 31

3.5 Image processing 33
3.6 Radiological evaluations 35
3.7 Statistical analysis 36
4 Results 37
4.1 Study I 37
4.2 Study II 39
4.3 Study III 41
4.4 Study IV 43
5 Discussion 47
5.1 Study I and II 47
5.1.1 Study limitations 48
5.1.2 Post-publication developments 49
5.2 Study III 50
5.2.1 Study limitations 51
5.2.2 Post-publication developments 51
5.3 Study IV 52
5.3.1 Study limitations 53
5.3.2 Post-publication developments 53
6 Conclusions 55
7 Future aspects 57
8 Populärvetenskaplig sammanfattning 59
9 Acknowledgements 61
10 References 63

LIST OF ABBREVIATIONS

ADL	Activities of daily life
ALFF	Amplitude of low-frequency fluctuations
ANCOVA	Analysis of covariance
ANOVA	Analysis of variance
ANTs	Advanced normalization tools
AUC	Area under curve
BET	Brain extraction tool
CBD	Corticobasal degeneration
CEST	Chemical exchange saturation transfer
Cho	Choline
COMT	Catechol-O-methyl transferase
CoV	Coefficient of variation
Cr	Creatine
CSF	Cerebrospinal fluid
DAT	Dopamine transporter
DKI	Diffusion kurtosis imaging
DLB	Dementia with lewy bodies
DTI	Diffusion tensor imaging
FA	Fractional anisotropy
FDG	Fludeoxyglucose
FLAIR	Fluid-attenuated inversion recovery
fMRI	FMRIb software library
FMRIb	Functional magnetic resonance imagin
FSE	Fast spin-echo
FSL	Oxford center for functional MRI of the brain
GABA	Gamma-amino butyric acid
GBA	Glucocerebrosidase
GCI	Glial cytoplasmic inclusions
Gln	Glutamine
Glu	Glutamate

GPi	Internal globus pallidus
GRE	Gradient recall echo
ICC	Intraclass correlation coefficient
iLSQR	Iterative least-squares
KIMOVE	Karolinska imaging in movement disorders
MAO	Monoamine oxidase
MCP	Middle cerebellar peduncle
MD	Mean diffusivity
MDS	The international Parkinson and movement disorder society
mI	Myo-inositol
MIBG	Metaiodobenzylguanidine
MNI	Montreal neurological institute
MPRAGE	Magnetization-prepared rapid acquisition gradient echo
MP-ratio	Midbrain-pons ratio
MRI	Magnetic resonance imaging
MRPI	Magnetic resonance parkinsonism index
MRS	Magnetic resonance spectroscopy
MSA	Multiple system atrophy
MSA-C	MSA with cerebellar syndrome
MSA-P	MSA with parkinsonism
MT	Magnetization transfer
MTR	Magnetization transfer ratio
NAA	N-acetylaspartate
NFL	Neurofilament light chain protein
NINDS	National institute of neurological disorders and stroke
NODDI	Neurite orientation dispersion and density imaging
PDF	Projection onto dipole fields
PET	Positron emission tomography
ppm	Parts per million
PSP	Progressive supranuclear palsy
PSP-CBS	PSP-corticobasal syndrome

PSP-P	PSP-parkinsonism
PSP-PAGF	PSP-pure akinesia with gait freezing
PSP-PNFA	PSP-progressive non-fluent aphasia
PSP-RS	PSP-Richardson-Steele
qMT	Quantitative magnetization transfer
QSM	Quantitative susceptibility mapping
RBD	REM-sleep behavior disorder
REM	Rapid eye movement
ROC	Receiving operator characteristic
rs-fMRI	Resting-state fMRI
SCP	Superior cerebellar peduncles
SHARP	Sophisticated harmonic artifact reduction on phase data
SPECT	Single-photon emission computed tomography
SPM	Statistical parametric mapping
SPSP	Society for progressive supranuclear palsy
STN	Subthalamic nucleus
SWI	Susceptibility weighted imaging
UMSARS	Unified multiple system atrophy rating scale
UPDRS	Unified Parkinson’s disease rating scale
VSGP	Vertical supranuclear gaze palsy
V-SHARP	Variable-kernel SHARP

1 INTRODUCTION

1.1 PARKINSON'S DISEASE

1.1.1 Background

When James Parkinson (1775–1824) published his renowned "An Essay on the Shaking Palsy" in 1817,[1] he gave a coherent and thoughtful description of a disease that was up until then overlooked and practically unknown. In this essay based on his keen observations of patients he probably had close contact with, as well as cases he met on the street, he describes the symptoms and traits of what was later to be known as Parkinson's disease (PD). He also refers back to earlier writings of Sylvius de la Boë and Boissier de Sauvages. The former describing the separation of tremors occurring during action from tremors occurring at rest ('*tremor coactus*'). De Sauvages notes that this form of tremor at rest can be observed as a leaping of the body part even when supported, whereas other forms of tremor ceases when movements stop, but returns when the limb moves again. He also describes a variant of '*scelotyrbe*' (meaning weakness) called '*scelotyrbe festinans*' (*festinans* meaning hastening), where patients trying to walk are instead forced to run. James Parkinson acknowledges that these two symptoms, the '*tremor coactus*' (resting tremor) and the '*scelotyrbe festinans*' together with the tendency to bend the trunk forwards, are the pathognomonic symptoms of the shaking palsy.

One person who brought more attention to this disorder, and also acknowledged the work of James Parkinson, was the famous neurologist Jean-Martin Charcot. He was also the one suggesting that the disorder should be referred to as Parkinson's disease.[2] He also expanded the description and identified rigidity and bradykinesia as the core features of the disorder and that while the resting tremor was common, it was not an obligatory feature. Charcot also noted that the patients were not distinctly weak, and that the term palsy should therefore be avoided.

1.1.2 Epidemiology

PD is the second most common neurodegenerative disease world-wide. Globally, over 6 million individuals are affected by this disease.[3] It is also the fastest growing neurological disorder included in Global Burden of Disease 2015 study. Age is the greatest risk factor, and PD is 40% more common in males than in females in most populations.[3,4] It has also been found that the incidence is greater in individuals exposed to pesticides and traumatic brain injury.[5] Smoking and caffeine, on the other hand, seem to be associated with a lower incidence of PD.[4] Whether smoking truly is protective or not has been debated, and it has also been shown that individuals with PD are able to quit smoking more easily than controls.[6] A map of global age-standardized prevalence of PD is shown in *Figure 1*.[3]

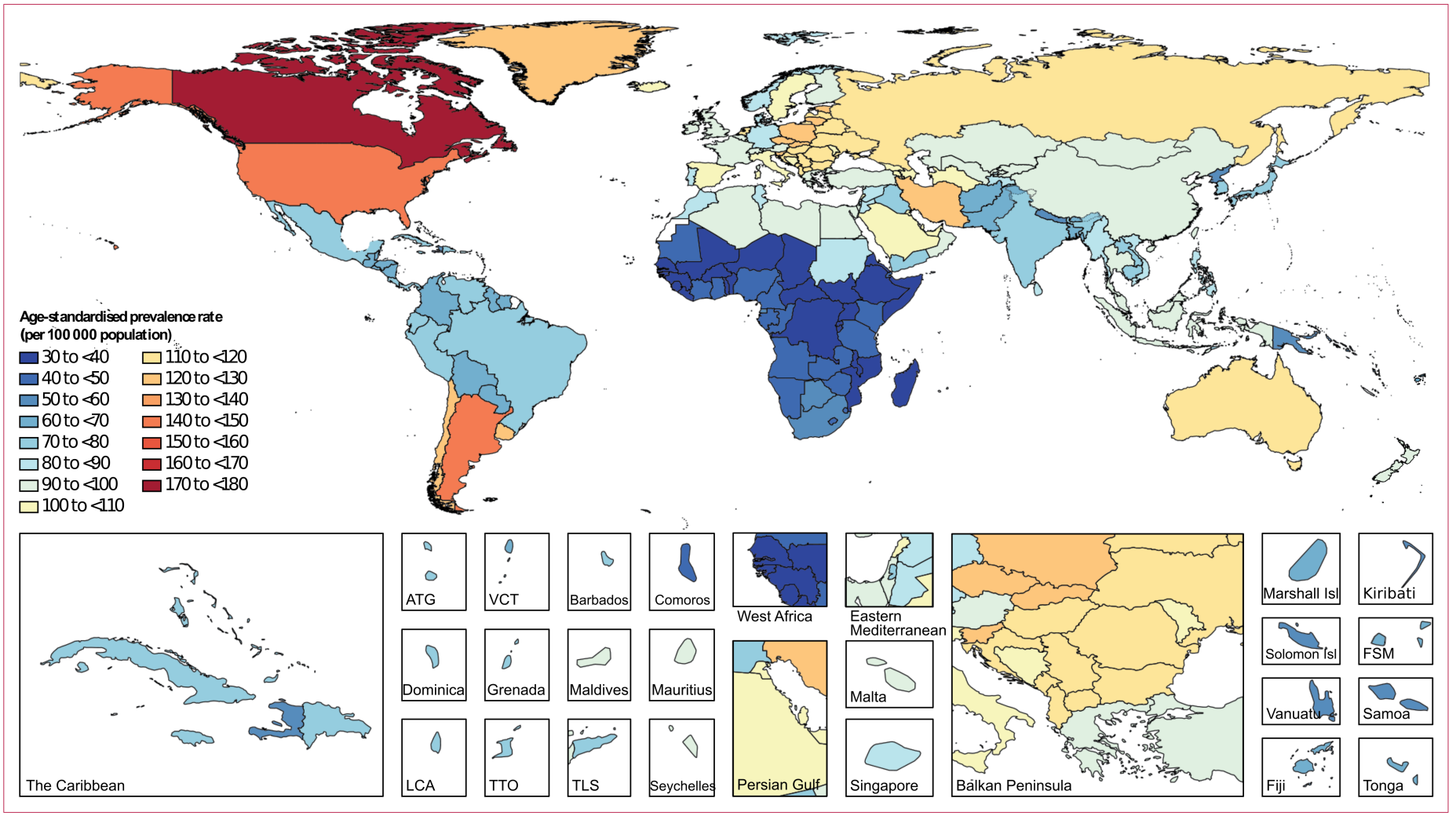

Figure 1: **Age-standardised prevalence of Parkinson's disease per 100 000 population by location for both sexes, 2016**
ATG=Antigua and Barbuda. FSM=Federated States of Micronesia. Isl=Islands. LCA=Saint Lucia. TLS=Timor-Lesta. TTO=Trinidad and Tobago. VCT=Saint Vincent and the Grenadines. Figure from Dorsey et al,[3] under creative commons license.

The global differences in age-standardized prevalence are not fully understood but may be due to a combination of methodology of the different underlying prevalence studies, differences in disease awareness, but also possible differences in risk factors as well as due to genetic factors. As stated above, the main risk factor is age. As seen in *Figure 2*, there is a marked increase in the prevalence of PD in both male and female with increasing age. PD is globally a major cause of death and disability, and caused 211 296 deaths and 3.2 million disability-adjusted life-years in 2016.[3]

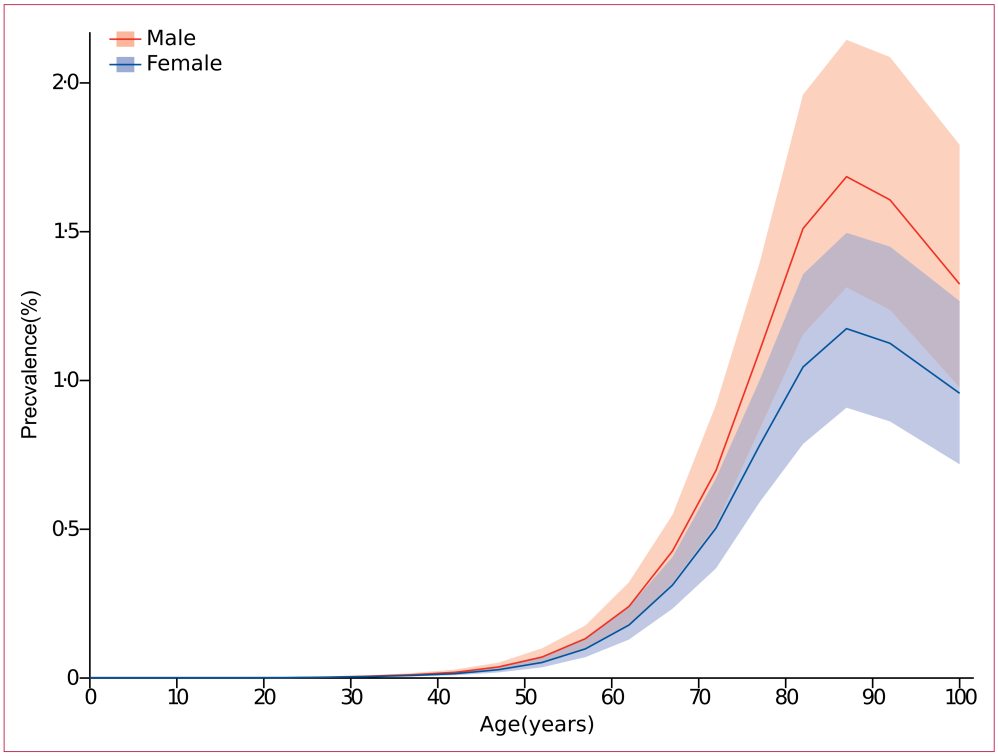

Figure 2: **Global prevalence of Parkinson's disease by age and sex, 2016**
Prevalence is expressed as the percentage of the population that is affected by the disease. Shading indicates 95% uncertainty intervals. Figure from Dorsey et al,[3] under creative commons license.

Concerning genetics, mutations in several different genes have been found to cause familial PD with autosomal dominant inheritance patterns shown for mutations or duplication in the alpha-synuclein gene, ubiquitin C-terminal hydrolase L1 and leucine rich repeat kinase 2 (LRRK2), among others.[7] Other genes found to cause an autosomal recessive inheritance pattern include parkin RBR E3 ubiquitin protein ligase and PTEN induced putative kinase 1 (PINK1).

While there are many known genetic mutations associated with familial PD, it has also been found that certain mutations increase the risk of developing the disease. Such identified genes associated with increased risk of developing PD are glucocerebrocidase (GBA) and MAPT.[7] Recently, much attention has been focused on mutations in the GBA gene, which were first described in patients with Gaucher's disease. Gaucher's disease is an autosomal recessive lysosomal storage disorder in which glucocerebroside is accumulated in multiple organs, bone and neural systems.[8] Mutations in the GBA gene have been implicated as risk factors for PD, and shown to be present in 4-10% of patients with PD as opposed to 0.4-1.0% reported in

healthy controls.[9] A possible mechanism is thought to be that the loss of glucocerebrosidase function impairs lysosomal activity and leads to accumulation of α-synuclein.[7] It should also be noted that the distinction between disease-causing genes and genes conveying an increased risk of disease is not always easily discernible, or even possible.

1.1.3 Etiology

PD is a neurodegenerative movement disorder. The core pathological feature in PD is the loss of dopaminergic neurons in the substantia nigra pars compacta in the midbrain.[5] This region contains neurons projecting unmyelinated axons mainly to the ipsilateral dorsal striatum. It has also been shown to occur neuronal loss in additional brain regions such as the locus coeruleus, raphe nucleus and the dorsal motor nucleus of the vagus nerve.[5]

Another important pathological feature of PD is the accumulation and aggregation of misfolded alpha-synuclein in both intra-cellular inclusions and in neurites, Lewy bodies and Lewy neurites respectively.[4,5] Lewy pathology has been found in practically all neuronal tissues including the brain, peripheral nervous system, spinal cord and adrenal glands.[5] Examples of Lewy bodies and Lewy neurites are shown in *Figure 3*.

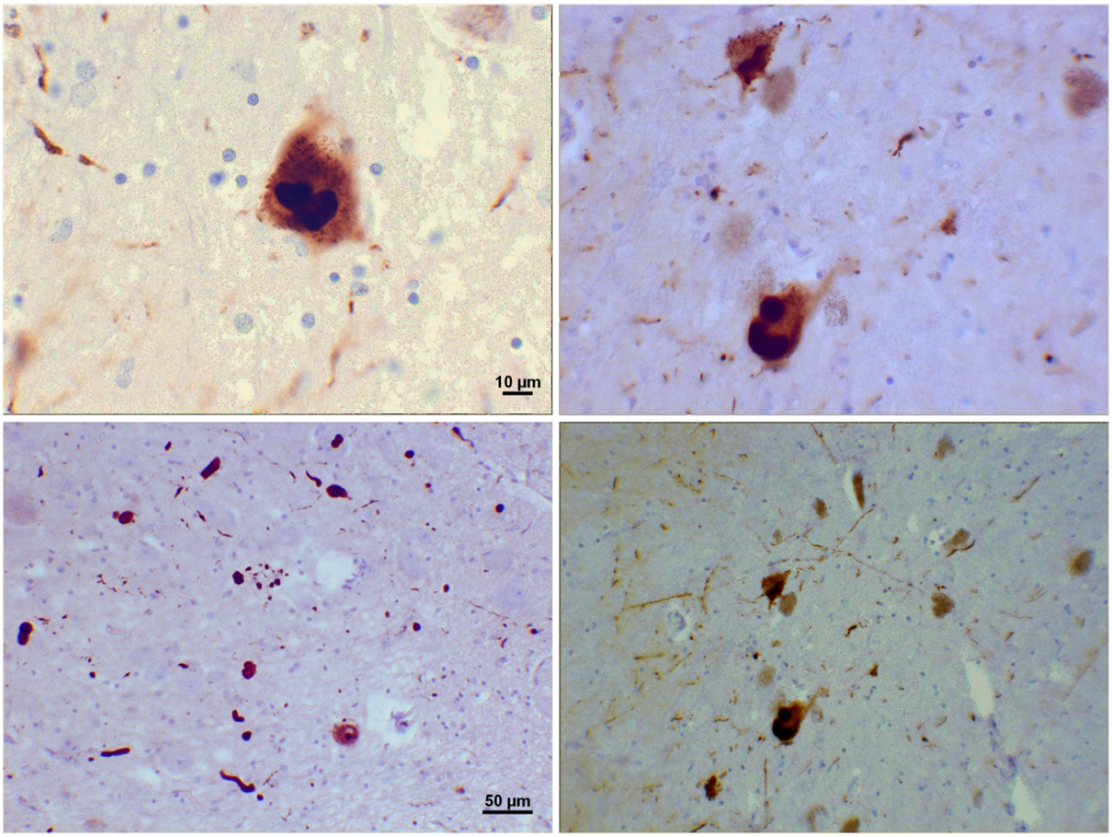

Figure 3: Photomicrograph of regions of substantia nigra in a Parkinson's patient showing Lewy bodies and Lewy neurites in various magnifications. Top panels show a 60-times magnification of the alpha synuclein intraneuronal inclusions aggregated to form Lewy bodies. The bottom panels are 20 × magnification images that show strand-like Lewy neurites and rounded Lewy bodies of various sizes. Neuromelanin laden cells of the substantia nigra are visible in the background. Stains used: mouse monoclonal alpha-synuclein antibody; counterstained with Mayer's haematoxylin. Image by Suraj Rajan, used under Creative Commons license (https://creativecommons.org/licenses/by-sa/3.0/), no changes made.

It has been hypothesized that the disease process initiates peripherally and then spreads in a caudal-to-rostral fashion.[10] This might in part explain the typical progression of symptoms commonly beginning with non-motor symptoms such as constipation and loss of the sense of smell, and then gradually moving higher to affect regulation of movements and lastly cortical functions. This model of disease progression was first proposed by the neuropathologist Heiko Braak and is commonly referred to as the Braak model.[10] A schematic depiction of this model is given in *Figure 4*.[11] This model has been debated and there are proponents of both the gut-first and the brain-first models on the pathogenesis of PD.

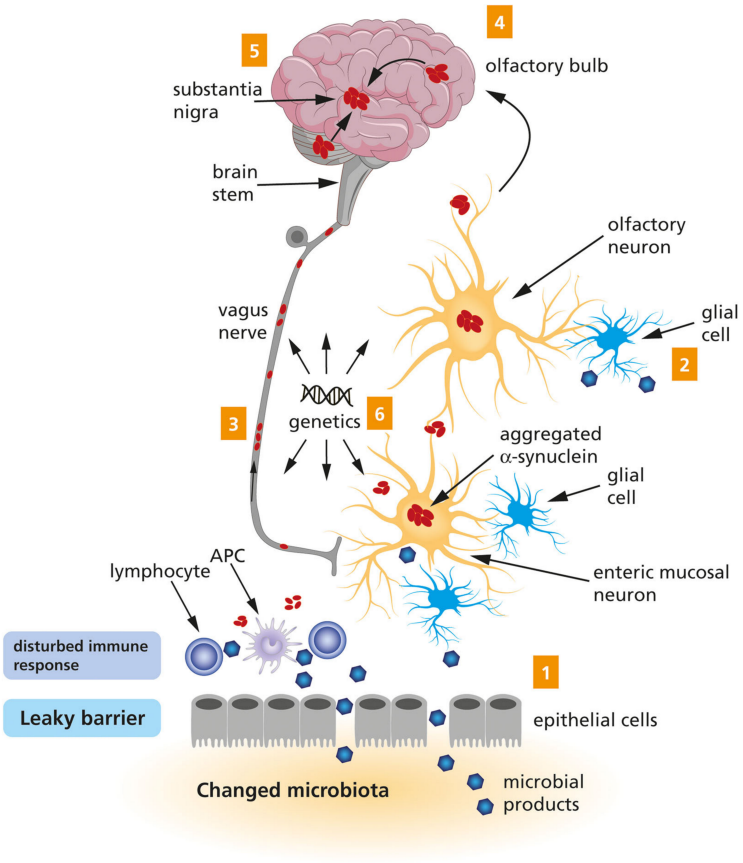

Figure 4: A schematic representation of the Braak's hypothesis of Parkinson's disease (PD). Microbial products come into contact with olfactory and/or enteric neurons, which trigger the aggregation of α-Synuclein (1 and 2). The aggregated α-Synuclein spreads toward the central nervous system via the olfactory bulb and the vagus nerve (3 and 4). Eventually, the aggregated α-Synuclein arrives at the substantia nigra (5). Genetic factors are likely to contribute to PD, but the exact mechanism remains to be elucidated (6). Figure from Rietdijk et al,[11] under creative commons license.

Iron in Parkinson's disease

It has been shown that there is an abnormal accumulation of iron in the substantia nigra in PD.[12–14] Coupled to this, there is a significant increase of ferritin, which binds Fe^{3+}, and a shift in the relationship of Fe^{2+} and Fe^{3+} in favor of the latter.[14,15] Neuromelanin, which is a dark pigment found in the substantia nigra, has been found to chelate and trap metals like iron. The

higher levels of iron in the substantia nigra in PD could saturate the chelating sites on neuromelanin and lead to an increase of toxic free irons.[15] Neuromelanin with iron overload has been found both intra- and extra-neuronally in the substantia nigra of patients with PD.[16] Iron in Fe^{3+} form has also been shown to bind to alpha-synuclein and accelerate its aggregation.[15,17] Evidence seems to point to that it might not be part of the initiation of the disease in PD, but that it could contribute to the progression of the neurodegeneration.[15]

1.1.4 Clinical manifestations

The loss of dopaminergic neurons in the substantia nigra leads to an imbalance in the basal ganglia circuitry, which leads to the typical symptoms of PD. A simplified schematic representation of the basal ganglia circuitry in health and in PD is shown in *Figure 5*.

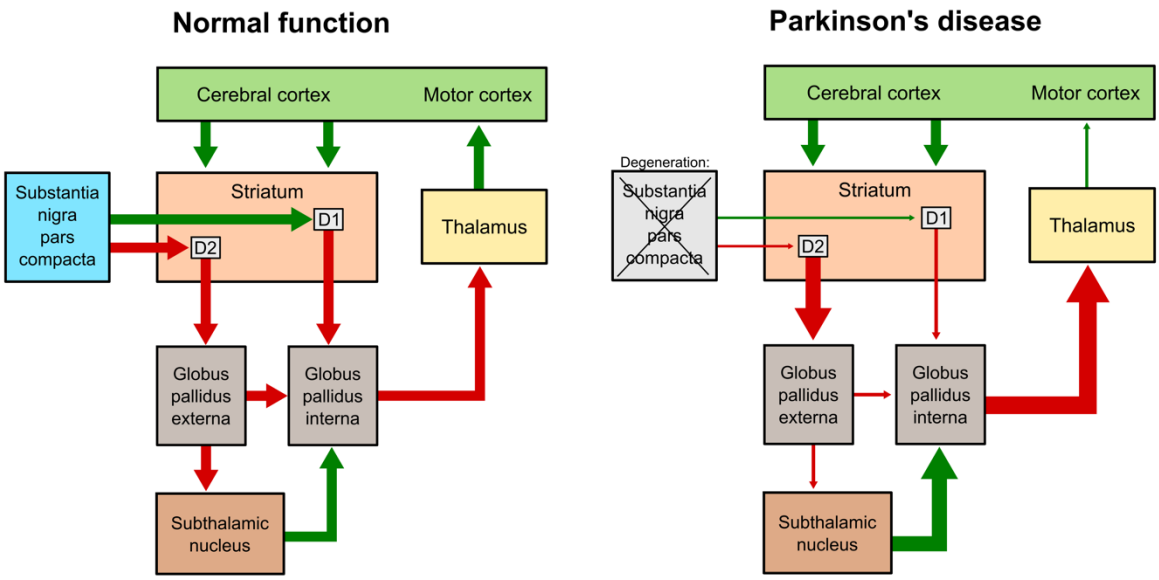

Figure 5: Schematic simplified representation of basal ganglia circuitry in health (left) and in Parkinson's disease (right). Green arrows represent activation and red arrows represent inhibition.

The typical motor symptoms of PD are bradykinesia, rigidity, resting tremors and postural instability.[4,5] The onset of the disease is normally unilateral, and this asymmetry typically persists also as the disease progresses. As seen in *Figure 2*, the prevalence of PD increases with age, and the average age of onset is in the late fifties.[4] What is also typical, is that in addition to these motor symptoms, there are so-called non-motor symptoms. These include REM-sleep behavior disorder (RBD), olfactory dysfunction, pain, depression and cognitive dysfunction.[4,5] Other common non-motor symptoms are those related to autonomic dysfunction, such as orthostatic hypotension and constipation. Som of these non-motor symptoms can often precede the onset of motor symptoms by years, and sometimes even decades.

1.1.5 Diagnosis

PD is a clinical diagnosis. For the diagnosis of PD, first the criteria for parkinsonism need to be fulfilled. Parkinsonism is defined based on three cardinal motor features. Bradykinesia, which is an obligate, must be present and combined with either rigidity, resting tremor, or

both.[18] Bradykinesia is defined as a combination of slow movement and a reduction in amplitude or speed as a movement is continued. It is tested by active movements such as finger tapping, pronation-supination of the hand or toe tapping. Rigidity is assessed by slowly moving the patient's extremity and is deemed present if a "lead-pipe" resistance is felt, with or without a cogwheel phenomenon.[18] Resting tremor is a relatively slow tremor 4–6 Hz in a resting extremity, and is suppressed when movements are initiated.[18]

When parkinsonism has been established as described above, a diagnosis of clinically established PD requires the following:[18]

- Absence of absolute exclusion criteria
- At least two supportive criteria
- No red flags

Absolute exclusion criteria	Supportive criteria	Red flags
Cerebellar abnormalities	**Clear and dramatic response to levodopa treatment**	**Rapid progression of gait impairment**
Downward supranuclear gaze palsy	**Presence of levodopa induced dyskinesias**	**No progression of motor symptoms over 5 or more years unless related to treatment.**
Diagnosis of behavioral variant FTD or primary progressive aphasia within 5 years of disease	**Rest tremor of an extremity**	**Early bulbar dysfunction.**
Parkinsonian features restricted to lower limbs for more than 3 years	**Loss of olfaction, or cardiac sympathetic denervation as measured by MIBG scintigraphy.**	**Inspiratory respiratory dysfunction.**
Treatment with dopamine receptor blocking or dopamine depleting consistent with drug-induced parkinsonism		**Severe autonomic failure in the first 5 years of disease.**
Absence of levodopa response		**Recurring falls due to impaired balance within 3 years of symptom onset.**
Cortical sensory loss, ideomotor apraxia or progressive aphasia		**Disproportionate anterocollis or contractures of hand or feet with the first 10 years.**
Normal functional imaging of the presynaptic dopaminergic system.		**Absence of non-motor symptoms despite 5 years disease duration.**
Alternative condition known to cause parkinsonism or other diagnosis more likely		**Unexplained pyramidal tract signs.**
		Bilateral symmetric parkinsonism.

Table 1. Absolute exclusion criteria, supportive critera and red flags, for the diagnosis of Parkinson's disease. From Postuma et al.[18]

If an individual does not meet the above criteria for clinically established PD, a diagnosis of clinically probable PD could still be possible. Clinically probable PD entails the following;[18]

- Absence of absolute exclusion criteria
- Red flags balanced by supportive criteria – one supportive criteria balances out one red flag, with a maximum of two red flags present to fulfil the criteria for probable PD.

While PD is a clinical diagnosis, neuroimaging such as magnetic resonance imaging or computed tomography is commonly performed, to rule out other possible causes of parkinsonism. Other ancillary testing such as ^{123}I-ioflupane single-photon emission computed tomography (SPECT), ^{18}F-fluorodeoxyglucose positron emission tomography (FDG-PET) and cerebrospinal fluid (CSF) tests can also be part of the investigation in parkinsonism and more details on these techniques will follow later in this text.

1.1.6 Treatment

The treatment of PD is mainly based on dopaminergic medication. These dopaminergic therapies can be divided into three main groups; levodopa, dopamine agonists and inhibitors of amine metabolism.[4,5]

Levodopa

Levodopa is a prodrug that, as opposed to dopamine, can enter through the blood-brain barrier. When inside the central nervous system, it is decarboxylated to dopamine. To minimize peripheral decarboxylation, which would cause side-effects, levodopa is administered together with a peripheral decarboxylase inhibitor such as benserazide or carbidopa.

Dopamine agonists

Dopamine agonists such as pramipexol, rotigotine and ropinirole exert their effect by directly activating dopamine receptors. They typically have a longer half-life than levodopa yielding a less pulsatile effect. This is believed to be coupled with a possibly reduced risk of motor fluctuations compared to levodopa.[4] They are also available in different dosage forms such as pills, transdermal patches and subcutaneous injections.

Metabolism inhibitors

Metabolism inhibitors can be further subdivided into monoamine oxidase (MAO) inhibitors and catechol-O-methyl transferase (COMT) inhibitors. The former inhibiting the clearance of dopamine by MAO in the synaptic cleft and thus increasing the dopamine concentration. The latter exerting its effect by peripheral inhibition of the COMT-dependent metabolism of levodopa, and in that way increasing the levels of circulating levodopa.[4] There are also variants of COMT inhibitors that in addition to this peripheral effect also have a central effect.

Treatment of non-motor symptoms

Regarding the non-motor symptoms, there is often a varied response to the dopaminergic therapy, and other medication is often needed to alleviate these symptoms.[5] For instance, depression can require treatment with selective noradrenaline and serotonin reuptake inhibitors, cognitive impairment might require acetylcholine esterase inhibitors and adrenergic agents can be used to treat orthostatic hypotension. In the case of hallucinations or other psychotic symptoms, the use of atypical neuroleptics can be warranted.

Advanced treatments

There are three commonly used forms of advanced treatments. These are considered when severe motor fluctuations cannot be sufficiently handled with the above-mentioned forms of medication. Levodopa gel can be continuously administered via a percutaneous endoscopic gastro-jejunostomy, and thus bypassing the ventricle giving a much more stable level of levodopa in the blood. Apomorphine can be administered subcutaneously via a pump, also giving a more even dopaminergic activation. Finally, using deep brain stimulation (DBS), one can via intracerebral electrodes stimulate certain basal ganglia regions to achieve a lesion-like effect without damaging the actual tissue.[4] The two most common targets for DBS are the subthalamic nucleus and the globus pallidus interna. By this stimulation, the balance in the basal ganglia circuitry can be shifted and parkinsonian symptoms such as bradykinesia, rigidity and tremors reduced.

1.1.7 Clinical scales

One of the most commonly used scales to assess symptoms and disability in PD are the Hoehn & Yahr scale.

Stage	Hoehn and Yahr scale[19]
1	Unilateral involvement only, usually with minimal or no functional disability
2	Bilateral or midline involvement, without impairment of balance
3	Bilateral disease: mild to moderate disability with impaired postural reflexes; physically independent
4	Severely disabling disease; still able to walk or stand unassisted
5	Confinement to bed or wheelchair unless aided

Table 2. The Hoehn and Yahr scale for rating of symptoms in Parkinson's disease.[19]

An updated version of the Hoehn and Yahr scale known as the modified Hoehn and Yahr scale also exists, with added stages 1.5 and 2.5.[20] The former representing "unilateral and axial involvement" and the latter "mild bilateral disease with recovery on pull test".

Another commonly used scale is the Unified Parkinson's Disease Rating Scale, or UPDRS. It is based on four sections;

- Part I: Evaluation of mentation, behavior and mood
- Part II: Self-evaluationof the activities of daily life (ADL)
- Part III: Clinician-scored motor evaluation
- Part IV: Complications of therapy

This UPDRS scale also exists in a revised edition sponsored by the Movement Disorders Society, the MDS-UPDRS.[21]

1.2 PROGRESSIVE SUPRANUCLEAR PALSY

1.2.1 Background

Progressive supranuclear palsy (PSP) was described by Steele, Richardson and Olszewski in 1964, as “a heterogenous degeneration involving the brain stem, basal ganglia and cerebellum with vertical gaze and pseudobulbar palsy, nuchal dystonia and dementia”.[22] They reported findings, including histopathology, from 9 patients developing this set of symptoms with the central ones being the vertical gaze palsy, axial rigidity and mild dementia.

1.2.2 Epidemiology

The prevalence of PSP is around 5-7 per 100 000,[23,24] making it a rare disorder, around a hundred times less common than PD. There are few known risk factors regarding PSP apart from age. Male gender is slightly over-represented in studies with around 55%, but the certainty in these numbers are not definite.[24] Lesser educational attainment has shown to be associated with an increased risk of developing PSP.[24] There has also been found an association between the H1 haplotype of the tau gene and PSP.[25]

1.2.3 Etiology

PSP is a tauopathy with pathological deposition of tau protein in the 4-repeat isoform in aggregates.[26] This tau pathology can be found in the frontal and parietal lobes, striatum, pallidum, subthalamic nucleus, substantia nigra, red nucleus, pons and cerebellum.[27,28] Pathologically, the picture is relatively typical with these 4-repeat tau inclusions, tufted astrocytes and coiled bodies, *Figure 6*.

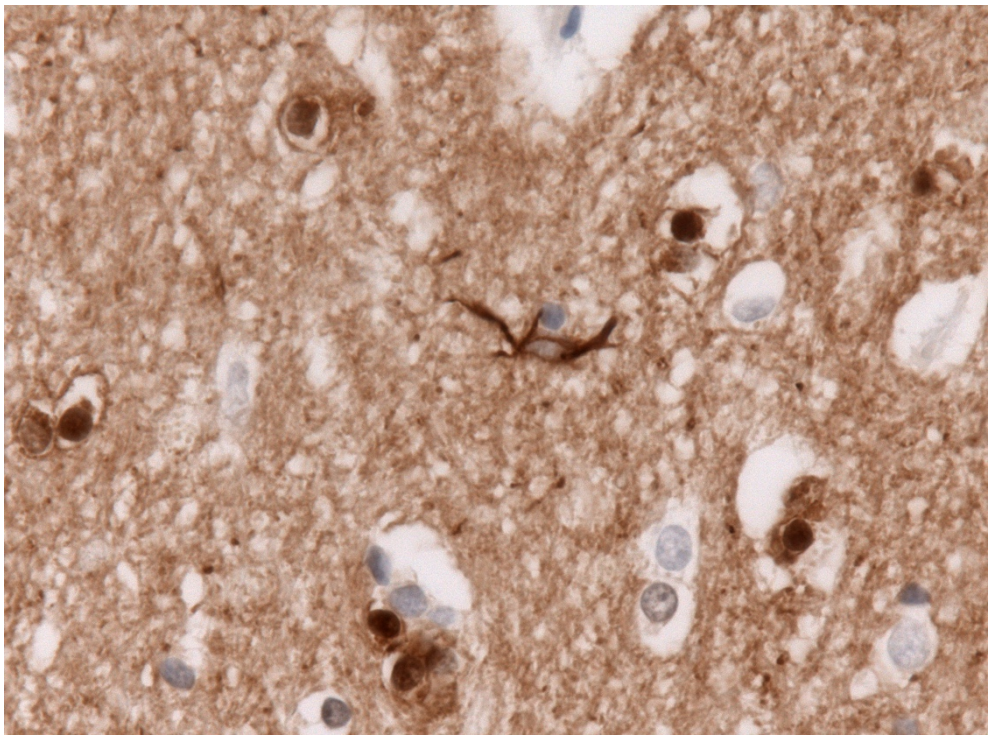

Figure 6: Autopsy specimen in progressive supranuclear palsy. Immunostaining for tau displaying a "tufted astrocyte" in the center (400x magnification). Image by Jensflorian, used under creative commons license (https://creativecommons.org/licenses/by-sa/3.0/), no changes made.

1.2.4 Clinical manifestations

The typical clinical manifestations in classical PSP, is the presence of vertical supranuclear gaze palsy, axial rigidity and early falls.[24] Mild to moderate cognitive impairment is also common, often with irritability or executive dysfunction.[27] While this picture is typical after a few years of disease, the initial symptoms are usually far more diverse and subtle, including gait disturbances, non-specific ocular issues and slowing of saccades.[27] The disease is severe and relatively rapidly progressive, with life expectancies of 5 to 8 years being reported.[27,29] Several subtypes have been described, with the classical variant being referred to as the Richardson-Steele (RS) phenotype. If more Parkinson-like features are present, such as more developed rigidity in the extremities, less ocular abnormalities, positive levodopa response or resting tremor, they are typically referred to as PSP-parkinsonism (PSP-P). These patients have been shown to have a less severe tau pathology compared to those with PSP-RS.[27] Other described variants are the PSP-corticobasal syndrome (PSP-CBS), PSP-pure akinesia with gait freezing (PSP-PAGF) and PSP-progressive non-fluent aphasia (PSP-PNFA).[27] In PSP-CBS, the picture is that of an asymmetric disease with prominent dystonia and cortical sensory loss. In PSP-PAGF, the central symptoms are gait disturbance and later on also a freezing of gait, and in PSP-PNFA a progressive non-fluent, expressive aphasia is present.

1.2.5 Diagnosis

The diagnosis of PSP is clinical, and a set of diagnostic criteria commonly used are those developed at the NINDS-SPSP international workshop.[30] These criteria divide the diagnostic certainty into three categories; possible, probable and definite:

PSP	**Mandatory inclusion criteria (Litvan et al)**[30]
Possible	• Gradually progressive disorder • Onset at age 40 or later • Either vertical (upward or downward gaze) supranuclear palsy or both slowing of vertical saccades and prominent postural instability with falls in the first year of disease onset • No evidence of other diseases that could explain the foregoing features
Probable	• Gradually progressive disorder • Onset at age 40 or later • Vertical (upward or downward gaze) supranuclear palsy and prominent postural instability with falls in the first year of disease onset • No evidence of other diseases that could explain the foregoing features
Definite	• Clinically probable or possible PSP and histopathologic evidence of typical PSP

Table 3. Mandatory inclusion criteria in the diagnosis of PSP. From Litvan et al.[30]

To fulfil these criteria, all of the following exclusion criteria must also be absent:

Mandatory exclusion criteria (Litvan et al)[30]
• Recent history of encephalitis • Alien limb syndrome, cortical sensory deficits, focal frontal or temporoparietal atrophy • Hallucinations or delusions unrelated to dopaminergic therapy • Cortical dementia of Alzheimer's type (severe amnesia and aphasia or agnosia, according to NINCDS-ADRA criteria) • Prominent, early cerebellar symptoms or prominent, early unexplained dysautonomia (marked hypotension and urinary disturbances) • Severe, asymmetric parkinsonian signs (i.e., bradykinesia) • Neuroradiologic evidence of relevant structural abnormality (i.e. basal ganglia or brainstem infarcts, lobar atrophy) • Whipple's disease, confirmed by polymerase chain reaction, if indicated

Table 4. Mandatory exclusion criteria in the diagnosis of PSP. From Litvan et al.[30]

Several supportive criteria are also listed, such as symmetric akinesia or rigidity, retrocollis and poor levodopa response. These are meant to be more of a guiding nature and not implemented in a rule-based way in the diagnostic criteria.

It has been found that these criteria, while having excellent specificity, might suffer from lower sensitivity in early disease and in other variants than PSP-RS.[31] This is due to the focus on ocular abnormalities, which are not always discernible until later stages. For this reason, among others, the MDS criteria for PSP were developed.[31] In these criteria, more variants of PSP are considered, and there is an additional level of certainty, “suggestive”, which is weaker than “possible”.

Additional testing and procedures are also commonly part of the investigation of suspected PSP, such as MRI, CSF examination and FDG-PET. MRI can show different signs consistent with PSP such as midbrain atrophy,[32] CSF examination can exhibit elevated neurofilament light chain protein (NFL)[33] and FDG-PET can help differentiate between atypical parkinsonian disorders.[34]

1.2.6 Treatment

Levodopa may have some effect on the rigidity and bradykinesia in PSP,[24] and is usually tried initially. In a cohort consisting of 103 pathologically proven PSP patients, 32% were reported to have had some response to levodopa.[35] Amantadine may provide some effect on gait and apathy.[24] Botolinum toxin can be used to ameliorate blefarospasm and apraxia of eyelid opening.[36,37]

1.2.7 Clinical scales

A clinical rating scale for assessing symptoms in PSP is the PSP rating scale, developed by Golbe et al.[38] It consists of 28 items divided into 6 categories; history/daily activities, behavioral symptoms, bulbar symptoms, supranuclear ocular motor symptoms, limb motor symptoms and gait/midline symptoms. The Hoehn and Yahr scale is also often used in PSP.[19]

1.3 MULTIPLE SYSTEM ATROPHY

1.3.1 Background

The name multiple system atrophy (MSA) was first used in 1969,[39] but other names for this disorder and its variants that were used even earlier were Shy-Drager syndrome, striato-nigral degeneration, olivopontocerebellar atrophy.[40,41] The last term was described as early as 1900 by Dejerine and Thomas.[42] They partly represent subtypes of what is today defined within the MSA entity.

1.3.2 Epidemiology

The prevalence of MSA is not completely known, but studies have placed it at ranges from 3.4 to 4.9 cases per 100 000 people making it roughly as rare as PSP.[43] No differences in prevalence has been found between the sexes.[43] The parkinsonian subtype of MSA is more common than the cerebellar subtype in Europe by 2 to 4 times.[43] However, the cerebellar subtype was around twice as frequent as the parkinsonian subtype in a Japanese cohort consisting of 230 patients with MSA.[44] This difference in proportions of the respective subtypes could be due to genetic or epigenetic factors.[43] No single mutations have been found linked to familial forms.[45]

1.3.3 Etiology

Pathologically, varying degrees of degeneration can be found in the striatum, substantia nigra, pons and cerebellum, as well as some degree of cortical atrophy.[43,45] Histologically, the findings are relatively specific for MSA, with alpha-synuclein inclusions within oligodendrocytes, so-called glial cytoplasmic inclusions (GCI).[42] Other findings include neuronal loss with axonal degeneration, myelin degeneration and microglial activation.[45] Examples of GCI within the cerebrum can be seen in *Figure 7.*

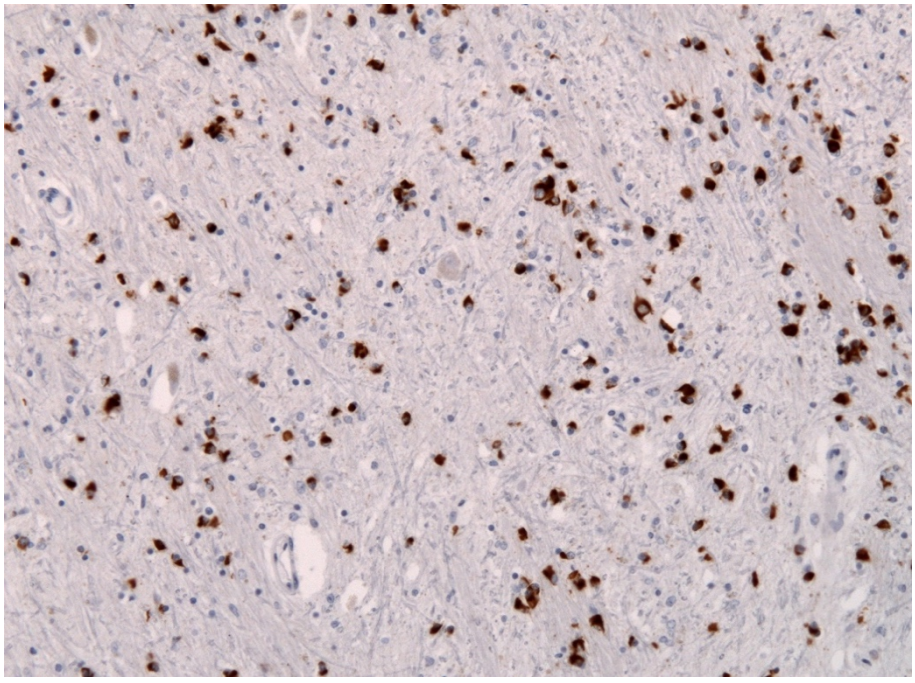

Figure 7: Alpha synuclein immunohistochemistry showing glial cytoplasmic inclusions in MSA. Image by Jensflorian, used under creative commons license (https://creativecommons.org/licenses/by-sa/3.0/), no changes made.

1.3.4 Clinical manifestations

The central feature of MSA is the early and prominent autonomic failure.[43] This autonomic dysfunction typically affects cardiovascular and/or urogenital systems. The cardiovascular dysfunction showing as severe orthostatic hypotension, and the urogenital dysfunction taking the form of erectile dysfunction and/or incontinence.[42] MSA is usually divided into subtypes; MSA with parkinsonism (MSA-P) and MSA with cerebellar symptoms (MSA-C). MSA-P may, especially in early stages, be hard to distinguish from PD.[42] It is typically associated with bradykinesia, rigidity and impaired balance. Different forms of tremor can be present, but classic Parkinsonian "pill-rolling" tremor is unusual.[43] Levodopa response is generally poor, but some degree of response can be found in around 40% of the patients with MSA-P.[43] In MSA-C, the picture is that of cerebellar ataxia and oculomotor abnormalities such as nystagmus.[43] Antecollis, dystonia, RBD, dysarthria, respiratory disturbances and dysphagia are also common symptoms in MSA.[42,43,45]

1.3.5 Diagnosis

The second consensus criteria for the diagnosis of MSA define three levels of diagnostic certainty; possible, probable and definite MSA.[46] It is defined as a sporadic, progressive, adult onset disease with the following criteria for the different degrees of certainty.

MSA	Criteria (Gilman et al)[46]
Possible	• Parkinsonism (bradykinesia with rigidity, tremor, or postural instability) **or** • A cerebellar syndrome (gait ataxia with cerebellar dysarthria, limb ataxia, or cerebellar oculomotor dysfunction) **and** • At least one feature suggesting autonomic dysfunction (otherwise unexplained urinary urgency, frequency or incomplete bladder emptying, erectile dysfunction in males, or significant orthostatic blood pressure decline that does not meet the level required in probable MSA) **and** • At least one of the additional features of possible MSA, see following table
Probable	• Autonomic failure involving urinary incontinence (inability to control the release of urine from the bladder, with erectile dysfunction in males) or an orthostatic decrease of blood pressure within 3 min of standing by at least 30 mm Hg systolic or 15 mm Hg diastolic **and** • Poorly levodopa-responsive parkinsonism (bradykinesia with rigidity, tremor, or postural instability) **or** • A cerebellar syndrome (gait ataxia with cerebellar dysarthria, limb ataxia, or cerebellar oculomotor dysfunction)
Definite	• Neuropathological findings congruent with MSA-P or MSA-C

Table 5. Diagnostic criteria for possible, probable and definite MSA. From Gilman et al.[46]

Additional features of possible MSA (Gilman et al)[46]
Possible MSA-P or MSA-C • Babinski sign with hyperreflexia • Stridor **Possible MSA-P** • Rapidly progressive parkinsonism • Poor response to levodopa • Postural instability within 3 y of motor onset • Gait ataxia, cerebellar dysarthria, limb ataxia, or cerebellar oculomotor dysfunction • Dysphagia within 5 y of motor onset • Atrophy on MRI of putamen, middle cerebellar peduncle, pons, or cerebellum • Hypometabolism on FDG-PET in putamen, brainstem, or cerebellum **Possible MSA-C** • Parkinsonism (bradykinesia and rigidity) • Atrophy on MRI of putamen, middle cerebellar peduncle, or pons • Hypometabolism on FDG-PET in putamen • Presynaptic nigrostriatal dopaminergic denervation on SPECT or PET

Table 6. Additional features for the diagnosis of possible MSA. From Gilman et al.[46]

These consensus criteria also list additional features supporting and not supporting a diagnosis of MSA, but these features are not included in a rule-based manner.

The investigation of suspected MSA commonly contains other testing such as CSF analysis, autonomic testing, MRI and FDG-PET.[47] CSF testing can show elevated levels of NFL[33] and autonomic testing can assess orthostatic hypotension as well as thermoregulatory dysfunction.[47] MRI may show signs consistent with MSA such as putaminal atrophy, pontocerebellar atrophy and hot cross bun sign.[48] FDG-PET can also show patterns of metabolism typical for MSA.[34]

1.3.6 Treatment

In MSA-P, initial levodopa response has been reported for a majority of the patients, although this response typically declines after a few years as the disease progresses.[42,45] Dopamine agonists, although probably not as effective as levodopa, can be tried in case of levodopa-induced dyskinesia.[43] Amantadine can potentially have some positive effect, and botulinum toxin treatments can be helpful for dystonia.[43] In case of orthostatic hypotension, treatment with anti-hypotensive medication such as adrenergic or mineral corticoid substances can be indicated.[42,43]

1.3.7 Clinical scales

A dedicated clinical scale for MSA is the Unified MSA Rating Scale (UMSARS), by Wenning et al.[49] It consists of 4 parts.

- Part I: Historical review
- Part II: Motor examination scale
- Part III: Autonomic examination
- Part IV: Global disability scale

As in PSP, the Hoehn and Yahr scale is also often used in MSA.[19]

1.4 OTHER TYPES OF ATYPICAL PARKINSONISM

Corticobasal degeneration (CBD) and dementia with lewy bodies (DLB) are two other disorders with parkinsonian symptoms often being part of the clinical picture.

1.4.1 Corticobasal degeneration

CBD is a 4-repeat tauopathy with astrocytic plaques and ballooned neurons typically found histologically. There is commonly an asymmetric cortical atrophy congruent with the asymmetric symptomatology in this disease. Clinically, the picture is of asymmetric rigidity, dystonia as well as cortical symptoms such as ideomotor apraxia and aphasia. No effective treatments are available, but levodopa or amantadine can be tried and evaluated. For the dystonia commonly associated with CBD, botulinum toxin or clonazepam can be helpful. The investigation is closely resembling that of PSP and MSA, with MRI, CSF analysis and FDG-PET commonly being performed. MRI can reveal an asymmetric cortical atrophy. An elevation of NFL in CSF is a common finding in CBD, and FDG-PET can often show an asymmetric cortical metabolism.

1.4.2 Dementia with lewy bodies

DLB is an alpha-synucleinopathy, and Lewy bodies are commonly seen in widespread cortical regions. Symptom-wise, a dementia, often with dysexecutive features, visuospatial dysfunction and variations in activity and wakefulness is typical. Patient also have fluctuating visual hallucinations. Some degree of parkinsonism, such as rigidity and bradykinesia, shall also be present. Also typical for DLB is sensitivity to certain medications, where dopaminergic drugs such as levodopa often can cause hallucinations and neuroleptics can cause severe rigidity and general worsening. To differentiate it from PD, the definition is that if the cognitive symptoms appear less than a year after the initial motor symptoms, it meets the criteria for DLB and not PD. The clinical investigation often includes MRI, CSF analysis, ^{123}I-ioflupane single-photon emission computed tomography as well as extensive neuropsychological testing. Memory deficits can be treated with choline esterase inhibitors, and for parkinsonian symptoms, low dosages of dopaminergic therapy may have a positive effect.

1.5 MAGNETIC RESONANCE IMAGING IN PARKINSONIAN DISORDERS

1.5.1 Conventional MRI sequences

Conventional MRI using standard sequences such as T_1-weighted imaging, T_2-weighted imaging including fluid-attenuated inversion recovery (FLAIR), is common in the clinical investigation of a patient presenting with parkinsonian symptoms, especially if there is possible uncertainty regarding symptomatology. Concerning primarily suspected idiopathic PD, MRI is used for the exclusion of alternative diagnoses.[50–52] Such alternative diagnoses with different typical MRI findings, possibly presenting with parkinsonism, include cerebrovascular disease, normal pressure hydrocephalus, brain tumor, multiple sclerosis, PSP, MSA and CBD. These disorders can sometimes present, in ways at least initially inseparable from idiopathic PD, with symptoms such as rigidity, tremor, bradykinesia or postural instability.[4,5,53] It is also important to exclude these alternative diagnoses since they may need different medical or surgical management. When suspecting atypical parkinsonian syndromes such as PSP, MSA or CBD, conventional MRI can in some cases aid clinicians in the diagnostic process.[50]

In PSP, mesencephalic atrophy is common. This is the basis for different radiological signs and measurements that have been proposed to assess these changes. Typical radiological signs of midbrain atrophy observed in PSP are the "hummingbird sign", the "mickey mouse sign" and the "morning glory sign".[32,50] The "hummingbird sign" referring to the appearance of the atrophic midbrain on sagittal slices, and the "mickey mouse sign" and "morning glory sign" describing the abnormal appearance on axial slices. Examples of these signs are shown in *Figure 8A-B*. For "hummingbird sign" and "morning glory sign" respective sensitivities of 68% and 50% have been reported, while the "mickey mouse sign" seems to be less prevalent and perhaps also less studied.[54]

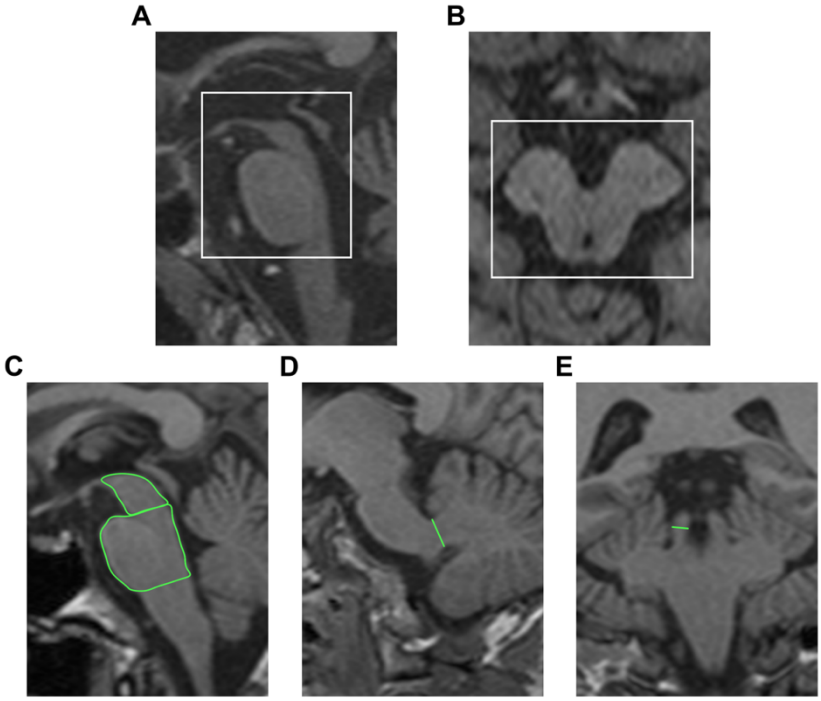

Figure 8: MRI in PSP. Hummingbird sign **(A)**. Mickey mouse sign / Morning glory sign **(B)**. Midbrain-to-pons area ratio **(C)**. Width of the middle cerebellar peduncle **(D)**. Width of the superior cerebellar peduncle **(E)**.

Commonly used measurements in PSP are the midbrain-to-pons ratio (MP-ratio) and the magnetic resonance parkinsonism index (MRPI), both showing excellent diagnostic discrimination between PSP and other types of parkinsonism as well as from controls. A wide range of sensitivities and specificities have been reported for both MP-ratio and MRPI: 64-100% sensitivity and 80-100% specificity for MP-ratio, and 69-100% sensitivity and 64-100% specificity for MRPI.[55] The MP-ratio is calculated by measuring the respective midline areas on a sagittal slice, illustrated in *Figure 8C*. For the MRPI, this ratio is inverted and multiplied by the width of the middle cerebellar peduncle divided by the width of the superior cerebellar peduncle on sagittal and coronal slices respectively, as illustrated in *Figure 8C-E*. While manual measurements such as the MRPI or MP-ratio inherently have the possibility for inter- and intra-rater disagreements, an Italian group has recently described a tool for automatic calculation of these measurements showing similar results as with manual calculations.[56] A newer version of MRPI called MRPI 2.0 has recently been proposed, taking into account also the width of the third ventricle and the width of the frontal horns. It has been shown to be better at separating PSP-P from PD in early stages of disease.[57]

In MSA, there are also a number of classical radiological signs reported to indicate disease. The most frequent ones are the "hot cross bun sign", the T_2-hyperintensity in the middle cerebellar peduncles ("MCP sign") and putaminal hypointensity on T_2-weighted images as well as a hyperintense ring around the putamen.[42,58] One study reports prevalence of hot cross bun sign and MCP sign in MSA at 58% and 50% respectively. Using a gradient recall echo (GRE) MRI sequence to assess putaminal hypointensity yielded a sensitivity of 73%. Examples of "hot cross bun sign", "MCP sign" and dorsolateral putaminal hypointensity are shown in *Figure 9*.

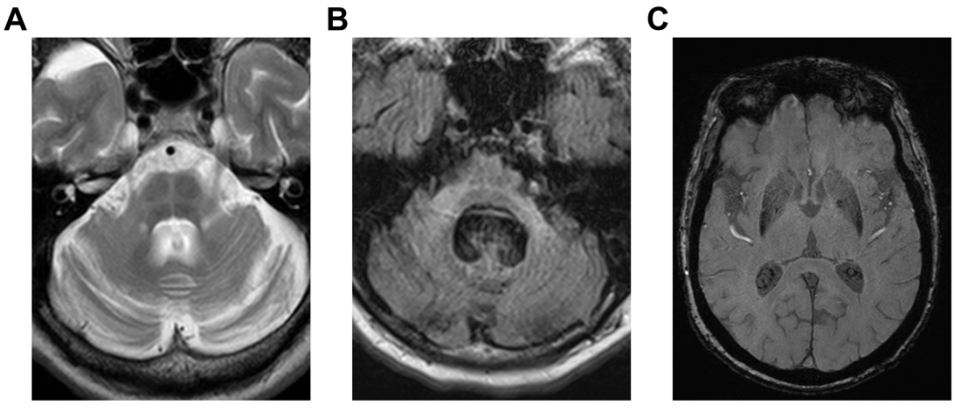

Figure 9: Signs of MSA. Hot cross bun sign with hyperintensity on T_2-weighted image **(A)**. Middle cerebellar peduncle hyperintensity (MCP sign) on T_2-weighted FLAIR image **(B)**. Hypointensity of the putamen on a gradient recall echo (GRE) sequence **(C)**.

1.5.2 Advanced MRI sequences

Susceptibility-related imaging

Susceptibility weighted imaging (SWI) is an imaging technique in which a GRE sequence is used to gather magnitude and phase images which are combined to give the final SWI volume, which is sensitive to venous blood, hemorrhage, calcifications and iron deposition.[59,60] In the SWI-processing, the phase is subjected to a variant of high-pass filtering in which the first step is a multiplication of the original complex image with a low-pass Hanning filter.[61] The original complex image is subsequently divided by the low-passed complex volume to yield a high-passed filtered phase. The high-pass filtered phase image is converted into a phase mask, where negative phase values are linearly distributed 0 to 1, and all positive phase values are set to 1. This mask is raised to the power of four and multiplied with the magnitude image to produce the final susceptibility weighted image.

It has been known for a long time that there is abnormal iron deposition in deep nuclei in parkinsonism,[62] which has been suggested to be due to disease-related disruption of the iron homeostasis.[63] Since SWI is sensitive to iron deposition, the presence of pathological brain iron accumulation can be assessed with SWI and one way of evaluating these changes in PD is the so-called "swallow tail sign".[64] It describes the normal hyperintense appearance of nigrosome-1 within the dorsolateral substantia nigra on SWI. This hyperintensity is commonly lost in parkinsonism.[65] A study on PD, MSA and PSP showed correct classification against healthy controls using this biomarker in 93.2% of the cases.[66] Another study on PD, MSA and PSP showed similar results with sensitivity and specificity against healthy controls of 88.8% and 83.6% respectively.[67] The presence and absence of the swallow tail sign is shown in Figure *10A-B*.

A newly developed technique also utilizing phase contrast to assess susceptibility is quantitative susceptibility mapping (QSM). QSM takes susceptibility imaging a step further and attempts to mathematically deconvolute tissue phase to underlying susceptibility,[68,69] which is a complex inverse and ill-posed problem due to the presence of zeroes along the magic angle of the dipole kernel. This problematic double cone is visualized in *Figure 10C*. Before the final deconvolution, the phase must be unwrapped and background fields have to be removed. Many techniques have been developed for background field removal including SHARP[70], V-SHARP[71] and projection unto dipole fields (PDF)[72]. After the tissue phase has been acquired, the susceptibility map is calculated using deconvolution with a dipole kernel. Commonly used methods include Iterative least-squares (iLSQR)[73] and Morphology enabled dipole inversion (MEDI)[74]. A recently described variant of the latter named MEDI+0 includes automatic referencing to CSF, enforcing of susceptibility homogeneity within CSF and suppression of artifacts near the lateral ventricles in the resulting susceptibility maps.[75] Examples of phase image, tissue phase and quantitative susceptibility map are shown in *Figure 10D-F*. Quantitative susceptibility maps have been shown to have a high degree of correlation to iron concentrations in brain tissue.[76–78]

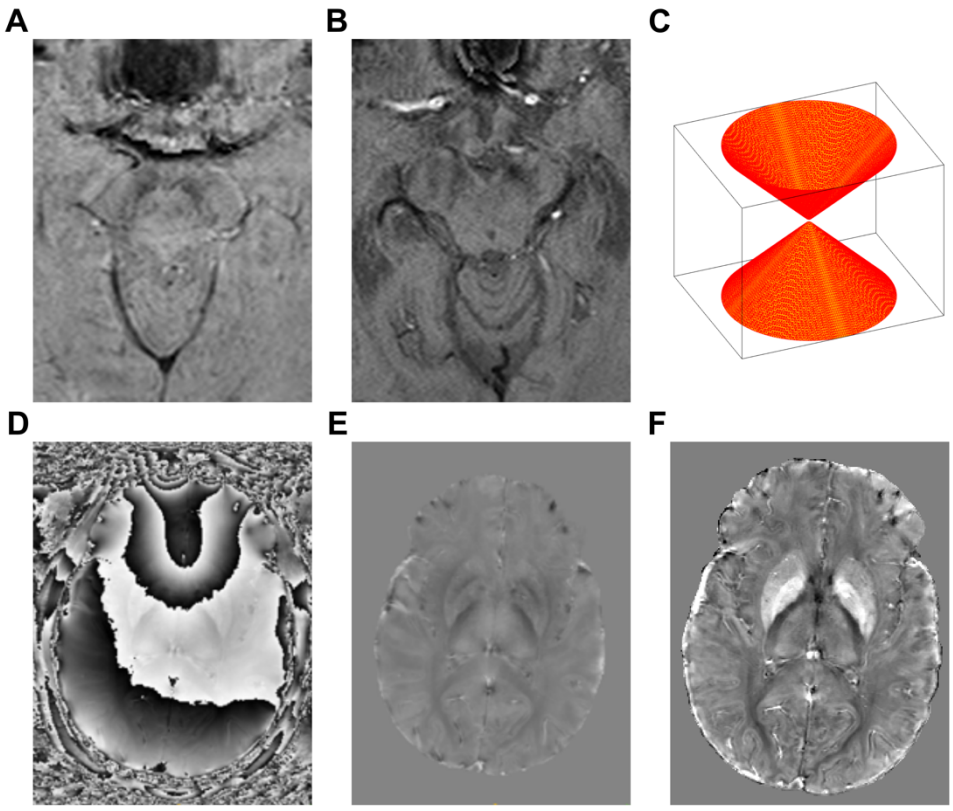

Figure 10: Presence of swallow tail sign in a healthy individual **(A)**. Absence of swallow tail sign in a patient with MSA **(B)**. Visualization of zeroes in the dipole kernel on the surface of a three-dimensional double cone **(C)**. Illustration of QSM processing in a healthy individual, with wrapped phase image **(D)**, tissure phase after phase unwrapping and background field removal **(E)** and the resulting quantitative susceptibility map after deconvolution **(F)**.

QSM techniques have been used in PD to investigate abnormal brain iron accumulation. One study reports increased susceptibility levels in the substantia nigra, red nucleus, thalamus and globus pallidus in PD compared to healthy controls.[79] Another study on QSM in PD vs. controls showed only significant increased susceptibility in the substantia nigra, but could from this region produce a good diagnostic separation with sensitivity 90% and specificity 86%.[80] In contrast, another study also using QSM in the substantia nigra to separate PD from healthy controls achieved lower diagnostic performance with sensitivities and specificities of around 70-75%.[81] Both these studies, however, show concordance in that QSM seems to be superior to R_2* in diagnostic performance. Other potential uses of QSM in PD is for structural visualization before surgical procedures. QSM has been shown to give higher contrast-to-noise ratio and higher inter-rater agreement in the delineation of the subthalamic nuclei (STN) compared to T_2*.[82] QSM also seems to provide contrast useful in identifying the internal globus pallidus (GPi) in both PD and controls.[83]

QSM has also been used in studies including atypical parkinsonian syndromes. One study used a combination of diffusion kurtosis imaging (DKI) and QSM of the lentiform nuclei, and could show sensitivities of 83-100% and specificities of 81-100% for diagnostic classification.[84] In the first QSM study investigating brainstem abnormalities in PSP and MSA, our group could show AUCs of 0.97 and 0.98 in separating PSP from PD and healthy controls respectively.

Sensitivities and specificities were around 90% or higher in both comparisons.[85] In CBD, a cortical pattern with layers of different susceptibility can be found.[86]

Diffusion weighted imaging

With specific diffusion weighted MRI sequences, it is possible to image the diffusion of protons *in vivo* in human tissue. One typical way of using this technique to quantify diffusion properties is to construct diffusion tensors by acquiring diffusion weighted images in a minimum of six directions. This is called diffusion tensor imaging (DTI).[87] The diffusion tensor mathematically describes the direction and amount of diffusion along three vectors. These values can be further evaluated by calculating different diffusion properties, such as mean diffusivity (MD), axial diffusivity (diffusion along the mean diffusion direction), and radial diffusivity (diffusion perpendicular to the main diffusion direction).[88] A commonly used measurement of microstructural integrity is the composite diffusion metric called fractional anisotropy (FA).[89]

A meta-analysis on DTI studies including 1087 patients with PD and 768 healthy controls showed significant differences in FA and MD between the groups in the substantia nigra, the corpus callosum, temporal cortex and cingulate cortex.[90] A DTI study performed at Karolinska University Hospital found reduced FA for substantia nigra in PD patients.[91] Another study on 66 PD patients and 65 healthy volunteers also describes changes in the parietal, occipital, insular and cerebellar white matter in PD.[92] A study using neuromelanin-based ROIs to assess FA in the substantia nigra found lower FA in PD compared to healthy controls.[93] In the same study, significant differences could not be found using ROIs in the substantia nigra based on T_2-weighted images. A longitudinal DTI study did not find any difference between PD and healthy controls at baseline, but showed a change in nigral FA-levels at the 1.5-2-year follow-up.[94] Callosal FA-values have been shown to yield diagnostic discrimination between PD and MSA patients without “hot cross bun sign”, with sensitivity 88% and specificity 83%, albeit examined in a small group of eight MSA patients.[95] A large meta-analysis also supports the findings of diffusional differences between PD and MSA, and showed that putaminal FA-values could separate MSA-P from PD with an overall sensitivity of 90% and overall specificity of 93%.[96] Other studies have shown extensive white matter involvement in MSA.[97,98] Visualizations of an FA-map and MD are shown in *Figure 11A-B*.

Tensor based imaging including FA does, however, have certain limitations.[99,100] For instance, in regions with crossing fibers and thus similar magnitudes of diffusion in all direction, such as in the centrum semiovale and deep grey matter structures, the FA-value will be close to 0.[101] Different techniques have been developed to give more detailed microstructural information, such as DKI and neurite orientation dispersion and density imaging (NODDI). These methods use multiple diffusion weightings in many directions to be able to assess non-Gaussian water diffusion.[102,103] A study using both DKI and NODDI showed changes in PD in different grey matter areas including the striatum and many cortical regions.[104] Using DKI, microstructural changes have also been shown in PSP and MSA in the midbrain tegmentum and pontine crossing tract.[105] A study using NODDI in 58 patients with PD and 36 healthy controls showed loss of intracellular volume in the substantia nigra and putamen in PD compared to controls. In

this study, a diagnostic separation between PD and controls was achieved with a sensitivity of 88% and a specificity of 83% using intracellular volume values from the substantia nigra pars compacta contralateral to the side of the more severe symptoms.[106] Examples of NODDI volumes showing intraneurite volume fractions and orientation dispersion index are shown in *Figure 11C-D*. It can be mentioned that for NODDI, the intracellular volume fraction and the orientation dispersion index are thought to together account for different microstructural properties that together can give rise to the same FA.[103]

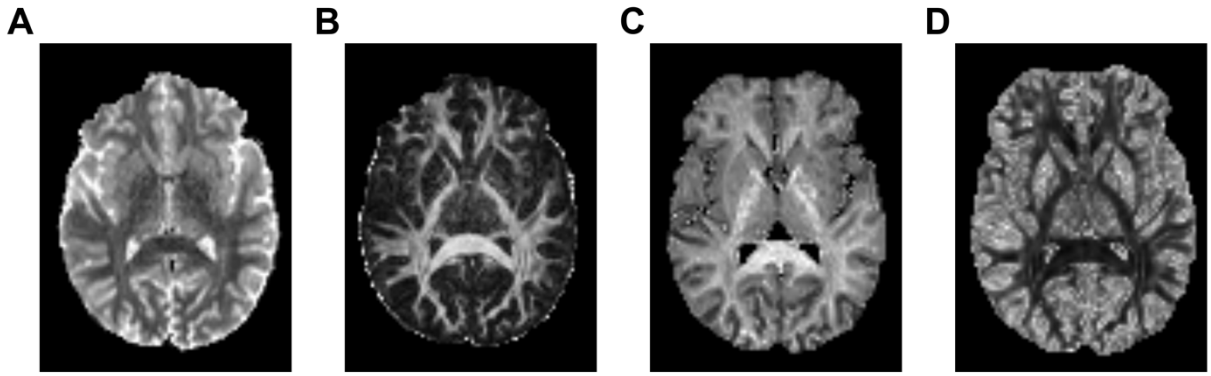

Figure 11: Diffusion imaging in a healthy control. Mean diffusivity **(A)**. Fractional anisotropy **(B)**. Map of intraneurite volume fraction in a healthy control calculated using the NODDI algorithm with diffusion data gathered in 32 directions with b=1000 and 64 directions with b=3000 **(C)**. Orientation dispersion index from NODDI **(D)**.

Functional magnetic resonance imaging

Functional magnetic resonance imaging (fMRI) employs different techniques to indirectly measure brain activity, with the most commonly used method being blood-oxygen level dependant (BOLD) contrast imaging.[107] Here, changes in blood oxygenation leads to signal differences that can be interpreted as changes in brain activity based on neurovascular coupling.

Studies have shown connectivity impairments in the striatum in PD patients in "off" state.[108] This reduced striatal interconnectivity was associated with decoupling of the striatum from the sensorimotor and thalamic networks. Increased striatocortical and thalamocortical connections but reduced striatothalamic connectivity is seen in PD when on dopaminergic therapy.[109] Intake of dopaminergic medication significantly improved striatal connectivity. A study on 51 patients with PD and 50 healthy controls showed a diagnostic separation with 92% sensitivity and 87% specificity using resting-state fMRI (rs-fMRI) to measure the amplitude of low-frequency fluctuations (ALFF) and employing SVM techniques for classification.[110] A large meta-analysis on rs-fMRI studies found evidence of functional impairment in the parietal lobes in PD compared to healthy controls.[111]

In PSP and CBD, increased functional connectivity was found within networks compared to controls, with a larger number of resting state networks affected in CBD.[112] Compared to healthy volunteers both patient groups exhibited reduced functional connectivity between the lateral visual and auditory networks. In PSP, lower functional connectivity was seen between the cerebellar and insular networks. Another study showed decreased connectivity in the

prefrontal cortex in PSP compared to healthy controls.[113] This study also found a correlation between lower functional midbrain connectivity and vertical gaze impairment. In MSA, changes in ALFF have been seen in different regions of visual cortex and in the right cerebellum compared to PD.[114] These changes are consistent with known pathological involvement in the respective parkinsonian disorder.[5,27,42]

Magnetization transfer and chemical exchange saturation transfer

Magnetization transfer (MT) is an imaging technique based on the fact that hydrogen atoms not only exist in free water but also in other more complex forms, for example bound to macromolecules such as myelin.[115] During MRI, the protons bound to macromolecules lose their magnetization rapidly and are thus challenging to image. It is, however, possible to image them indirectly by MT.[116] The MT technique is based on using a preparation pulse aimed to resonate with and saturate the protons bound to macromolecules. The bound protons will interact and transfer some of their magnetization to the free protons from which signal can be obtained (S_{MT}). By repeating the procedure without a saturation pulse (S_0), it is possible to determine the ratio of which magnetization has been transferred, referred to as the magnetization transfer ratio (MTR):

$$MTR = \frac{S_0 - S_{MT}}{S_0}$$

A study on PD, PSP, MSA and healthy controls using MTR found significantly lower levels in the globus pallidus in PSP compared to all other groups and in the putamen in MSA compared to PD and controls. They also found decreased levels in the substantia nigra in all parkinsonian disorders compared to controls.[117] A study on PD showed MTR reduction in the substantia nigra, the striatum, thalamus and in white matter.[118] Two MTR studies on MSA showed significantly lower MTR in the pyramidal tracts compared to healthy controls.[119,120] A study using quantitative MT (qMT), an extension of ordinary MT allowing calculation of additional magnetization transfer-related properties, showed significant differences in the substantia nigra pars compacta in PD compared to healthy controls.[121]

Another imaging technique related to MT is chemical exchange saturation transfer (CEST), in which saturation pulses are used to achieve a contrast based on chemical exchange. It allows imaging of a multitude of contrasts, including pH imaging, imaging of peptides, metal ion detection, temperature imaging, imaging of polyamines and nucleic acids, among others.[122] Two CEST studies using amide proton transfer protocols found significantly lower signals in the substantia nigra in PD compared to healthy controls.[123,124] Another study using CEST and DTI in PD found that while both CEST and DTI found significant changes in the substantia nigra PD compared to controls, only CEST could visualize changes also in the putamen and the caudate nucleus.[125]

Neuromelanin-sensitive imaging

Techniques have been developed to visualize melanin using T_1-weighted fast spin-echo (FSE) sequences.[126,127] It is known that neurons in the substantia nigra contain a melanin pigment known as neuromelanin. The signal intensity in the above mentioned FSE-sequence has been shown to be reduced in the substantia nigra in PD, reflecting degeneration of neuromelanin-containing neurons. The contrast mechanism for this is thought to be a T_1 reduction caused by melanin-iron complexes.[128] Using neuromelanin-sensitive imaging and a fully automated segmentation technique of the substantia nigra and locus coeruleus, excellent discrimination between PD and healthy controls have been reported with a sensitivity of 91-92% and a specificity of 89%.[129] A study exploring neuromelanin-sensitive imaging in atypical parkinsonian syndromes has shown reduced nigral volumes with neuromelanin-positivity compared to controls in PD, PSP, MSA and CBD.[130] In this study, no significant differences were seen between the atypical parkinsonian disorders and PD.

Magnetic resonance spectroscopy (MRS)

Magnetic resonance spectroscopy (MRS) can be used to measure different metabolites in living tissue, such as N-acetylaspartate (NAA), creatine (Cr), choline (Cho), glutamate (Glu), glutamine (Gln), myo-inositol (mI) and gamma-amino butyric acid (GABA).[131,132] From the magnetic resonance spectrums, calculations are made to assess either ratios between these metabolites or direct quantifications of single metabolites. An MRS study on PD, PSP and MSA found reduced NAA/Cho and NAA/Cr ratios in the putamen and pallidum in PSP and MSA, suggesting neuronal loss.[133] Another study by the same group found reduced NAA/Cho ratio in the lentiform nucleus in MSA and PSP compared to PD and healthy controls, and reduced NAA/Cr in MSA, PSP and PD compared to controls.[134] It has also been shown that PSP, CBD, MSA and vascular parkinsonism, but not PD, had reduction of NAA/Cr in the frontal cortex.[135] This study also reports that PSP, CBD, MSA and PD had lower NAA/Cr levels in the putamen, and that CBD had an asymmetry in the putamen compared to controls and the other patient groups. A study using quantitative MRS to assess absolute quantities of metabolites as opposed to ratios, found lower NAA levels in PSP and MSA compared to PD and healthy controls. [136] A study exploring MRS of the cerebellum found reduced NAA/Cr ratio in PSP compared to PD and controls, and in MSA of cerebellar subtype (MSA-C) compared to all other groups.[137] A recent study found lower NAA/Cr in the substantia nigra in PD than in controls and a negative correlation between these levels and UPDRS score.[138] Another study found decreased GABA levels in the basal ganglia of PD patients compared to controls.[139] These findings suggest that different metabolic changes are present in parkinsonism, and that these vary between the different parkinsonian disorders. While not used clinically at present, further development of these techniques could prove useful in the diagnostics of parkinsonism.

Ultra high-field MRI

By increasing the field strength in MRI beyond the typically used 1.5 and 3.0 Tesla (T), it is possible to achieve higher signal-to-noise ratio and increased T_2*-effects. For research purposes there have been studies using 7 T, which provides increased spatial/temporal resolution and contrast, allowing better depiction of smaller structures such as the substantia nigra.[140] The importance of these studies are highlighted by the fact that 7 T was approved for clinical use for neurological and musculoskeletal application in Europe and the United States in 2017. Using 7 T T_2*-weighted MRI, it is possible to visualize anatomical alterations of the substantia nigra in PD patients.[141] A 7 T study on 30 patients with PD, 7 with MSA, 3 with PSP and 26 healthy controls using T_2*-weighted imaging found bilateral nigral hyperintensity in all healthy controls, and loss of the hyperintensity in all patients with PD, all patients with PSP and in all but one of the patients with MSA.[142] Another group investigated the consistency of the nigrosome-1 visibility in 46 healthy controls.[143] They found that nigrosome 1 was at least unilaterally visible in 93% of the cases. Another study assessing the same question in 13 healthy adults found the sign present in 81% of the cases.[144] It has been shown that using 7 T imaging, a better separation of the subthalamic nucleus from the substantia nigra is possible.[145] Using 7 T imaging and volume analysis of the subthalamic nucleus, a good diagnostic separation between PSP and healthy controls (ROC AUC = 0.89) can be achieved.[146] Ultra high-field imaging may also assist in surgical planning for DBS of the subthalamic nucleus[147] and the internal globus pallidus.[148] A study using 7 T proton MRS describes elevated GABA levels in pons and putamen in PD compared to healthy controls.[149] This latter finding is contradictory to the newer study mentioned above where lower levels of GABA was seen in the putamen using 3 T MRS.[139]

1.6 SINGLE-PHOTON EMISSION COMPUTED TOMOGRAPHY AND POSITRON EMISSION TOMOGRAPHY IN PARKINSONIAN DISORDERS

There are several nuclear medicine imaging methods used to assess patients with parkinsonian symptoms, to aid in the diagnostics. The most commonly used are the SPECT and PET methods, where a radiotracer ligand binds to a target of interest and allows imaging of it.

1.6.1 ^{123}I-ioflupane single-photon emission computed tomography

In the investigation of parkinsonism, ^{123}I-ioflupane single-photon emission computed tomography (DaTSCAN™) can often be a useful ancillary tool. By binding of this ligand to the dopamine transporter, it is possible to image the presynaptic dopaminergic system.[150] It can be useful when facing tremors, to differentiate PD from essential tremor.[34] An example of such imaging is shown in *Figure 12*.

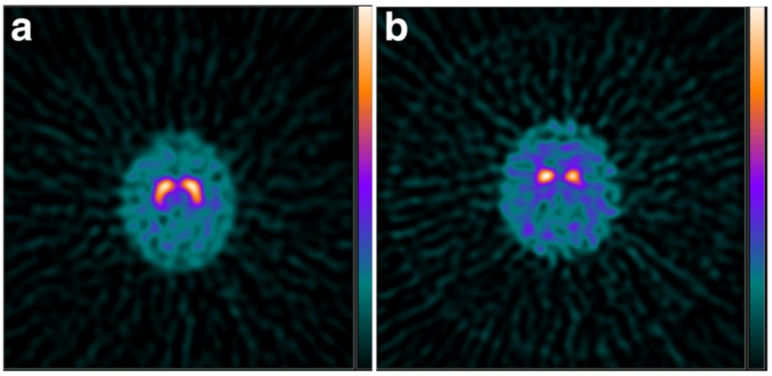

Figure 12: ^{123}I-ioflupane single-photon emission computed tomography in a patient with essential tremor **(A)**, and a patient with Parkinson's disease **(B)**. Image adapted from Nichols et al. (2018)[151]. Under creative commons license (https://creativecommons.org/licenses/by/4.0/).

It may also be used more broadly to differentiate neurodegenerative from non-degenerative causes of parkinsonism.[152] However, it does not allow reliable separation on the individual level between the different parkinsonian disorders.[34]

1.6.2 ^{18}F-fluorodeoxyglucose positron emission tomography

Using FDG-PET, it is possible to image the cerebral glucose metabolism, and reveal regional changes.[34] An example of an FDG-PET examination is shown in *Figure 13*.

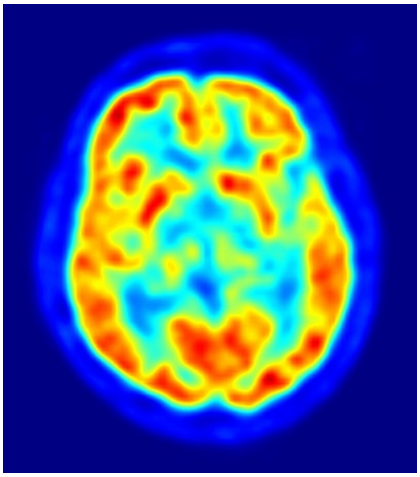

Figure 13: ^{18}F-fluorodeoxyglucose positron emission tomography (FDG-PET) in 56-year old man. Image is public domain.

Typical patterns can often be seen in PD, PSP, MSA and CBD.[150] In PD, changes with increased activity in basal ganglia areas, pons and cerebellum as well as reductions in certain cortical areas have been reported.[152] In PSP, decreased metabolism in basal ganglia, brainstem and frontal cortical areas can be seen.[150] In MSA, the typical picture is that of reduced metabolism in areas such as the putamen and cerebellum.[34,152] CBD typically shows a lateralized decrease in metabolism in the basal ganglia and cortical areas contralateral to the clinically most affected side.[150] Several studies have shown high sensitivity and specificity in separating PD from atypical parkinsonism as well as separating between the different atypical parkinsonian disorders.[34]

2 AIMS

The overall aim of this thesis was to evaluate new MRI techniques and their application in parkinsonian disorders. This application includes both the diagnostic capabilities as well as the potential knowledge they can bring regarding the different underlying disease pathologies.

The specific research aims for the studies were:

- To investigate pathological brain iron accumulation between parkinsonian disorders (**Studies I & II**)

- To assess whether different patterns of brain iron accumulation as measured by QSM can be used for diagnostic separation between parkinsonian disorders. (**Studies I & II**)

- To evaluate an automated approach to brainstem segmentation in PD, PSP and MSA. (**Study III**)

- To compare automated brainstem segmentation with manual brainstem metrics in the diagnostics of parkinsonism. (**Study III**)

- To investigate the newly developed T_1/T_2-weighted ratio in PD and atypical parkinsonian syndromes, and to assess whether underlying pathology causes different patterns of signal change allowing diagnostic separation. (**Study IV**)

3 MATERIAL AND METHODS

3.1 ETHICAL CONSIDERATIONS

The Regional Ethical Review Board in Stockholm approved Study I, III and IV (registration number 2015/1607-31). The Regional Ethical Review Board in Lund approved Study II and IV (registration numbers 290/2008, 557/2008 and 2013/202).

For the retrospective Study I and III, as well as the retrospective cohort in Study IV, informed consent was waived in the groups with disease, in accordance with approval from the Regional Ethical Review Board in Stockholm. This waiving of consent was based on the retrospective nature of these studies, age of data, full anonymization and the fact that a large proportion of the participants were deceased at the time of study initiation. For the healthy controls in Study I, written informed consent was obtained. For Study II and the prospective cohort in Study IV, written informed consent was obtained from all participants.

3.2 PROCEDURES AND PARTICIPANTS

This thesis is based on two patient cohorts; the retrospective Karolinska Imaging in Movement Disorders (KIMOVE) cohort and the prospective Biomarkers For Identifying Neurodegenerative Disorders Early and Reliably (BioFINDER) cohort (www.biofinder.se).

Retrospective KIMOVE cohort – included in this cohort are patients who received a diagnosis of PD, PSP or MSA at the Neurology Clinic, Karolinska University Hospital, Huddinge, Sweden, between the years 2001 to 2015, and underwent a routine MRI examination as part of the clinical investigation of their disease. Additionally, 14 healthy controls were recruited, matched by age and sex.

Prospective BioFINDER cohort – included in this cohort are patients and controls and recruited from the Neurology Clinic, Skåne University Hospital, Sweden, between 2008 and 2016. The participants were assessed by a medical doctor with experience in movement disorders, including neurological examination and different rating scales.

Study I included participants from the retrospective KIMOVE cohort who underwent SWI as part of their routine clinical investigation for parkinsonian symptoms. A total of 102 participants were included, with 62 PD, 15 PSP, 11 MSA and 14 healthy controls.

Study II included participants from the prospective BioFINDER cohort who underwent SWI during their research MRI scan. A total of 199 participants were included; 134 PD, 11 PSP, 10 MSA and 44 healthy controls.

Study III included participants from the KIMOVE cohort who had undergone 3D high resolution T_1-weighted imaging. 196 participants were included, with 140 PD, 29 PSP and 27 MSA.

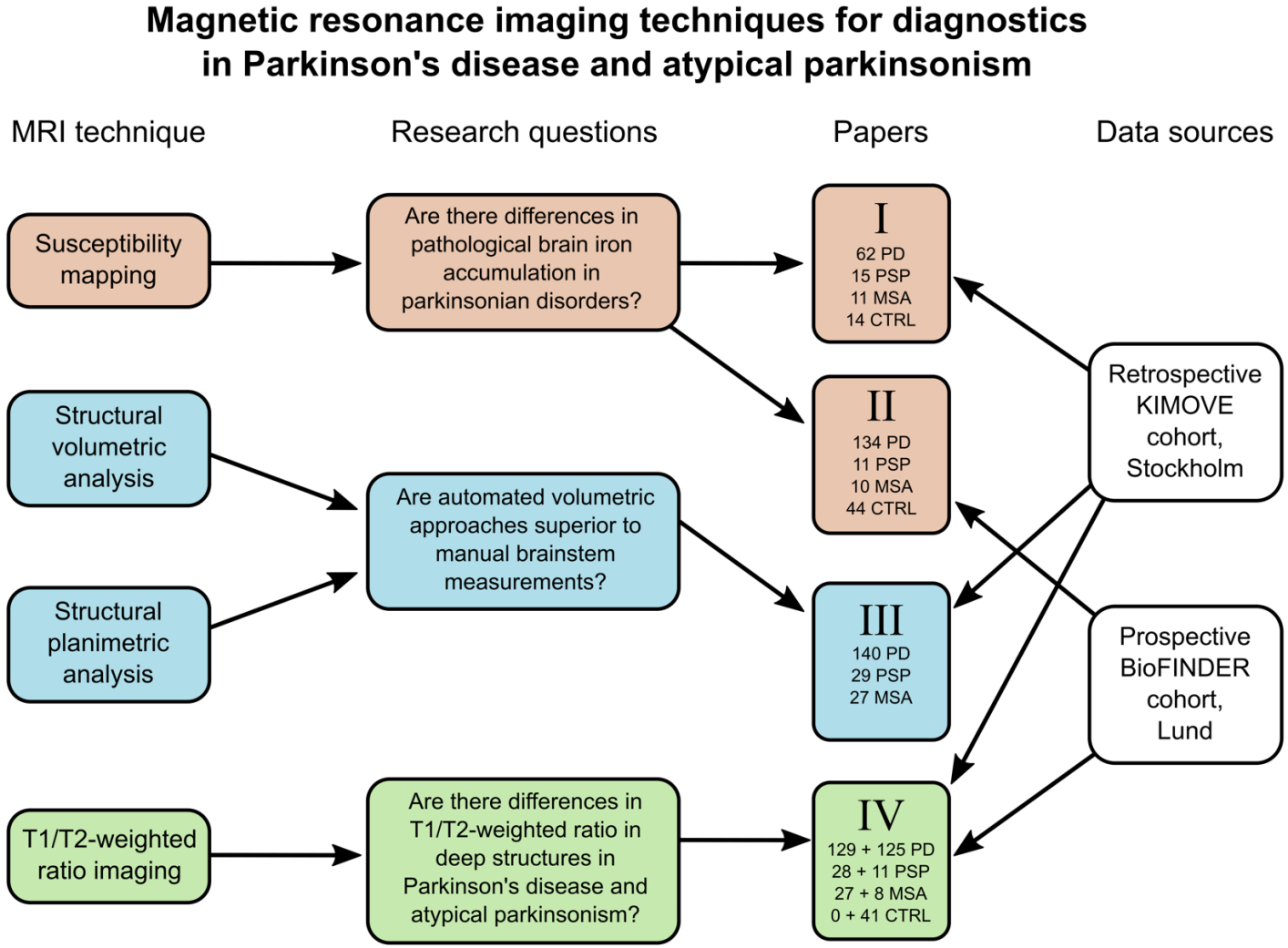

Figure 14. Schematic representation of research questions in relation MRI techniques, scientific papers and data sources.

Study IV included patients from both the retrospective KIMOVE cohort and the prospective BioFINDER cohort who had undergone both T_1-weighted and T_2-weighted MRI. From the KIMOVE cohort, 184 participants were included; 129 PD, 28 PSP and 27 MSA. From the BioFINDER cohort, 185 participants were included; 125 PD, 11 PSP, 8 MSA and 41 healthy controls.

A schematic representation of the research questions in relation to data sources/participants and MRI techniques is shown in *Figure 14*.

3.3 CLINICAL EVALUATIONS

The patients from the KIMOVE cohort were reviewed by assessing patient charts. From these, Hoehn & Yahr grading was assessed retrospectively. For patients with PSP, the presence of vertical gaze palsy at time of MRI investigation was noted. The length of clinical follow-up was also registered, as well as changed status of the presence of vertical gaze palsy in the patients with PSP.

Stage	Hoehn & Yahr scale[19]
1	Unilateral involvement only, usually with minimal or no functional disability
2	Bilateral or midline involvement, without impairment of balance
3	Bilateral disease: mild to moderate disability with impaired postural reflexes; physically independent
4	Severely disabling disease; still able to walk or stand unassisted
5	Confinement to bed or wheelchair unless aided

Table 2, reiterated. Hoehn and Yahr scale.

The patients from the BioFINDER cohort were assessed by a medical doctor with experience in movement disorders. The study includes follow-up for up to 10 years, with annual visits including (but not limited to) UPDRS, Mini-mental state examination (MMSE) and Hoehn & Yahr grading. MRI examinations are performed biannually. Blood tests as well as CSF examinations were also performed as part of the full BioFINDER study. For **Study II** and **Study IV**, the visit with first available MRIs of the relevant types described above was used, with clinical evaluations of UPDRS part III, MMSE and Hoehn & Yahr staging recorded.

3.4 BRAIN IMAGING

Study I. Acquisition parameters for the MRI sequences used on three Siemens MRI scanners, between the years 2008 and 2015, for the SWI in Study I are listed in *Table 7*.

Siemens MRI Scanner	Field strength (T)	Slice thickness (mm)	In-plane resolution (mm)	Flip angle (°)	Repetition time (ms)	Echo time (ms)
Trio	3	1.6	0.7 x 0.7	15	28	20
Avanto	1.5	2.0	0.9 x 0.9	20	49	40
Aera	1.5	1.6	0.9 x 0.9	20	49	40
Aera	1.5	2.0	0.9 x 0.9	20	49	40

Table 7. Acquisition parameters for SWI sequences in Study I.

Study II. For Study II, SWI as well as 3D magnetization-prepared rapid acquisition gradient echo (MPRAGE) T_1-weighted imaging were acquired using a 3 T Siemens Skyra scanner. The parameters are shown in *Table 8*.

Sequence	Slice thickness (mm)	In-plane resolution (mm)	Flip angle (°)	Repetition time (ms)	Echo time (ms)	Inversion time (ms)
SWI	1.5	0.86 x 0.86	15	27	20	N/A
T_1-weighted MPRAGE	1.0	1.0 x 1.0	9	1900	2.54	900

Table 8. Acquisition parameters for MPRAGE and SWI sequences in Study II.

Study III. For Study III, MPRAGE T_1-weighted images were acquired between 2001 and 2015 using different acquisition protocol variants, with 1.5 T (Aera, Avanto and Symphony) and 3 T (Trio) Siemens scanners. For the 1.5 T scanners, the following acquisition parameters were used: slice thickness 1.0 mm to 1.6 mm, in-plane resolution 0.4 x 0.4 mm to 1.3 x 1.3 mm, repetition time 1110 ms to 2400 ms, echo time 2.41 ms to 4.38 ms, inversion time 790 ms to 1100 ms, flip angle 8° to 15°. For the 3 T Trio scanner, the following acquisition parameters were used: slice thickness 0.9 mm to 1.5 mm, in-plane resolution 0.9 x 0.9 mm to 1.0 x 1.0 mm, repetition time 1900 ms to 2300 ms, echo time 2.57 ms to 3.42 ms, inversion time 900 ms, flip angle 9°. More details regarding the different protocol variants can be found in Paper III, *supplementary table 1*.

Study IV. For Study IV, participants from the KIMOVE and BioFINDER cohorts who had undergone MPRAGE T_1-weighted imaging as well as T_2-weighted imaging were included. The acquisition parameters are summarized in *Table 9*.

Cohort	MRI Sequence	Field strength (T)	Slice thickness (mm)	In-plane resolution (mm)	Flip angle (°)	Repetition time (ms)	Echo time (ms)	Inversion time (ms)
KIMOVE	T_1-weighted MPRAGE	1.5	1.0–1.6	0.4 x 0.4 – 1.3 x 1.3	8–15	1110– 2400	2.29–4.38	300–1100
	T_1-weighted MPRAGE	3	0.9–1.5	0.9 x 0.9 – 1.0 x 1.0	9	1900–2300	2.57–3.39	900
	T_2-weighted spin-echo	1.5	3.0–5.0	0.4 x 0.4 – 1.0 x 1.0	150–180	2500–5474	82–122	N/A
	T_2-weighted spin-echo	3	3.0–4.0	0.3 x 0.3 – 1.0 x 1.0	120–150	5530–7150	76–111	N/A

Cohort	MRI Sequence	Field strength (T)	Slice thickness (mm)	In-plane resolution (mm)	Flip angle (°)	Repetition time (ms)	Echo time (ms)	Inversion time (ms)
BioFINDER	T_1-weighted MPRAGE	3	1.0	1.0 x 1.0	9	1900	2.54	900
	T_2-weighted spin-echo	3	5.0	0.4 x 0.4	150	6000	99	N/A

Table 9. Acquisition parameters for T_1-weighted MPRAGE and T_2-weighted spin-echo sequences for Study IV. For the KIMOVE cohort, 4 different Siemens scanners were used; Aera (1.5 T), Avanto (1.5 T), Symphony (1.5 T) and Trio (3 T). For the BioFINDER cohort, a Siemens Skyra (3 T) was used.

3.5 IMAGE PROCESSING

Study I

Susceptibility processing: High-pass filtered phase and magnitude images were acquired. Brain extraction was performed on the magnitude images using FMRIb Software Library Brain Extraction Tool (FSL BET).[153] This mask was then further three-dimensionally eroded and used together with the high-pass filtered phase in the QSM processing. The high-pass filtered phase was unwrapped using a Laplacian phase unwrapping algorithm and variable-kernel sophisticated harmonic artifact reduction on phase data (V-SHARP) was applied for background phase removal.[71] Finally, the improved sparse linear equation and least-squares method (iLSQR) was used to create the final susceptibility maps.[73]

Manual segmentation: The susceptibility maps were manually segmented by myself, using ITK-SNAP software.[154] The two most representative and artefact free slices were chosen from each region. The putamen, globus pallidus, substantia nigra and the red nucleus were segmented, and susceptibility values extracted. The susceptibility values were normalized using CSF in the lateral ventricles. The processing stream is illustrated in *Figure 15*.

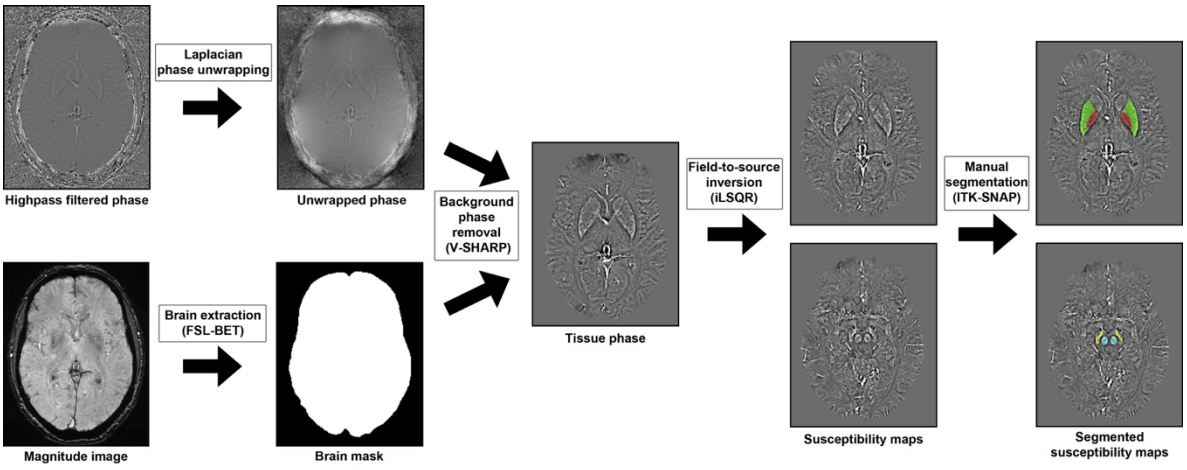

Figure 15. Schematic illustration of the processing in Study I. Figure from Sjöström et al. (2017), supplementary material.[85]

Study II

Susceptibility processing: The susceptibility processing for Study II follows the same pipeline as described above for Study I.

Manual segmentation: The substantia nigra, the red nucleus and the cerebellar dentate nucleus were segmented by a neurologist, Yulia Surova. Susceptibility data from these regions were extracted. The manual segmentation is visualized in *Figure 16B-C*.

Automated segmentation: FSL FIRST was used to automatically segment globus pallidus and putamen from the T_1-weighted MPRAGE images.[155] The magnitude image was then registered to the T_1-weighted image using FSL FLIRT,[156] and this transformation subsequently applied to the susceptibility map. These regions of interest were also subjected to minor manual adjustments using ITK-SNAP by myself, to ensure goodness of fit. The automated segmentation is shown in *Figure 16A*.

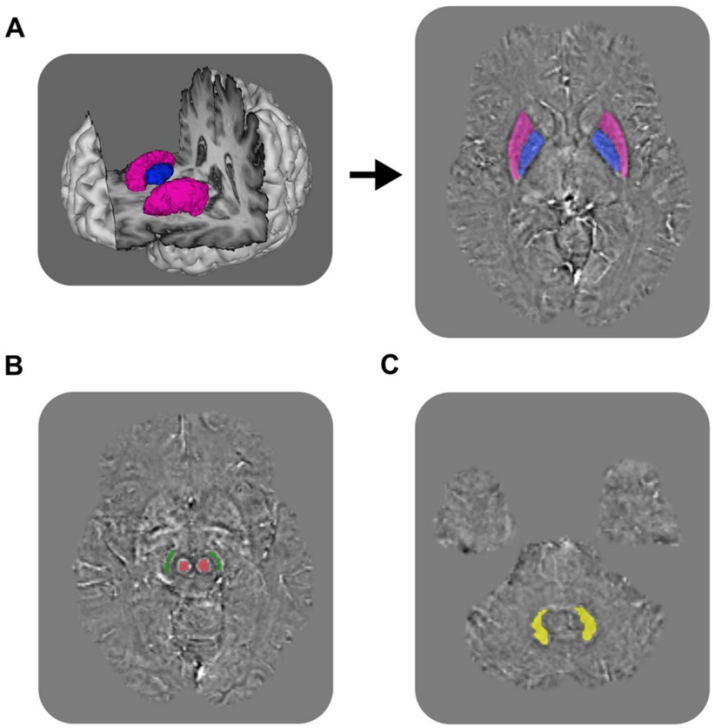

Figure 16. Illustration of automated segmentation using FSL FIRST (**A**) and manual segmentations (**B-C**) for Study II. Figure from Sjöström et al. (2019).[157]

Study III

Automated segmentation: FreeSurfer was used to automatically segment brainstem substructures; the midbrain, superior cerebellar peduncles, pons and medulla oblongata.[158,159] The volumes in all patient groups were subsequently normalized using the slope of the relation between the respective structure and the total intracranial volume in the group with PD, since this group was the largest and expected to have the least degree of atrophy compared to PSP and MSA.

Study IV

T_1/T_2-weighted ratio: T_1/T_2-weighted ratio images were created using the MRTool toolbox[160,161] running in Statistical Parametric Mapping (SPM) software.[162] To summarize, the histograms of the T_1-weighted and T_2-weighted images were normalized using a non-linear matching to CSF, soft tissues and bone. The images were then registered together and a T_1/T_2-weighted ratio was calculated. The ratio images were further normalized using the mean white matter ratio levels of the respective participants.

Automated segmentation: FreeSurfer was used to automatically segment brain structures from the T_1-weighted MPRAGE images, including tissue types and subcortical structures.

Registration to Montreal Neurological Institute (MNI) space and atlas-based region extraction: T_1-weighted volume was non-linearly registered to the MNI152 template using Advanced Normalization Tools (ANTs).[163,164] This transform was then applied to the T_1/T_2-weighted ratio volumes. For data extraction from the subthalamic nucleus, substantia nigra and the red nucleus, respective FSL MIST atlas regions in MNI space were used, and further three-dimensionally eroded to minimize potential partial volume effects with neighboring tissue.

3.6 RADIOLOGICAL EVALUATIONS

Study III

I manually measured planimetric MP-ratio, MRPI and MRPI 2.0 on all subjects. A random subset of 25% of the participants were remeasured by myself and also measured by a specialist in neuroradiology, Farouk Hashim, to calculate intra-rater and inter-rater reliabilities using intraclass correlation coefficients (ICC). The manual measurements are shown in *Figure 17*.

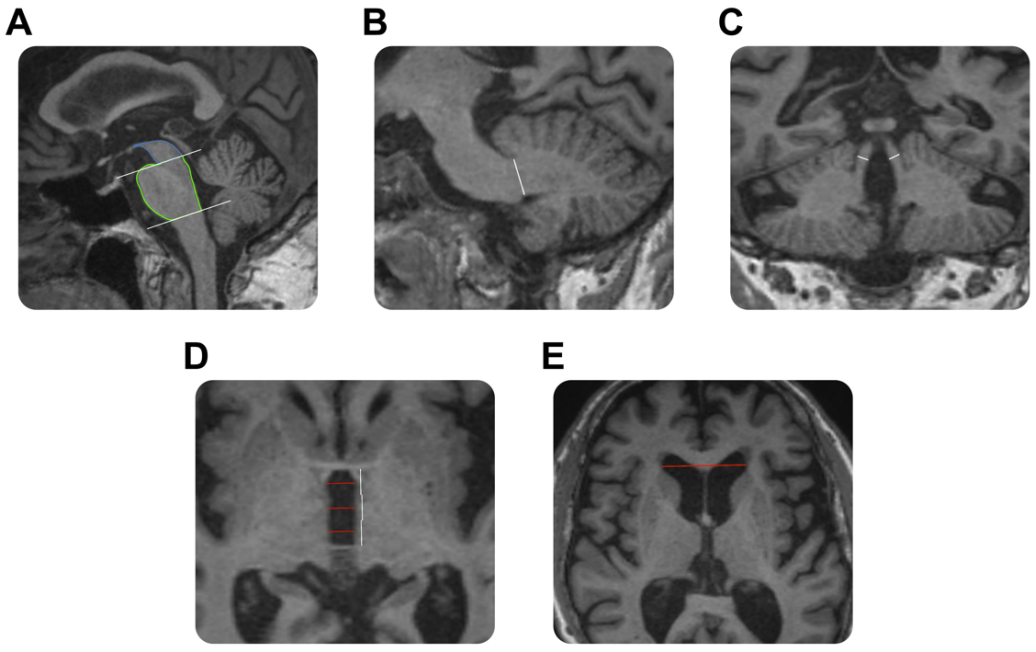

Figure 17. Manual segmentation of midbrain and pons are (**A**), middle cerebellar peduncle width (**B**), width of superior cerebellar peduncles (**C**), width of the third ventricle (**D**) and the width of the frontal horns (**E**)

3.7 STATISTICAL ANALYSIS

SPSS 23.0 (IBM, USA) was used for Study I, SPSS 24.0 for Study II, and SPSS 26.0 for Study III and Study IV. Normality was assessed using Shapiro-Wilk test for Study I, Study III and Study IV. Normality was assessed using Kolmogorov-Smirnov for Study II. Group comparisons were performed using one-way ANOVA or independent samples Kruskal-Wallis test, and pairwise comparisons were performed using independent samples t-test or Mann-Whitney u-test. For Study I and Study II, two-way ANCOVA and one-way ANCOVA was also used to asses group differences, respectively. In Study I, ordinal logistic regression was used to assess effects of increased susceptibility in different regions on the Hoehn & Yahr score in patients with PD. For Study II, Pearson partial correlation was used to assess correlations between variables. Differences in distribution between groups were tested using Pearson's χ^2 test. Diagnostic accuracy was investigated using area under receiver operating characteristic curves (ROC AUC). Diagnostic performance in Study III was also further assessed using McNemar test. Pairwise comparisons in Study I and III were corrected for multiple comparisons using the False Discovery Rate procedure as described by Benjamini and Hochberg.[165] Pairwise comparisons in Study III were corrected for multiple comparison using the Bonferroni method. Intra- and inter-rater reliabilities for Study III were calculated using intraclass correlation coefficients (ICC), with a two-way mixed model for absolute agreement on single measures. Intra- and inter-scanner reliabilities in Study III were also assessed by calculating coefficients of variation (CoV). Statistical significance was defined as an α-level of 0.05, after correction for multiple comparisons where such was performed.

4 RESULTS

4.1 STUDY I

Demographics of study participants

88 patients who had undergone SWI as part of routine clinical investigation as well as 14 age- and sex-matched controls were included in this study. The demographics of the participants are shown in *Table 10*.

	N	Mean age (Y)	Gender (F/M)	Mean symptom Duration (Y)	Associated features at time of MRI	DAT SPECT positive/total examined (N/N)
PD	62	65.2 ± 10.5	19/43	4.7 ± 4.4	Hoehn & Yahr Stage 1/2/3/4/5 (N): 17/24/16/5/0	46/46
PSP	15	69.1 ± 6.0	3/12	2.8 ± 1.0	Hoehn & Yahr Stage 1/2/3/4/5 (N): 0/1/7/5/2 Postural instability (93.3%, n=14) Vertical gaze palsy (80.0%, n=12) DOPA-responsive (0%, n=0)	8/8
MSA	11	68.9 ± 13.1	5/6	3.6 ± 2.7	Hoehn & Yahr Stage 1/2/3/4/5 (N): 0/1/0/8/2 Orthostatism (36.4%, n=4) Incontinence (54.5%, n=6) DOPA-responsive (27.3%, n=3)	3/3
Controls	14	63.5 ± 5.3	5/9			

Table 10. Demographics of the participants in Study I. Abbreviations: F = female; M = male, DAT = dopamine transporter.

Reliability and reproducibility

To investigate reproducibility, one of the healthy controls was examined on all three different MRI scanners. No significant differences in susceptibility were found in any of the regions of interest between the scanners. Susceptibility differences in all regions between the scanners were also investigated within the different groups using one-way ANOVA, and no such differences were found.

Validity of QSM measurements

Susceptibility values in 8 different regions in the healthy controls in our study were compared to known iron concentrations in these regions, as measured by Langkammer et al. in a post-mortem validation study.[76] A strong correlation was found, with $r = 0.96$, $p < 0.001$.

Group differences

Differences in susceptibility between the groups are shown in *Figure 18*. Notably, higher susceptibility was seen in the red nucleus and globus pallidus in PSP compared to all other groups. Higher susceptibility was also found in the substantia nigra in all patient groups compared to healthy controls.

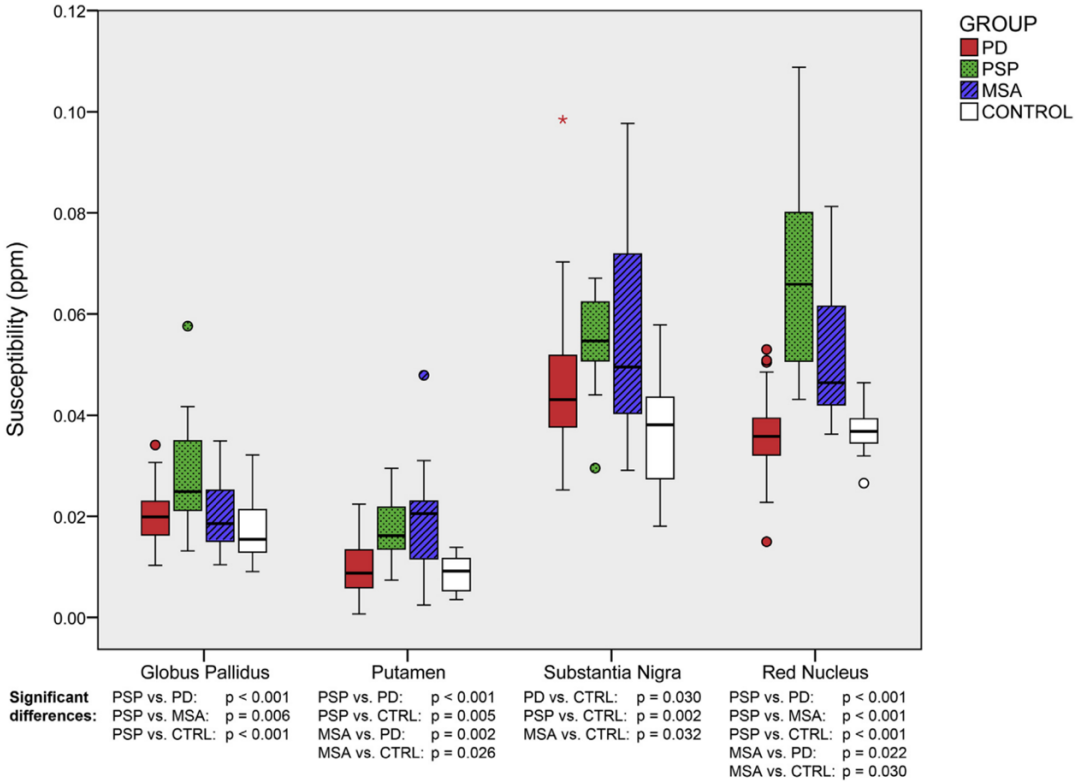

Figure 18. Susceptibility levels in the regions of interest. Significant differences are shown below the plot. Abbreviations: CTRL = control; ppm = parts per million. Figure from Sjöström et al. (2017).[85]

Diagnostic performance

The highest degrees of diagnostic separation were found in the red nucleus for separating PSP from PD (AUC 0.97), MSA from PD (AUC 0.86), PSP from MSA (AUC 0.75), PSP from controls (AUC 0.98) and MSA from controls (AUC 0.86). For separating PD from controls, best diagnostic performance was seen in the substantia nigra with AUC 0.71.

Features associated with odds of having higher Hoehn and Yahr score in the PD group

Using ordinal logistic regression, features including age, gender, disease duration and susceptibility in the globus pallidus, putamen, substantia nigra and the red nucleus were entered into a model to investigate associations with odds of having higher Hoehn and Yahr scores. An increase in age and disease duration were found to be associated with increased odds of having a higher Hoehn and Yahr score ($p = 0.012$ and $p = 0.002$ respectively). Increased susceptibility in the putamen was associated with increased odds of having a higher Hoehn and Yahr score ($p = 0.040$).

4.2 STUDY II

Demographics of study participants

For this susceptibility mapping study, 199 participants from the BioFINDER cohort were included; 134 PD, 11 PSP, 10 MSA and 44 healthy controls. The demographics of the study participants are shown in Table 11.

Demographic variables	PD	PSP	MSA	Controls
Participants, N	134	11	10	44
Age at clinical visit, y, mean ± SD	66.9 ± 9.6	72.2 ± 5.5	63.4 ± 11.4	66.0 ± 7.8
Gender, F/M	48/86	6/5	6/4	26/18
Disease duration, y, mean ± SD	6.0 ± 5.0	5.5 ± 2.8	4.7 ± 2.2	N/A
UPDRS-III, score, median (IQR)	13.5 (7-22.25)	36 (28-58)	38.5 (24-52.5)	1 (0-2)
Hoehn & Yahr, score, median (IQR)	2 (1-2.5)	4 (3-5)	4 (3-5)	0 (0-0)
MMSE, score, median (IQR)	28 (27-29)	27 (19-28)	29 (26.75-29)	29 (28-30)
Dementia, N	18	4	0	0

Table 11. Demographics of participants in Study II. Abbreviations: IQR = interquartile range.

Group differences

Susceptibility levels and their distribution between the groups are shown in *Figure 19*.

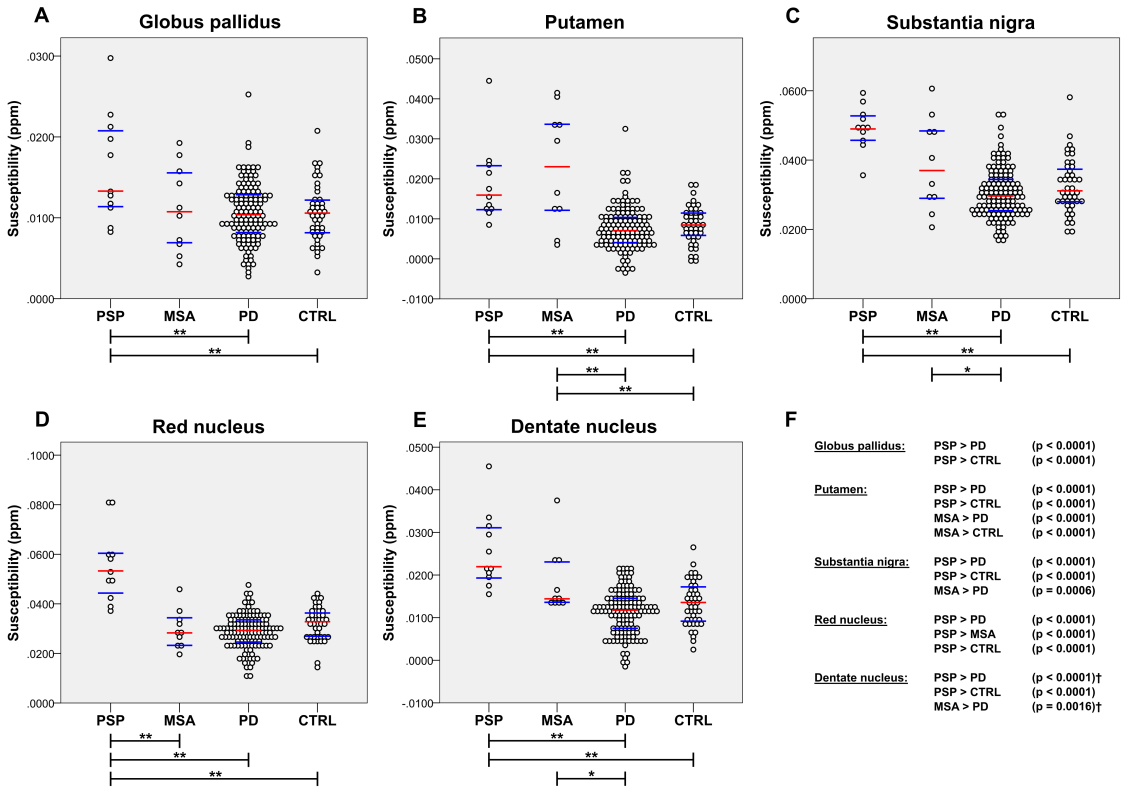

Figure 19. Susceptibility levels in the different groups. Red line denotes median and blue lines represent the interquartile range. Dagger (†) indicates the use of Mann-Whitney U-test due to non-normality of data. Significant differences are shown beneath respective plots. One asterisk (*) represents a p-value of less than the Bonferroni corrected α-level of 0.0017, two asterisks (**) represent p < 0.0001. Figure from Sjöström et al. (2019).[157]

There is a marked increase in susceptibility in the red nucleus in PSP compared to all other groups (all p-values < 0.0001). There was also an increased susceptibility in globus pallidus in PSP compared to PD and controls (both p-values < 0.0001). Susceptibility in the putamen was increased in PSP and MSA compared to PD and healthy controls (all p-values < 0.0001). The dentate nucleus also exhibited elevated susceptibility in PSP compared to PD and controls (both p-values < 0.0001), and in MSA compared to PD (p = 0.0016).

Diagnostic performance

ROC curves were used to investigate diagnostic performance in separating the groups using susceptibility levels from the different regions. As seen in *Figure 20*, the highest AUC for separating PSP from PD, MSA and controls was found in the red nucleus, with respective AUCs 0.98, 0.96 and 0.96. There was also excellent diagnostic separation between PSP and PD in the putamen, substantia nigra and the dentate nucleus. For separation between PSP and controls, excellent performance was also seen in the substantia nigra (AUC 0.95) and in the dentate nucleus (AUC 0.92)

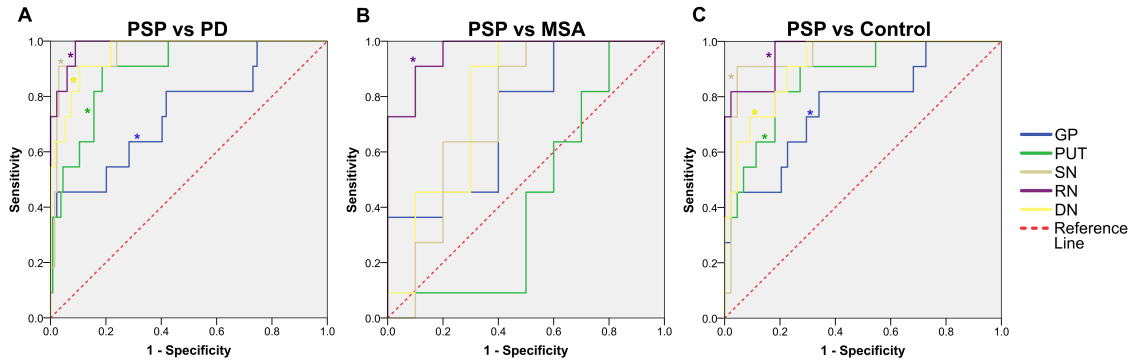

ROI	AUC	Sens. %	Spec. %
GP	0.74 (0.57-0.92)	81.8	58.2
PUT	0.90 (0.82-0.98)	90.9	81.3
SN	0.96 (0.92-1.00)	90.9	97.0
RN	0.98 (0.96-1.00)	100	91.0
DN	0.96 (0.91-1.00)	90.9	89.6

ROI	AUC	Sens. %	Spec. %
GP	0.73 (0.50-0.95)	81.8	60.0
PUT	0.56† (0.29-0.84)	50.0†	90.9†
SN	0.75 (0.51-0.98)	90.9	60.0
RN	0.96 (0.90-1.00)	90.9	90.0
DN	0.79 (0.57-1.00)	90.9	70.0

ROI	AUC	Sens. %	Spec. %
GP	0.77 (0.60-0.94)	81.8	65.9
PUT	0.87 (0.76-0.98)	81.8	81.8
SN	0.95 (0.88-1.00)	90.9	95.5
RN	0.96 (0.92-1.00)	100	81.8
DN	0.92 (0.84-0.99)	90.9	77.3

Figure 20. ROC curves depicting the diagnostic separation between PSP and the other groups. Dagger (†) indicates that the sensitivities and specificities are for the reverse comparison. Abbreviations: DN = dentate nucleus; GP = globus pallidus; PUT = putamen; RN = red nucleus; SN = substantia nigra. Figure from Sjöström et al. (2019).[157]

For MSA, good separation from PD and controls was seen using putaminal susceptibility (AUC 0.82 and AUC 0.80, respectively). Using dentate nucleus susceptibility, good diagnostic separation between MSA and PD was also seen (AUC 0.80). By combining all regions of interest in a discriminant analysis 97.2% of cases were correctly classified in PSP vs PD. Using the same method for separating PSP and MSA, 90.5% of cases were correctly classified.

Correlations between susceptibility, clinical scores and disease duration in the PD group

In the PD group, we found a significant correlation between putaminal susceptibility levels and UPDRS-III (r = 0.213, p = 0.015). There were also significant correlations between disease duration and susceptibility in the globus pallidus (r = 0.198, p = 0.023) and substantia nigra (r = 0.251, p = 0.004).

4.3 STUDY III

Demographics of the study participants

In this retrospective study, 196 participants in the KIMOVE cohort who had undergone T_1-weighted MPRAGE imaging as part of routine clinical investigation were included. The demographics of the study participants are shown in *Table 12*.

	N	Mean age, Y±SD	Gender Female/Male, N	Mean symptom Duration, Y±SD	Hoehn & Yahr Stage 1/2/3/4/5, N	MRI field strength 1.5T/3T, N/N	VSGP at time of MRI
PD	140	65.3 ± 9.8	48/92	5.3 ± 5.0	32/64/25/19/0	95/45	-
PSP	29	69.1 ± 6.7	11/18	3.1 ± 1.8	1/2/13/10/3	23/6	15/29
MSA	27	68.6 ± 8.5	14/13	2.4 ± 1.5	2/4/3/17/1	20/7	-

Table 12. Demographics of the participants in Study III. Abbreviations: VSGP = vertical supranuclear gaze palsy.

Reliability assessments

Volumetric reliability: To assess intra- and inter-scanner reliabilities, 3 healthy controls were examined using 3 of the different MRI scanners, with 2 examinations in each scanner. Brainstem substructures were segmented, and intra- and inter-scanner intraclass correlation coefficients were calculated. ICC-values showed excellent intra-scanner reliabilities for the midbrain (ICC 0.95), pons (ICC 1.00) and medulla oblongata (ICC 0.97). In the superior cerebellar peduncles (SCP), a lower intra-scanner ICC was seen at 0.53. Examining inter-scanner ICC, we found excellent reliability for the midbrain (ICC 0.91), pons (ICC 0.99) and medulla oblongata (ICC 0.93). A lower inter-scanner ICC was seen in the SCP (ICC 0.27).

Planimetric reliability: A randomly selected subset of 25% of the participants were re-measured by the original rater (Henrik Sjöström, a specialist in neurology) and measured by a second rater (Farouk Hashim, a specialist in neuroradiology) for calculation of reliability measures. Intra-rater reliability was found to be excellent for the manual scores; MP-ratio (ICC 0.96), MRPI (ICC 0.92) and MRPI 2.0 (ICC 0.97). Inter-rater ICC between the raters was excellent for MP-ratio (ICC 0.94), good for MRPI 1.0 (ICC 0.88) and excellent for MRPI 2.0 (ICC 0.93).

Pooling of data: No group differences were found regarding distribution across the four MRI scanners ($p = 0.167$), in field strength ($p = 0.424$), pixel spacing ($p = 0.719$) or slice thickness ($p = 0.705$). No differences in brainstem volumes depending on field strength were found in any of the groups. The data were hereafter combined for the remaining analyses.

Group comparisons of normalized brainstem volumes

Distribution of the normalized brainstem volumes are visualized in *Figure 21*. PSP exhibited lower volumes compared to PSP and MSA in the midbrain (both p-values < 0.001), SCP (p < 0.001 and p = 0.028, respectively) and the medulla oblongata (both p-values < 0.001). In PSP and MSA, lower pons volumes were seen compared to PD (both p-values < 0.001).

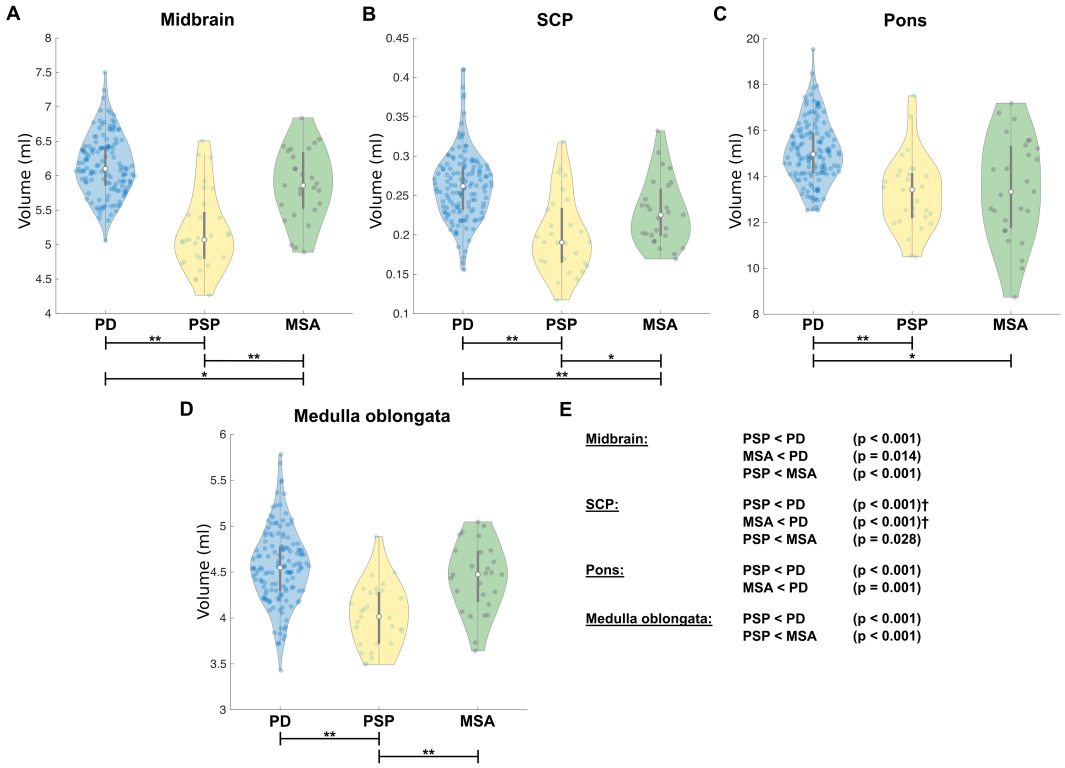

Figure 21. Normalized brainstem volumes in the different groups. One asterisk (*) indicates differences with p < 0.05 and two asterisks (**) indicated differences with p < 0.001, after correction for multiple comparisons using the False Discovery Rate procedure. Dagger (†) indicates the use of Mann-Whitney U-test due to non-normality of data.

Diagnostic performance

Midbrain and medulla oblongata volumes were the most successful brainstem volumes in separating PSP from PD (AUC 0.90 and 0.85, respectively) and PSP from MSA (AUC 0.80 for both volumes). Using the midbrain volume to separate PSP from PD, we found a sensitivity of 79% and a specificity of 89% at an optimal cut-off defined as the point on the ROC curve closest to the upper left corner. For separation between PSP and MSA, the volume with best diagnostic performance was also the midbrain, with a sensitivity of 76% and specificity of 78%. Composite variables were created, and the product of the midbrain and medulla oblongata volumes was excellent at separating PSP from PD (AUC 0.92) and at separating PSP from MSA (AUC 0.85). By comparing ROC AUC, we found that the midbrain volume showed significantly better diagnostic performance than MP-ratio (p = 0.019), MRPI (p = 0.007) and MRPI 2.0 (p = 0.021) in separating PSP from PD. We also found that the product of the midbrain and medulla oblongata volumes also had significantly better performance than MP-ratio (p = 0.005), MRPI (p = 0.003) and MRPI 2.0 (p = 0.007 respectively) in separating PSP from PD. The volumetric midbrain-to-pons ratio performed significantly worse than its planimetric counterpart. No volumetric variable had significantly better diagnostic performance than any of the planimetric variables in separating PSP from MSA.

4.4 STUDY IV

Demographics of study participants

This study on T_1/T_2-weighted ratio in parkinsonism included patients from both the retrospective KIMOVE cohort and the prospective BioFINDER cohort, who had undergone T_1-weighted and T_2-weighted MRI. 184 participants were included from the KIMOVE cohort, and 185 participants were included and from the BioFINDER cohort. Demographics of the included study participants are shown in *Table 13*.

KIMOVE cohort	N	Mean age, Y±SD	Gender Female/ Male, N	Mean symptom Duration, Y±SD	Hoehn & Yahr Stage 1/2/3/4/5,N	MRI field strength 1.5T/3T, N/N	VSGP at time of MRI, N
PD	129	65.3 ± 9.6	45/84	5.2 ± 4.9	31/58/23/17/0	89/40	-
PSP	28	68.8 ± 6.6	11/17	3.1 ± 1.7	1/2/13/9/3	22/6	17
MSA	27	68.6 ± 8.5	14/13	2.4 ± 1.5	2/4/3/17/1	20/7	-
BioFINDER cohort	**N**	**Median age, Y (IQR)**	**Gender Female/ Male, N**	**Mean symptom duration, Y±SD**	**Hoehn & Yahr Stage 0/1/2/3/4/5,N**	**UPDRS-3 Mean score±SD**	**MMSE Mean score±SD**
PD	125	68 (11.5)	46/79	6.1 ± 5.1	1/39/60/18/6/1	16.7 ± 11.8	27.2 ± 3.3
PSP	11	72 (5.0)	6/5	5.5 ± 2.9	0/0/0/6/2/3	35.7 ± 17.3	25.8 ± 4.3
MSA	8	62 (19.5)	5/3	5.0 ± 2.2	0/0/0/2/3/3	40.9 ± 18.5	27.9 ± 1.7
Controls	41	68 (12.5)	23/18	-	41/0/0/0/0/0	1.5 ± 2.4	28.6 ± 1.4

Table 13. Demographics of the participants in Study IV. Abbreviations: IQR = interquartile range; VSGP = vertical supranuclear gaze palsy.

Group comparisons

KIMOVE cohort

In the retrospective cohort, we found higher T_1/T_2-weighted ratio in PSP compared to PD in the caudate nucleus ($p = 0.015$) and putamen ($p = 0.001$), and lower ratio in the thalamus ($p = 0.015$), red nucleus ($p = 0.013$) and subthalamic nucleus ($p = 0.019$). We found lower T_1/T_2-weighted ratio in PSP compared to MSA in the thalamus ($p = 0.017$), red nucleus ($p = 0.006$) and subthalamic nucleus ($p = 0.012$). When comparing MSA to PD, a higher T_1/T_2-weighted ratio was seen in the caudate nucleus ($p = 0.028$) and putamen ($p = 0.011$). When comparing MSA to PD tendencies of higher pallidal T_1/T_2-weighted ratio in MSA and lower pontine ratio was also seen, with significant pairwise tests but non-significant ANOVA at the group level. T_1/T_2-weighted ratio values in the different regions in the KIMOVE cohort are visualized in *Figure 22*.

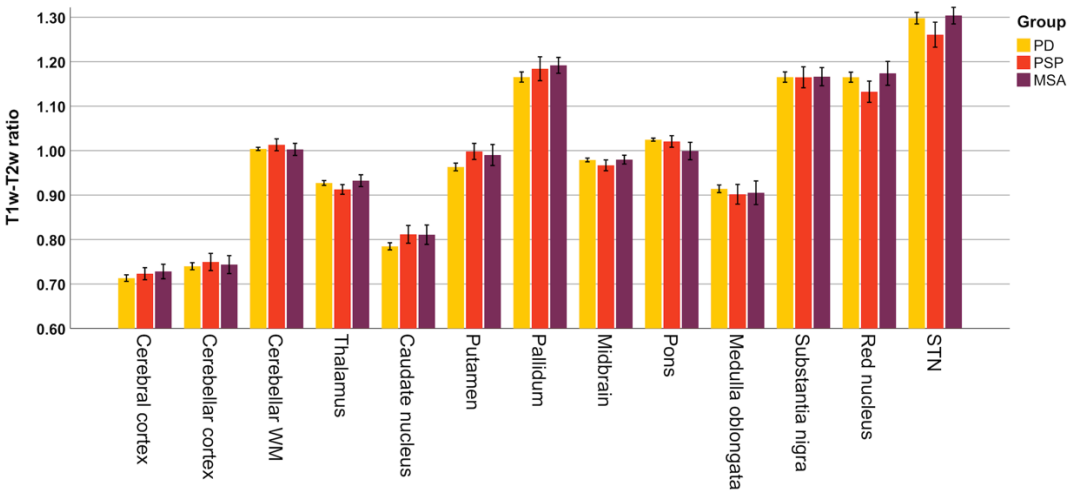

Figure 22. Mean T_1/T_2-weighted ratio in the different regions in the retrospective KIMOVE cohort. Error bars show 95% confidence intervals of the mean.

BioFINDER cohort

Regions displaying significant differences, with the addition of the substantia nigra and midbrain, were carried on for analysis in the prospective BioFINDER cohort. Here, we could validate the findings of lower T_1/T_2-weighted ratio in PSP compared to PD, MSA and controls in the red nucleus ($p = 0.006$, $p = 0.012$ and $p = 0.008$ respectively) and in the subthalamic nucleus ($p = 0.013$, $p = 0.033$ and $p = 0.047$ respectively). We also found lower ratio in the midbrain in PSP compared to PD ($p = 0.026$) and MSA ($p = 0.009$). There were also tendencies of higher T_1/T_2-weighted ratio in PD and MSA in the substantia nigra compared to controls, with significant pairwise tests but non-significant ANOVA in the group level analysis. In the same way, PSP showed tendencies of higher ratio in the caudate nucleus compared to controls, and MSA showed tendencies of higher pallidal T_1/T_2-weighted ratio compared to controls. T_1/T_2-weighted ratio values in the different regions in the BioFINDER cohort are shown in *Figure 23*. Significant p-values from the pairwise comparisons are visualized in *Figure 24*.

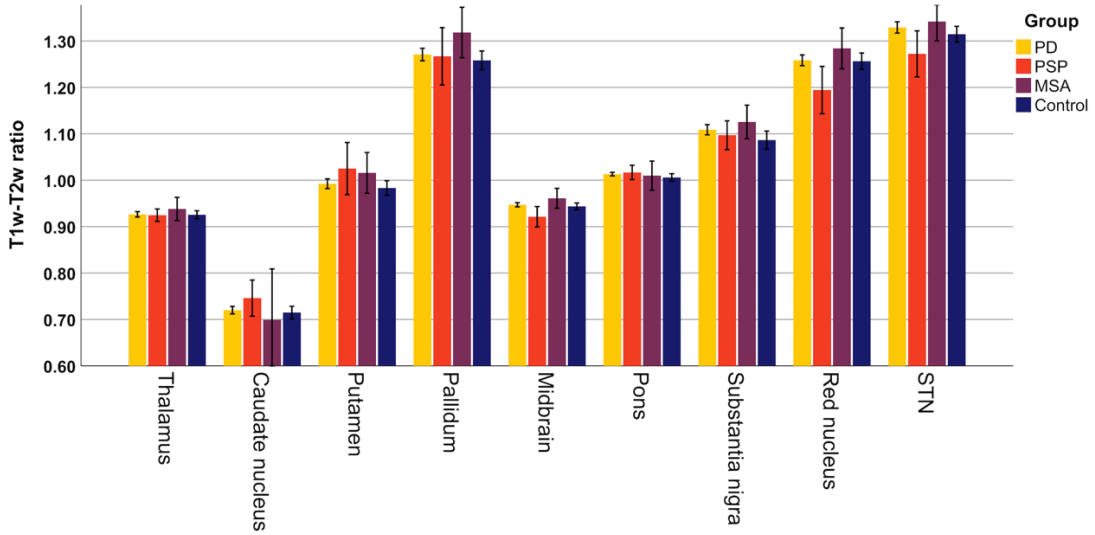

Figure 23. Mean T_1/T_2-weighted ratio in the different regions in the prospective BioFINDER cohort. Error bars show 95% confidence intervals of the mean.

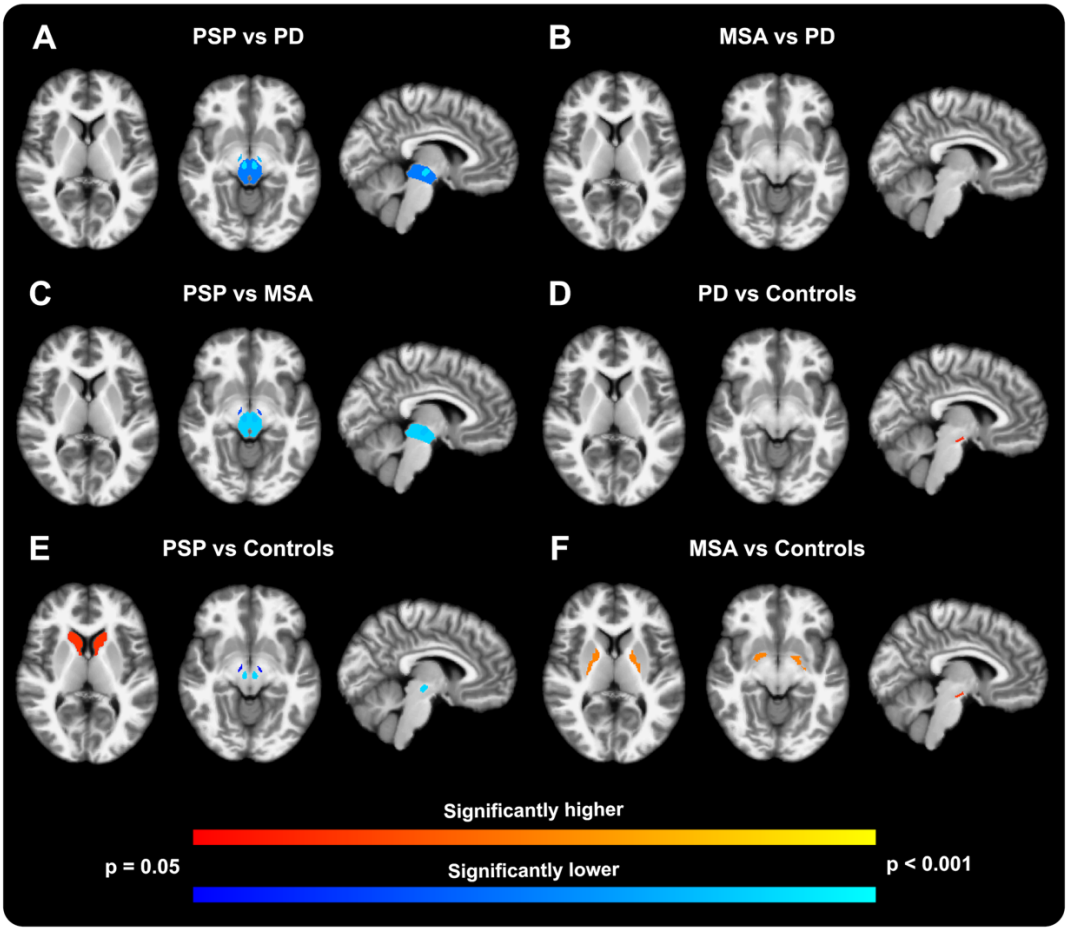

Figure 24. Visualization of significant group differences in white matter normalized T_1/T_2-weighted ratio in the prospective BioFINDER cohort. Regions with significant difference in pairwise testing are colored according to p-value to indicate the level of significance of increased (red – yellow) or decreased (dark blue – light blue) ratio. Note that all $p < 0.05$ from pairwise testing are depicted, regardless of results from ANOVA or Kruskal-Wallis test.

Diagnostic performance

Diagnostic performance of the T_1/T_2-weighted ratio was first analyzed in the KIMOVE cohort using ROC AUC. The regions showing the best diagnostic performances in differentiating PSP from PD were the thalamus (AUC 0.65), caudate nucleus (AUC 0.67), putamen (AUC 0.69), red nucleus (AUC 0.65) and the subthalamic nucleus (AUC 0.65). For differentiating MSA from PD, the best diagnostic performances were found in the caudate nucleus (AUC 0.64), putamen (AUC 0.66), pallidum (AUC 0.63) and pons (AUC 0.63). The regions with best diagnostic performances in separating PSP from MSA were the thalamus (AUC 0.69), red nucleus (AUC 0.72) and the subthalamic nucleus (AUC 0.72).

Composite variables based on the regions with significant differences in the KIMOVE cohort were then diagnostically evaluated in the BioFINDER cohort. For separating PSP from PD, this variable consisted of ratios from the following regions; (Caudate * Putamen) / (Thalamus * Red nucleus * Subthalamic nucleus) and yielded an AUC of 0.82. For separating MSA from PD, the composite variable consisted of (Caudate * Putamen * Pallidum) / Pons and yielded and AUC of 0.59. For separating PSP from MSA, the composite variable consisted of (thalamus * red nucleus * subthalamic nucleus) and yielded and AUC of 0.86.

5 DISCUSSION

A common problem in the movement disorder clinic is to differentiate PD from PSP and MSA. While being distinct disease entities when considering underlying pathophysiology, they often present with similar symptoms of parkinsonism. A correct and early diagnosis is important in the choice of medication and involvement of other health specialties such as physiotherapists, speech therapists and dieticians.

The overarching aim of my thesis is to investigate different MRI techniques and evaluate their potential as diagnostic biomarkers in parkinsonian disorders, to hopefully contribute to better clinical care and to build more knowledge regarding these disorders and techniques together with the research community.

5.1 STUDY I AND II

The results from Study I show that it is possible to process high-pass filtered phase images from clinical SWI examinations into susceptibility maps by using QSM techniques, and that these maps can be used to investigate pathological brain iron accumulation in parkinsonian disorders. There was a substantial elevation of susceptibility in different regions in PSP and in MSA compared to PD. Most notable is the increased susceptibility in the red nucleus and globus pallidus in PSP compared to all other groups. These findings are congruent with known pathological involvement in these regions.[27,150] Another interesting finding in Study I is the elevated susceptibility in the putamen in MSA compared to PD and controls. This finding is also in line with the picture in MSA with both pre- and post-synaptic dopaminergic degeneration and histopathological findings in this region.[166] All patient groups exhibited elevated susceptibility levels in the substantia nigra compared to healthy controls. Regarding diagnostic performance, the results from Study I showed that the red nucleus susceptibility stood out as a promising potential biomarker in the separation of PSP from other causes of parkinsonism.

Study II largely corroborates our findings from Study I in a coherent and prospectively recruited cohort, with elevated susceptibility in the red nucleus in PSP compared to all other groups, and elevated susceptibility in the globus pallidus compared to PD and healthy controls. The diagnostic performance of the red nucleus susceptibility in separating PSP from other parkinsonian disorders and controls was also corroborated, and it remained the most promising biomarker region. Other notable findings in Study II are the elevated putaminal susceptibility levels in MSA compared to PD and controls, consistent with the results from Study I. The elevated pallidal susceptibility in PSP was replicated in Study II in relation to PD and controls but not to MSA. We believe this might, in part, be due to the slightly lower number of PSP and MSA patients in the BioFINDER cohort (11 PSP and 10 MSA in BioFINDER, compared to 15 PSP and 11 MSA in the KIMOVE cohort).

To our knowledge, we are the first group to demonstrate this highly increased susceptibility in the red nucleus in PSP compared to PD (Study I and II), MSA (Study I and II) and controls (Study II). Using this region as a diagnostic biomarker to separate PSP from PD, MSA and

controls, we find promising accuracies as measured by ROC AUC. Other potential biomarker regions are the putamen and the dentate nucleus for separating atypical parkinsonism from PD.

Regarding associations and correlations between susceptibility measurements and clinical scores in PD, results from Study I showed that an increase in putaminal susceptibility was associated with an increased risk of having a higher Hoehn and Yahr score. Study II could similarly show that that there is a correlation between putaminal susceptibility and UPDRS part III. This is interesting considering that the putamen is an area that, together with the substantia nigra, has been shown to have increased iron accumulation in PD both in MRI and postmortem studies.[167]

When viewed in relation to QSM studies in Parkinsonism, such as those by Murakami et al[168] and Barbosa et al,[81] they found increased susceptibility in in the substantia nigra in PD compared to controls. While we found similar findings in Study I, we could not validate this in Study II. We cannot definitively explain this, but one possible reason could be differences in the methodology of the manual segmentations. In Study I, the two centermost representative slices were segmented in all regions. In Study II, all slices where the respective regions were visible and artefact-free were segmented. This difference could lead to an effective decrease, in Study II, of the resulting levels in the groups with higher susceptibility since all slices with lower susceptibility would also be included until the region was not visible for segmentation.

5.1.1 Study limitations

Study I

Firstly, the retrospective nature of the study means that the assessments of Hoehn and Yahr scores and screening for clinical signs such as vertical supranuclear gaze palsy or autonomic dysfunction is done through review of the clinical patient charts. The diagnoses have, however, been determined by specialists in neurology according to established diagnostic criteria,[30,46,169] and the diagnostic certainty is also strengthened by the fact that the patients were subjected long-time follow up at the neurology department. Secondly, the study participants were scanned using three different Siemens scanners. No differences were found between the susceptibility levels in the different MRI protocols in any of the groups. One of the healthy controls was examined using all three scanners, and no differences in susceptibility was found in any of the regions of interest between the scanners. The main group analysis was also carried out as a two-way ANCOVA where the MRI protocol was one of the factors to further account for possible differences.

Study I and II

When considering the common methodology for Study I and II, there are some possible limitations that apply to both studies. The high-pass filtered nature of the phase images used in these studies, which is done as part of the standard clinical SWI processing, can possibly reduce the contrast of the phase image. Technically, it is a form of background field removal. Background field removal is also part of the standard QSM processing, but more recently

developed techniques using projection onto dipole fields[72] or laplacian variants[71] that combine phase unwrapping and background field removal are typically more suited to preserving such contrast. The results from our studies prove, however, that useful information regarding susceptibility differences are still preserved and can extracted from this type of data. The data is also representative of MRI procedures commonly performed in routine clinical practice. Another limitation common to both studies, is the somewhat low number of patients with atypical parkinsonian syndromes. This, however, is a universal issue shared with most studies on PSP and MSA, considering that these are indeed rare disorders.

5.1.2 Post-publication developments

After publication, there has been some research activity in the field of QSM in parkinsonian disorders. A study by Jin et al. investigated the combination of neuromelanin-sensitive MRI and QSM imaging of nigrosome-1, and found that these two biomarkers together can aid in the differentiation of PD from essential tremor.[170] Shahmaei et al. investigated differences between patients with PD and healthy controls, and also correlations to disease stage as measured by Hoehn and Yahr.[171] Similar to our findings in Study I, they also show increased nigral susceptibility in PD, but also report elevated susceptibility in the red nucleus, thalamus and globus pallidus compared to healthy controls. They found a significant association with disease stage in all nuclei. There are still some differences in the reports of susceptibility levels between studies, with the original studies on QSM in PD by Barbosa et al.[81] and Murakami et al.[168] only showed significant increase of susceptibility in the substantia nigra. Langkammer et al., on the other hand, found elevations also in the red nucleus, thalamus and globus pallidus in addition to the substantia nigra.[79] Not only the actual levels of susceptibility but also their texture seem to be different between patients with PD and controls. Li et al. report that first- and second-order texture characteristics from QSM images of the substantia can be used to separate PD from controls.[172] More specific regional analysis in the substantia nigra has led to deeper understanding of where the susceptibility changes are most prominent. Bergsland et al. have now shown that iron accumulation in the substantia nigra in PD is located mainly in the ventral parts of the structure.[173] There has also been additional studies in QSM in atypical parkinsonism. Miyata et al. have shown interesting results in separating CBD from PSP by assessing CBD-specific susceptibility layers in the cerebral cortex.[86]

More closely related to our Studies I and II, two studies assessing the red nucleus as a possible biomarker have been published recently. One smaller study by Azuma et al. found, slightly in discordance with our results, that the globus pallidus and not the red nucleus seemed to be most promising in separating PSP from PD.[174] This study, however, only included 8 patients with PSP and thus makes the reported ROC AUCs and diagnostic performance less reliable. A larger study by Mazzuchi et al. including 15 patients with PSP, report that the susceptibility in the red nucleus yielded the highest diagnostic accuracy for PSP,[175] which is in concordance with our results from Study I and Study II.

5.2 STUDY III

To our knowledge, this is the first study directly comparing automated brainstem volumetry to manual planimetric measurements in the differentiation of PSP from other causes of parkinsonism. Our results show that there are significantly lower volumes in the midbrain, superior cerebellar peduncles and medulla oblongata in PSP compared to PD and MSA. There were also reduced pontine volumes in both PSP and MSA compared to PD.

The results from Study III clearly show that normalized midbrain volume can potentially be used as a biomarker to separate PSP from PD, and that a product of the normalized midbrain and medulla oblongata volumes could improve the diagnostic separation of PSP from both PD and MSA. We did not find any particular brainstem structure where the volume could be used to distinguish MSA from PD in any reliable way. The midbrain volume performed better than planimetric measurements (MP-ratio, MRPI 1.0 and MRPI 2.0) in separating PSP from PD, and on par with planimetry for separation between PSP and MSA. Our findings are in line with the results of a recent study by Pyatigorskaya et al.,[176] where significant midbrain atrophy with loss of volume was found in PSP using automated segmentation techniques. Also, Bocchetta et al. show similar findings with lower brainstem volumes in PSP and MSA compared to controls.[177]

Another most interesting finding in our study is that the volumetric midbrain-to-pons ratio showed significantly lower accuracy than its planimetric counterpart. We speculate that this could be due to an atrophy mostly affecting the midline and hence more directly giving a lower midbrain-to-pons area ratio, since this measure is done at the midline on sagittal slices on the structural T_1-weighted MRI. Further studies on local volume changes, perhaps with measurements of structural deformation, would be needed to elucidate this matter further.

In our study, we find somewhat lower diagnostic accuracies when assessing the manual planimetric measurements compared to what some other groups have shown earlier.[57,178] We believe that this may be due to the fact that PSP patients in our study were in relatively early stages of disease, considering that only 15 of 29 PSP patients had a vertical gaze palsy at the time of MRI. This does not mean that our PSP group is of a less certain diagnosis, since all but two individuals developed vertical gaze palsy during follow-up. Of the remaining two PSP patients, one received a diagnosis of definite PSP upon autopsy, leaving only one PSP patient remaining as a "possible" diagnosis at the end of the follow-up. A study by Mangesius et al. showed a similar tendency as our results, where a group with early PSP and parkinsonism was included and exhibited a lower diagnostic accuracy compared to those with later disease stages.[179]

Another factor to take into consideration is how such an automated approach could be incorporated in an existing radiological infrastructure. The automated FreeSurfer-based segmentation itself takes many hours, compared to a few minutes for a manual planimetric variable. However, there could still be a potential advantage with a method that does not require manual labor by a radiologist and that could be run as a background process on a server and

deliver volumetric results as the runs are completed. Such volumetric results could then be included in the reports to the referring clinician.

5.2.1 Study limitations

There are some limitations to this study. Firstly, this is a retrospective study, and the diagnosis and degree of symptoms have been classified based on review of patient charts. However, the diagnoses have been set by specialists in neurology and the patients have been recruited consecutively, creating a representative clinical cohort which we believe lends it well to generalization to other similar populations. The patients have been subject to long-term follow-up, which also strengthens the reliability of the respective diagnoses.

Another point is that the patients in our cohort have been scanned using different Siemens MRI scanner and different acquisition protocols. There were however no significant differences between the groups regarding distribution across the different scanners or voxel sizes. We also investigated intra- and inter-scanner reliability using intraclass correlation coefficients. More importantly, the volumetric and planimetric measurements are inherently matched on the patient level since they are performed on the same structural MRI volume, so the comparisons between the two types of analysis are perfectly valid.

Thirdly, the planimetric manual measurements were not performed by a radiologist, but by a specialist in neurology with 4 years' experience in neuroimaging, Henrik Sjöström. Therefore, to assess the reliabilities in these measurements a specialist in neuroradiology, Farouk Hashim also performed the planimetric measurements in a randomly selected subset of 25% of the participants. Henrik Sjöström also re-measured this subset of subset to also allow intra-rater reliability assessments. Intraclass correlation coefficients were calculated and found to be excellent for all intra-rater reliabilities and good to excellent for the inter-rater reliabilities.

5.2.2 Post-publication developments

At the time of submission of this thesis from printing, the manuscript for this study is under review. Therefore, no new data is available for discussion.

5.3 STUDY IV

In this first study on T_1/T_2-weighted ratio in atypical parkinsonism, we found most interesting differences in T_1/T_2-weighted ratio in the striatum, thalamus, subthalamic nucleus and the red nucleus in PSP compared to PD in the retrospective KIMOVE cohort. In the same cohort, we also found differences in the striatum between MSA and PD, and differences in the thalamus, subthalamic nucleus and the red nucleus between PSP and MSA.

In the prospective BioFINDER cohort, significant differences in T_1/T_2-weighted ratio were corroborated in the subthalamic nucleus and the red nucleus in PSP compared to PD and MSA. There, we also found a lower ratio in the midbrain in PSP compared to the other groups. Although not significant at group level ANOVA analysis, we still found significantly higher T_1/T_2-weighted ratio in PD compared to healthy controls in the pairwise analysis, in line with earlier findings by Du et al.[180] These nigral elevations in PD as well as in MSA compared to controls must however be interpreted with caution considering the lack of significant ANOVA.

What causes these changes in T_1/T_2-weighted ratio in subcortical gray matter structures is not completely known. We speculate that a possible explanation for elevated T_1/T_2-weighted ratio in the red nucleus in PSP compared to the other groups could be found in Study I and Study I, in which higher susceptibility reflecting pathological iron accumulation in the red nucleus was found in PSP compared to PD and MSA. This could possibly lead to changes in the T_1-weighted and/or T_2-weighted image and thus a change in T_1/T_2-weighted ratio. Other factors potentially affecting the signal could of course be myelin content, but also considering the known association between neurite density and the T_1/T_2-weighted ratio,[181] cell death as part of the neurodegenerative process could also contribute to such changes.

We also assessed the diagnostic performance of the T_1/T_2-weighted ratio in parkinsonism. When using single regions as biomarkers for diagnostic separation in the KIMOVE cohort, no regions yielded particularly good performance. Moving on, all regions with significant differences in the pairwise comparisons between the groups in the KIMOVE cohort were used to create composite variables. When applied to the prospective BioFINDER cohort, these multi-region variables yielded good diagnostic performance, as measured by ROC AUC for PSP vs PD and PSP vs MSA, where we found AUCs of 0.82 and 0.86 respectively.

The major strengths of Study IV are the application of the T_1/T_2-weighted ratio to new patient groups, and that the results clearly show findings that we interpret as signs of neurodegeneration in subcortical grey matter regions. Another strength is the use of two cohorts; one retrospective cohort for explorative analysis and one prospective for validation and testing of diagnostic performance. Interestingly, many of the substantial findings in the KIMOVE cohort such as the lower T_1/T_2-weighted ratio in the red nucleus in PSP could be validated in the BioFINDER cohort.

To summarize, the results from Study IV show that there are different patterns of T_1/T_2-weighted ratio in PSP compared to PD and MSA, reflecting underlying differences in pathology in these disorders. These differences could potentially be used as biomarkers is the

diagnostic process and the assessment of the parkinsonian patient. While there are currently no disease modifying therapies for these disorders, there is still a need for a high diagnostic certainty also when considering involvement in clinical trials of new medications. T_1- and T_2-weighted imaging are two of the most performed sequences, and it is worth considering the vast amount of possible data already existing. The routine use of these acquisitions in any MRI examination could also simplify a possible inclusion of such a ratio method in clinical practice, considering that the underlying data is already acquired.

5.3.1 Study limitations

As in Study I and Study III, the retrospective KIMOVE cohort included patients who had received diagnosis of PD, PSP or MSA at Karolinska University Hospital Huddinge. In these patients, diagnoses and assessments of disease severity were done through review of patient charts. They were, however, consecutively referred for brain MRI from the neurology department and subjected to a long-term follow-up as part of the routine neurological care.

The participants from the KIMOVE cohort were imaged using four different Siemens MRI scanners and different acquisition protocol variants. We found no differences in distributions of scanner model or field strength between the groups. It is also important to note that the construction of T_1/T_2-weighted ratio images involves histogram-based non-linear normalization to signals from bone, soft tissue and CSF. This is to allow comparison of combinations of different sequences and acquisition parameters. We also added an additional normalization step by dividing ratio levels in all regions by the mean of each individual's white matter ratio values. This was to further enhance the comparability between the different protocol variants.

The acquisition protocols for the T_2-weighted images included a relatively high slice thickness, yet the resulting ratio images yielded significant results and differences between the groups indicating that this type of data can also be used to assess changes related to neurodegeneration. Another limitation common to all studies is the relatively small number of patients with PSP and MSA in the BioFINDER cohort. This could in part explain why some of the findings in the KIMOVE cohort could not be replicated in the prospective BioFINDER cohort.

5.3.2 Post-publication developments

At the time of submission of this thesis from printing, the manuscript for this study is under review. Therefore, no new data is available for discussion.

6 CONCLUSIONS

Susceptibility mapping

In summary, Study I and Study II, showed that susceptibility mapping techniques can be used to investigate disease-related changes reflecting pathological brain iron accumulation occurring in parkinsonian disorders.

- The changes in susceptibility differ between the disease groups and could thus be used as diagnostic biomarkers, to potentially help clinicians in the separation of these disorders. Such separation of disorders is important in the clinical management of the disease and also when considering recruitment to clinical trials.

- These studies have added to the growing research field and after we were able to show the most interesting findings of increased susceptibility in the red nucleus in PSP, other groups have since been able to corroborate these findings.[175]

Automated brainstem volumetry

Study III investigated the use of automated brainstem segmentation in PD, PSP and MSA, and compared this technique to planimetric manual measurements.

- Automated brainstem segmentation is a promising new technique for assessing pathological changes in PSP.

- The volume of the midbrain performed better than any of the planimetric manual measurements in separating PSP from PD.

T_1/T_2-weighted ratio

The results from Study IV show that T_1- and T_2-weighted images, commonly acquired in routine MRI examinations, can be combined into a T_1/T_2-weighted ratio which reveals differences between parkinsonian disorders.

- Lower T_1/T_2-weighted ratio is found in the red nucleus and subthalamic nucleus in PSP.

- By combining ratio values from multiple regions, a higher degree of separation of PSP from PD and MSA can be achieved.

7 FUTURE ASPECTS

While we and others have shown that novel MRI techniques such as QSM and automated segmentation techniques can be used as an aid in the diagnostics in parkinsonism, there is still a need for further studies delving deeper into the diagnostic properties. There is also a need for work regarding investigation into the different subtypes of the atypical parkinsonian syndromes. Regarding the T_1/T_2-weighted ratio imaging we are, to our knowledge, the first to use this technique in PSP and MSA. Although we can show interesting findings with changes in this ratio in atypical parkinsonism, more research in needed with further analysis, validation and elucidation.

Another point needing further investigation is how changes over time can be followed using different MRI techniques, especially in the rarer atypical parkinsonian disorders. Such longitudinal studies would also be necessary to better evaluate these methods' potential as tools for assessing treatment effects in clinical trials.

One of the main advantages of MRI, beside the lack of ionizing radiation and ability to visualize small pathological changes in tissues, is the method's extreme versatility. With MRI, it is possible to image everything from the diffusion properties of water molecules to neurovascular coupling, to magnetic properties such as susceptibility and even electrical properties like conductance. In my opinion, when given a method that can measure so many different tissue properties in different ways, it would be reasonable to use this method in a multi-modal way to yield as true a picture as possible of the tissue or problem at hand.

All in all, and probably the most important point I want to stress, I believe there is great need for more efforts into making new MRI techniques clinically available. This work is of course a vast endeavor with everything from validation and studies on reliability to cooperation with developers of software and systems to build working and effective pipelines for data managements and processing. However, if this work is not done, then the full potential of such promising new methods might never be reached.

8 POPULÄRVETENSKAPLIG SAMMANFATTNING

Parkinsons sjukdom (PS) är den näst vanligaste degenerativa sjukdomen i nervsystemet, efter Alzheimers sjukdom. Vid PS uppstår en förlust av nervceller i övre delen av hjärnstammen, i ett område som heter substantia nigra, ”den svarta substansen”. Dessa nervceller producerar i vanliga fall en signalsubstans som heter dopamin. En minskning av dopaminnivåerna i hjärnan, som vid PS, kan leda till stelhet, långsamma rörelser, skakningar och nedsatt balans. Denna symtombild kallas för parkinsonism, och den vanligaste orsaken till parkinsonism är PS. Förutom dessa symtom som drabbar rörelseförmågan, så kallade motoriska symtom, är det vanligt med icke-motoriska symtom, såsom depression, förstoppning, nedsatt luktsinne, sömnstörningar och lågt blodtryck. Sådana icke-motoriska symtom kan ofta uppkomma flera år innan de motoriska symtomen framträder. Diagnosen PS ställs genom en klinisk bedömning och undersökning av neurolog men även bildundersökningar såsom skiktröntgen (DT) eller magnetkameraundersökning (MR) brukar utföras för att utesluta andra förklaringar till symtombilden. Sådana alternativa förklaringar kan till exempel vara stroke, hjärntumör eller multipel skleros (MS). En viktig del av omhändertagandet vid PS är även att följa och utvärdera effekten av insatt medicinering. Vid PS är målet att, med mediciner, ersätta effekten av det förlorade dopaminet; ofta genom att ge ett förstadium till dopamin, levodopa, som sedan omvandlas till dopamin i hjärnan.

Förutom PS finns ett antal ovanliga sjukdomar som också brukar debutera med parkinsonism. Dessa sjukdomar brukar sammantaget benämnas atypisk parkinsonism. Med detta begrepp innefattas vanligen på fyra olika sjukdomar; progressiv supranukleär pares (PSP), multipel systematrofi (MSA), kortikobasal degeneration (CBD) och Lewy body-demens. Dessa sjukdomar kan ofta vara svåra att skilja från PS, särskilt tidigt i sjukdomsförloppet, då symtombilden kan vara i stort sett identisk. De orsakas dock av andra underliggande processer och är i grund och botten andra sjukdomar. Det som förenar framförallt PSP, MSA och CBD är att de ofta svarar mycket sämre på Parkinsonmediciner såsom levodopa, och att de har ett klart mer aggressivt förlopp med snabbare försämring och tillkomst av andra symtom som ögonrörelsestörningar eller blodtrycksbesvär. För att försöka skilja dessa tillstånd från PS görs ofta ryggmärgsvätskeprov och MR-undersökning. På MR är det välkänt att det, åtminstone i senare stadier av sjukdom, ibland kan finnas typiska tecken på förtvining i särskilda områden vilket kan stärka diagnosen.

Syftet med denna avhandling är att undersöka nya magnetkameratekniker vid PS, PSP och MSA – både för att lära oss mer om dessa sjukdomar och för att ta reda på om dessa metoder kan användas diagnostiskt, för att skilja sjukdomarna från varandra. Att tidigt kunna skilja sjukdomarna från varandra är viktigt, då vård och medicinering bättre kan anpassas, och för att kunna ge mer sanningsenliga prognoser till patienter och anhöriga. Även vid läkemedelsstudier av nya potentiella bromsmediciner är det viktigt med tidiga och korrekta diagnoser.

Det är sedan tidigare känt att nedbrytning av nervceller kan leda till rubbningar i den lokala järnomsättningen. I Studie I och Studie II undersökte vi om sparade magnetkamerabilder med så kallad susceptibility weighted imaging (SWI) kunde vidarebehandlas för att avslöja skillnader i sjukdomsrelaterad järninlagring vid PS, PSP och MSA. Vi fann i dessa studier tydliga skillnader, där PSP uppvisade kraftig järninlagring i ett område kallat nucleus ruber, ”den röda kärnan”. Med hjälp av dessa nivåer var det även möjligt att skilja ut patienter med PSP från de med PS, MSA och friska kontrollpersoner. Vi fann även tecken till ökad järninlagring i putamen, ”skalkärnan”, vid MSA jämfört med PS.

I Studie III använde vi automatiska segmenteringsverktyg för att från magnetkamerabilder beräkna volymer av hjärnstamsdelar. Vi jämförde sedan dessa områdens diagnostiska egenskaper med manuella mätningar, på samma bilder, som också brukar användas vid dessa sjukdomar. Genom att använda volymen av övre delen av hjärnstammen, mitthjärnan, kunde vi urskilja patienter med PSP från de med PS eller MSA bättre än när vi använde de klassiska manuella måtten. Om volymen av mitthjärnan kombinerades med volymen av förlängda märgen förbättrades den diagnostiska förmågan att skilja de olika parkinsonismvarianterna åt ännu mer.

I Studie IV studerade vi en ny metod, T_1/T_2-viktad kvot, och dess användbarhet vid PS och atypisk parkinsonism. T_1/T_2-viktad kvot går ut på att det räknas ut en kvot mellan två vanliga MR-bildtyper, och på så sätt skapas ett bättre mått på vävnadsegenskaper. Vi kunde, i den här studien, visa förändrad T_1/T_2-viktad kvot i bland annat nucleus ruber och i den subthalamiska kärnan i PSP jämfört med alla andra grupper. Genom att kombinera resultaten från flera olika områden i hjärnan kunde vi ännu bättre skilja PSP från PS och MSA.

9 ACKNOWLEDGEMENTS

I am eternally grateful for all the outstanding help and support I have received, which has made this thesis possible. In particular, I would like to thank:

My main supervisor, professor **Per Svenningsson**, for your kind support, wise suggestions and great patience. Thank you for letting me be a part of your dynamic and brilliant group. Your guidance in this world of science has meant everything to me and this project.

Dr. **Tobias Granberg**, my co-supervisor, for your support, your enthusiasm, and for pointing me in the right direction when needed. For patiently putting up with all my technical questions. For getting me started in science and, of course, for your friendship.

Professor **Eric Westman**, my co-supervisor, who with your knowledge and positive encouragement has always been available for discussions. Thank you for letting me be part of the journal clubs and activities also at your department.

My friends and colleagues at the Academic Specialist Center; **Mattias Andréasson**, **Erika Fritz**, **Lisa Hainke**, **Ellen Hertz**, **Anders Johansson**, **Anita Karlsson**, **Ioanna Markaki**, **Kerstin Pålsson**, **Mathias Sundgren**, **Panagiota Tsitsi,** among others. Thank you for your help and support, for always having your doors open and for making this a great place to be!

My former and current bosses at the Academic Specialist Center, to **Eva Lindström**, **Sofia Ernestam**, **Linda Kjerr** and **Christian Bartholomäus**.

Ingela Nilsson-Remahl, for giving me a job in Stockholm and for being my first boss in Huddinge, and also my mentor. Thank you!

The fantastic MRI nurses at Karolinska Huddinge.

The MRI physicists who have helped me out when testing new ideas and things I wanted to implement in the MRI protocols – **Love Engström Nordin**, **Sven Petersson** and **Tomas Jonsson**.

Sten Fredrikson, for letting me into the world of teaching by allowing me to be clinical amanuensis for the medical students, also allowing more precious research time.

Per-David Alm and **Tahir Osman**, for getting me started in the world of neurology. For your knowledge, kindness and patience. Thank you!

My movement disorder interested friends and colleagues; **Lovisa Brodin**, **Karolina af Edholm**, **Patrik Fazio**, **Martin Paucar** and **Thomas Willows**.

My fellow researchers **Russell Oullette, Michael Plattén** and **Jonathan Tjerkaski**, for stimulating conversations and for assistance with MRI scans.

My old colleagues in Huddinge; to **Amir Ahoromazdae**, **Sanno Chamoun**, **Björn Evertsson**, **Katarina Fink, Agnes Gorczyca**, **Caroline Ingre**, **Mustafa Ismail**, **Jesper Jacobsen**, **Ulla Lindbom**, **Cecilia Lundgren**, **Magnus Lundkvist**, **Benno Mahler**, **Rayomand Press**, **Ulf Kläppe**, **Kosta Kostulas**, **Mircea Oprica**, **Salma Samara**, **Kristin Samuelsson**, **Anna Sundholm**, and so many other great people!

Oskar Hansson, **Danielle van Westen** and **Yulia Surova**, for fruitful collaboration with Lund University.

All my friends and family, thank you for encouragement, for good times. You are too many to name, but you know who you are!

My mother-in-law **Kristina** and my father-in-law **Torbjörn**, for your support, for great discussions, for your insights in the world of science and for making the life puzzle more manageable.

My parents, **Ann-Christine** and **Birger**, for your love and endless support. For your encouragement, and for making it possible to combine life and work.

My children **Astrid** and **Freja,** for all the happiness you bring and for showing me what really matters in life.

My wife **Anna**, thank you my love, for your never-ending patience and kindness. Without you, this would not have been possible.

10 REFERENCES

1. Parkinson J. An Essay on the Shaking Palsy. JNP. American Psychiatric Publishing; 2002;14:223–236.

2. Obeso JA, Stamelou M, Goetz CG, et al. Past, present, and future of Parkinson's disease: A special essay on the 200th Anniversary of the Shaking Palsy. Mov Disord. 2017;32:1264–1310.

3. Dorsey ER, Elbaz A, Nichols E, et al. Global, regional, and national burden of Parkinson's disease, 1990–2016: a systematic analysis for the Global Burden of Disease Study 2016. The Lancet Neurology. Elsevier; 2018;17:939–953.

4. Poewe W, Seppi K, Tanner CM, et al. Parkinson disease. Nat Rev Dis Primers. 2017;3:17013.

5. Kalia LV, Lang AE. Parkinson's disease. Lancet. 2015;386:896–912.

6. Ritz B, Lee P-C, Lassen CF, Arah OA. Parkinson disease and smoking revisited: ease of quitting is an early sign of the disease. Neurology. 2014;83:1396–1402.

7. Deng H, Wang P, Jankovic J. The genetics of Parkinson disease. Ageing Res Rev. 2017;42:72–85.

8. Roshan Lal T, Sidransky E. The Spectrum of Neurological Manifestations Associated with Gaucher Disease. Diseases. 2017;5.

9. Han F, Grimes DA, Li F, et al. Mutations in the glucocerebrosidase gene are common in patients with Parkinson's disease from Eastern Canada. Int J Neurosci. 2016;126:415–421.

10. Braak H, Del Tredici K, Rüb U, de Vos RAI, Jansen Steur ENH, Braak E. Staging of brain pathology related to sporadic Parkinson's disease. Neurobiol Aging. 2003;24:197–211.

11. Rietdijk CD, Perez-Pardo P, Garssen J, van Wezel RJA, Kraneveld AD. Exploring Braak's Hypothesis of Parkinson's Disease. Front Neurol. 2017;8:37.

12. Dexter DT, Wells FR, Agid F, et al. Increased nigral iron content in postmortem parkinsonian brain. Lancet. 1987;2:1219–1220.

13. Dexter DT, Wells FR, Lees AJ, et al. Increased nigral iron content and alterations in other metal ions occurring in brain in Parkinson's disease. J Neurochem. 1989;52:1830–1836.

14. Youdim MBH, Ben-Shachar D, Riederer P. Is Parkinson's disease a progressive siderosis of substantia nigra resulting in iron and melanin induced neurodegeneration? Acta Neurologica Scandinavica. 1989;80:47–54.

15. Mochizuki H, Choong C-J, Baba K. Parkinson's disease and iron. J Neural Transm (Vienna). 2020;127:181–187.

16. Jellinger K, Kienzl E, Rumpelmair G, et al. Iron Melanin Complex in Substantia-Nigra of Parkinsonian Brains - an X-Ray-Microanalysis. J Neurochem. Hoboken: Wiley; 1992;59:1168–1171.

17. Levin J, Högen T, Hillmer AS, et al. Generation of ferric iron links oxidative stress to α-synuclein oligomer formation. J Parkinsons Dis. 2011;1:205–216.

18. Postuma RB, Berg D, Stern M, et al. MDS clinical diagnostic criteria for Parkinson's disease. Mov Disord. 2015;30:1591–1601.

19. Hoehn MM, Yahr MD. Parkinsonism: onset, progression and mortality. Neurology. 1967;17:427–442.

20. Goetz CG, Poewe W, Rascol O, et al. Movement Disorder Society Task Force report on the Hoehn and Yahr staging scale: status and recommendations. Mov Disord. 2004;19:1020–1028.

21. Goetz CG, Fahn S, Martinez-Martin P, et al. Movement Disorder Society-sponsored revision of the Unified Parkinson's Disease Rating Scale (MDS-UPDRS): Process, format, and clinimetric testing plan. Movement Disorders. 2007;22:41–47.

22. Steele JC, Richardson JC, Olszewski J. Progressive supranuclear palsy. A heterogeneous degeneration involving the brain stem, basal ganglia and cerebellum with vertical gaze and pseudobulbar palsy, nuchal dystonia and dementia. Arch Neurol. 1964;10:333–359.

23. Schrag A, Ben-Shlomo Y, Quinn NP. Prevalence of progressive supranuclear palsy and multiple system atrophy: a cross-sectional study. Lancet. 1999;354:1771–1775.

24. Golbe LI. Progressive supranuclear palsy. Semin Neurol. 2014;34:151–159.

25. Baker M, Litvan I, Houlden H, et al. Association of an extended haplotype in the tau gene with progressive supranuclear palsy. Hum Mol Genet. 1999;8:711–715.

26. Goedert M, Spillantini MG. Propagation of Tau aggregates. Mol Brain. 2017;10:18.

27. Williams DR, Lees AJ. Progressive supranuclear palsy: clinicopathological concepts and diagnostic challenges. Lancet Neurol. 2009;8:270–279.

28. Hattori M, Hashizume Y, Yoshida M, et al. Distribution of astrocytic plaques in the corticobasal degeneration brain and comparison with tuft-shaped astrocytes in the progressive supranuclear palsy brain. Acta Neuropathol. 2003;106:143–149.

29. Goetz CG, Leurgans S, Lang AE, Litvan I. Progression of gait, speech and swallowing deficits in progressive supranuclear palsy. Neurology. 2003;60:917–922.

30. Litvan I, Agid Y, Calne D, et al. Clinical research criteria for the diagnosis of progressive supranuclear palsy (Steele-Richardson-Olszewski syndrome): report of the NINDS-SPSP international workshop. Neurology. 1996;47:1–9.

31. Höglinger GU, Respondek G, Stamelou M, et al. Clinical diagnosis of progressive supranuclear palsy: The movement disorder society criteria. Mov Disord. 2017;32:853–864.

32. Sakurai K, Tokumaru AM, Shimoji K, et al. Beyond the midbrain atrophy: wide spectrum of structural MRI finding in cases of pathologically proven progressive supranuclear palsy. Neuroradiology. 2017;59:431–443.

33. Sako W, Murakami N, Izumi Y, Kaji R. Neurofilament light chain level in cerebrospinal fluid can differentiate Parkinson's disease from atypical parkinsonism: Evidence from a meta-analysis. J Neurol Sci. 2015;352:84–87.

34. Thobois S, Prange S, Scheiber C, Broussolle E. What a neurologist should know about PET and SPECT functional imaging for parkinsonism: A practical perspective. Parkinsonism Relat Disord. 2019;59:93–100.

35. Williams DR, de Silva R, Paviour DC, et al. Characteristics of two distinct clinical phenotypes in pathologically proven progressive supranuclear palsy: Richardson's syndrome and PSP-parkinsonism. Brain. 2005;128:1247–1258.

36. Krack P, Marion MH. "Apraxia of lid opening," a focal eyelid dystonia: clinical study of 32 patients. Mov Disord. 1994;9:610–615.

37. Piccione F, Mancini E, Tonin P, Bizzarini M. Botulinum toxin treatment of apraxia of eyelid opening in progressive supranuclear palsy: report of two cases. Arch Phys Med Rehabil. 1997;78:525–529.

38. Golbe LI, Ohman-Strickland PA. A clinical rating scale for progressive supranuclear palsy. Brain. 2007;130:1552–1565.

39. Graham JG, Oppenheimer DR. Orthostatic hypotension and nicotine sensitivity in a case of multiple system atrophy. J Neurol Neurosurg Psychiatry. 1969;32:28–34.

40. Adams RD, Vanbogaert L, Vandereecken H. STRIATO-NIGRAL DEGENERATION. J Neuropathol Exp Neurol. 1964;23:584–608.

41. Shy GM, Drager GA. A neurological syndrome associated with orthostatic hypotension: a clinical-pathologic study. Arch Neurol. 1960;2:511–527.

42. Wenning GK, Colosimo C, Geser F, Poewe W. Multiple system atrophy. Lancet Neurol. 2004;3:93–103.

43. Fanciulli A, Wenning GK. Multiple-system atrophy. N Engl J Med. 2015;372:249–263.

44. Watanabe H, Saito Y, Terao S, et al. Progression and prognosis in multiple system atrophy: an analysis of 230 Japanese patients. Brain. 2002;125:1070–1083.

45. Jellinger KA. Multiple System Atrophy: An Oligodendroglioneural Synucleinopathy1. J Alzheimers Dis. 62:1141–1179.

46. Gilman S, Wenning GK, Low PA, et al. Second consensus statement on the diagnosis of multiple system atrophy. Neurology. 2008;71:670–676.

47. Palma J-A, Norcliffe-Kaufmann L, Kaufmann H. Diagnosis of multiple system atrophy. Auton Neurosci. 2018;211:15–25.

48. Brooks DJ, Tambasco N. Imaging synucleinopathies. Mov Disord. 2016;31:814–829.

49. Wenning GK, Tison F, Seppi K, et al. Development and validation of the Unified Multiple System Atrophy Rating Scale (UMSARS). Mov Disord. 2004;19:1391–1402.

50. Heim B, Krismer F, De Marzi R, Seppi K. Magnetic resonance imaging for the diagnosis of Parkinson's disease. J Neural Transm (Vienna). 2017;124:915–964.

51. Nobili F, Westman E, Kogan RV, et al. Clinical utility and research frontiers of neuroimaging in movement disorders. Q J Nucl Med Mol Imaging. 2017;61:372–385.

52. Baglieri A, Marino MA, Morabito R, Di Lorenzo G, Bramanti P, Marino S. Differences between conventional and nonconventional MRI techniques in Parkinson's disease. Funct Neurol. 2013;28:73–82.

53. Etemadifar M, Afshar F, Nasr Z, Kheradmand M. Parkinsonism associated with multiple sclerosis: A report of eight new cases and a review on the literature. Iran J Neurol. 2014;13:88–93.

54. Massey LA, Micallef C, Paviour DC, et al. Conventional magnetic resonance imaging in confirmed progressive supranuclear palsy and multiple system atrophy. Mov Disord. 2012;27:1754–1762.

55. Whitwell JL, Höglinger GU, Antonini A, et al. Radiological biomarkers for diagnosis in PSP: Where are we and where do we need to be? Mov Disord. 2017;32:955–971.

56. Nigro S, Arabia G, Antonini A, et al. Magnetic Resonance Parkinsonism Index: diagnostic accuracy of a fully automated algorithm in comparison with the manual measurement in a large Italian multicentre study in patients with progressive supranuclear palsy. Eur Radiol. 2017;27:2665–2675.

57. Quattrone A, Morelli M, Nigro S, et al. A new MR imaging index for differentiation of progressive supranuclear palsy-parkinsonism from Parkinson's disease. Parkinsonism Relat Disord. 2018;54:3–8.

58. Saeed U, Compagnone J, Aviv RI, et al. Imaging biomarkers in Parkinson's disease and Parkinsonian syndromes: current and emerging concepts. Transl Neurodegener. 2017;6:8.

59. Haacke EM, Xu Y, Cheng Y-CN, Reichenbach JR. Susceptibility weighted imaging (SWI). Magn Reson Med. 2004;52:612–618.

60. Di Ieva A, Lam T, Alcaide-Leon P, Bharatha A, Montanera W, Cusimano MD. Magnetic resonance susceptibility weighted imaging in neurosurgery: current applications and future perspectives. J Neurosurg. 2015;123:1463–1475.

61. Wang Y, Yu Y, Li D, et al. Artery and vein separation using susceptibility-dependent phase in contrast-enhanced MRA. J Magn Reson Imaging. 2000;12:661–670.

62. Lhermitte J, Kraus WM, McAlpine D. Original Papers: ON THE OCCURRENCE OF ABNORMAL DEPOSITS OF IRON IN THE BRAIN IN PARKINSONISM WITH SPECIAL REFERENCE TO ITS LOCALISATION. J Neurol Psychopathol. 1924;5:195–208.

63. Lee DW, Andersen JK. Iron elevations in the aging Parkinsonian brain: a consequence of impaired iron homeostasis? J Neurochem. 2010;112:332–339.

64. Wang Z, Luo X-G, Gao C. Utility of susceptibility-weighted imaging in Parkinson's disease and atypical Parkinsonian disorders. Transl Neurodegener. 2016;5:17.

65. Mahlknecht P, Krismer F, Poewe W, Seppi K. Meta-analysis of dorsolateral nigral hyperintensity on magnetic resonance imaging as a marker for Parkinson's disease. Mov Disord. 2017;32:619–623.

66. Reiter E, Mueller C, Pinter B, et al. Dorsolateral nigral hyperintensity on 3.0T susceptibility-weighted imaging in neurodegenerative Parkinsonism. Mov Disord. 2015;30:1068–1076.

67. Bae YJ, Kim J-M, Kim E, et al. Loss of Nigral Hyperintensity on 3 Tesla MRI of Parkinsonism: Comparison With (123) I-FP-CIT SPECT. Mov Disord. 2016;31:684–692.

68. Wang Y, Liu T. Quantitative susceptibility mapping (QSM): Decoding MRI data for a tissue magnetic biomarker. Magn Reson Med. Epub 2014 Jul 17.

69. Haacke EM, Liu S, Buch S, Zheng W, Wu D, Ye Y. Quantitative susceptibility mapping: current status and future directions. Magn Reson Imaging. 2015;33:1–25.

70. Schweser F, Deistung A, Lehr BW, Reichenbach JR. Quantitative imaging of intrinsic magnetic tissue properties using MRI signal phase: an approach to in vivo brain iron metabolism? Neuroimage. 2011;54:2789–2807.

71. Li W, Avram AV, Wu B, Xiao X, Liu C. Integrated Laplacian-based phase unwrapping and background phase removal for quantitative susceptibility mapping. NMR Biomed. 2014;27:219–227.

72. Liu T, Khalidov I, de Rochefort L, et al. A novel background field removal method for MRI using projection onto dipole fields (PDF). NMR Biomed. 2011;24:1129–1136.

73. Li W, Wang N, Yu F, et al. A method for estimating and removing streaking artifacts in quantitative susceptibility mapping. Neuroimage. 2015;108:111–122.

74. Liu J, Liu T, de Rochefort L, et al. Morphology enabled dipole inversion for quantitative susceptibility mapping using structural consistency between the magnitude image and the susceptibility map. Neuroimage. 2012;59:2560–2568.

75. Liu Z, Spincemaille P, Yao Y, Zhang Y, Wang Y. MEDI+0: Morphology enabled dipole inversion with automatic uniform cerebrospinal fluid zero reference for quantitative susceptibility mapping. Magn Reson Med. Epub 2017 Oct 11.

76. Langkammer C, Schweser F, Krebs N, et al. Quantitative susceptibility mapping (QSM) as a means to measure brain iron? A post mortem validation study. Neuroimage. 2012;62:1593–1599.

77. Sun H, Walsh AJ, Lebel RM, et al. Validation of quantitative susceptibility mapping with Perls' iron staining for subcortical gray matter. NeuroImage. 2015;105:486–492.

78. Zheng W, Nichol H, Liu S, Cheng Y-CN, Haacke EM. Measuring iron in the brain using quantitative susceptibility mapping and X-ray fluorescence imaging. Neuroimage. 2013;78:68–74.

79. Langkammer C, Pirpamer L, Seiler S, et al. Quantitative Susceptibility Mapping in Parkinson's Disease. PLoS ONE. 2016;11:e0162460.

80. Murakami Y, Kakeda S, Watanabe K, et al. Usefulness of quantitative susceptibility mapping for the diagnosis of Parkinson disease. AJNR Am J Neuroradiol. 2015;36:1102–1108.

81. Barbosa JHO, Santos AC, Tumas V, et al. Quantifying brain iron deposition in patients with Parkinson's disease using quantitative susceptibility mapping, R2 and R2. Magn Reson Imaging. 2015;33:559–565.

82. Alkemade A, de Hollander G, Keuken MC, et al. Comparison of T2*-weighted and QSM contrasts in Parkinson's disease to visualize the STN with MRI. PLoS ONE. 2017;12:e0176130.

83. Ide S, Kakeda S, Ueda I, et al. Internal structures of the globus pallidus in patients with Parkinson's disease: evaluation with quantitative susceptibility mapping (QSM). Eur Radiol. 2015;25:710–718.

84. Ito K, Ohtsuka C, Yoshioka K, et al. Differential diagnosis of parkinsonism by a combined use of diffusion kurtosis imaging and quantitative susceptibility mapping. Neuroradiology. 2017;59:759–769.

85. Sjöström H, Granberg T, Westman E, Svenningsson P. Quantitative susceptibility mapping differentiates between parkinsonian disorders. Parkinsonism Relat Disord. 2017;44:51–57.

86. Miyata M, Kakeda S, Toyoshima Y, et al. Potential usefulness of signal intensity of cerebral gyri on quantitative susceptibility mapping for discriminating corticobasal degeneration from progressive supranuclear palsy and Parkinson's disease. Neuroradiology. 2019;61:1251–1259.

87. Hagmann P, Jonasson L, Maeder P, Thiran J-P, Wedeen VJ, Meuli R. Understanding diffusion MR imaging techniques: from scalar diffusion-weighted imaging to diffusion tensor imaging and beyond. Radiographics. 2006;26 Suppl 1:S205-223.

88. Lebel C, Treit S, Beaulieu C. A review of diffusion MRI of typical white matter development from early childhood to young adulthood. NMR Biomed. Epub 2017 Sep 8.

89. Basser PJ, Pierpaoli C. Microstructural and physiological features of tissues elucidated by quantitative-diffusion-tensor MRI. J Magn Reson B. 1996;111:209–219.

90. Atkinson-Clement C, Pinto S, Eusebio A, Coulon O. Diffusion tensor imaging in Parkinson's disease: Review and meta-analysis. Neuroimage Clin. 2017;16:98–110.

91. Skorpil M, Söderlund V, Sundin A, Svenningsson P. MRI diffusion in Parkinson's disease: using the technique's inherent directional information to study the olfactory bulb and substantia nigra. J Parkinsons Dis. 2012;2:171–180.

92. Chiang P-L, Chen H-L, Lu C-H, et al. White matter damage and systemic inflammation in Parkinson's disease. BMC Neurosci. 2017;18:48.

93. Langley J, Huddleston DE, Merritt M, et al. Diffusion tensor imaging of the substantia nigra in Parkinson's disease revisited. Hum Brain Mapp. 2016;37:2547–2556.

94. Loane C, Politis M, Kefalopoulou Z, et al. Aberrant nigral diffusion in Parkinson's disease: A longitudinal diffusion tensor imaging study. Mov Disord. 2016;31:1020–1026.

95. Chen B, Fan G, Sun W, et al. Usefulness of diffusion-tensor MRI in the diagnosis of Parkinson variant of multiple system atrophy and Parkinson's disease: a valuable tool to differentiate between them? Clin Radiol. 2017;72:610.e9-610.e15.

96. Bajaj S, Krismer F, Palma J-A, et al. Diffusion-weighted MRI distinguishes Parkinson disease from the parkinsonian variant of multiple system atrophy: A systematic review and meta-analysis. PLoS ONE. 2017;12:e0189897.

97. Rulseh AM, Keller J, Rusz J, et al. Diffusion tensor imaging in the characterization of multiple system atrophy. Neuropsychiatr Dis Treat. 2016;12:2181–2187.

98. Wang P-S, Yeh C-L, Lu C-F, Wu H-M, Soong B-W, Wu Y-T. The involvement of supratentorial white matter in multiple system atrophy: a diffusion tensor imaging tractography study. Acta Neurol Belg. 2017;117:213–220.

99. Jones DK, Cercignani M. Twenty-five pitfalls in the analysis of diffusion MRI data. NMR Biomed. 2010;23:803–820.

100. Tournier J-D, Mori S, Leemans A. Diffusion tensor imaging and beyond. Magn Reson Med. 2011;65:1532–1556.

101. Pfefferbaum A, Adalsteinsson E, Rohlfing T, Sullivan EV. Diffusion tensor imaging of deep gray matter brain structures: effects of age and iron concentration. Neurobiol Aging. 2010;31:482–493.

102. Jensen JH, Helpern JA. MRI quantification of non-Gaussian water diffusion by kurtosis analysis. NMR Biomed. 2010;23:698–710.

103. Zhang H, Schneider T, Wheeler-Kingshott CA, Alexander DC. NODDI: practical in vivo neurite orientation dispersion and density imaging of the human brain. Neuroimage. 2012;61:1000–1016.

104. Kamagata K, Zalesky A, Hatano T, et al. Gray Matter Abnormalities in Idiopathic Parkinson's Disease: Evaluation by Diffusional Kurtosis Imaging and Neurite Orientation Dispersion and Density Imaging. Hum Brain Mapp. Epub 2017 May 4.

105. Ito K, Sasaki M, Ohtsuka C, et al. Differentiation among parkinsonisms using quantitative diffusion kurtosis imaging. Neuroreport. 2015;26:267–272.

106. Kamagata K, Hatano T, Okuzumi A, et al. Neurite orientation dispersion and density imaging in the substantia nigra in idiopathic Parkinson disease. Eur Radiol. 2016;26:2567–2577.

107. Chow MSM, Wu SL, Webb SE, Gluskin K, Yew DT. Functional magnetic resonance imaging and the brain: A brief review. World J Radiol. 2017;9:5–9.

108. Bell PT, Gilat M, O'Callaghan C, et al. Dopaminergic basis for impairments in functional connectivity across subdivisions of the striatum in Parkinson's disease. Hum Brain Mapp. 2015;36:1278–1291.

109. Agosta F, Caso F, Stankovic I, et al. Cortico-striatal-thalamic network functional connectivity in hemiparkinsonism. Neurobiol Aging. 2014;35:2592–2602.

110. Tang Y, Meng L, Wan C-M, et al. Identifying the presence of Parkinson's disease using low-frequency fluctuations in BOLD signals. Neurosci Lett. 2017;645:1–6.

111. Tahmasian M, Eickhoff SB, Giehl K, et al. Resting-state functional reorganization in Parkinson's disease: An activation likelihood estimation meta-analysis. Cortex. 2017;92:119–138.

112. Bharti K, Bologna M, Upadhyay N, et al. Abnormal Resting-State Functional Connectivity in Progressive Supranuclear Palsy and Corticobasal Syndrome. Front Neurol. 2017;8:248.

113. Rosskopf J, Gorges M, Müller H-P, et al. Intrinsic functional connectivity alterations in progressive supranuclear palsy: Differential effects in frontal cortex, motor, and midbrain networks. Mov Disord. 2017;32:1006–1015.

114. Wang N, Edmiston EK, Luo X, et al. Comparing abnormalities of amplitude of low-frequency fluctuations in multiple system atrophy and idiopathic Parkinson's disease measured with resting-state fMRI. Psychiatry Res. 2017;269:73–81.

115. Sled JG. Modelling and interpretation of magnetization transfer imaging in the brain. Neuroimage. Epub 2017 Dec 5.

116. Wolff SD, Balaban RS. Magnetization transfer contrast (MTC) and tissue water proton relaxation in vivo. Magn Reson Med. 1989;10:135–144.

117. Eckert T, Sailer M, Kaufmann J, et al. Differentiation of idiopathic Parkinson's disease, multiple system atrophy, progressive supranuclear palsy, and healthy controls using magnetization transfer imaging. Neuroimage. 2004;21:229–235.

118. Tambasco N, Belcastro V, Sarchielli P, et al. A magnetization transfer study of mild and advanced Parkinson's disease. Eur J Neurol. 2011;18:471–477.

119. Naka H, Imon Y, Ohshita T, et al. Magnetization transfer measurements of brain structures in patients with multiple system atrophy. Neuroimage. 2002;17:1572–1578.

120. da Rocha AJ, Maia ACM, da Silva CJ, et al. Pyramidal tract degeneration in multiple system atrophy: the relevance of magnetization transfer imaging. Mov Disord. 2007;22:238–244.

121. Trujillo P, Summers PE, Smith AK, et al. Pool size ratio of the substantia nigra in Parkinson's disease derived from two different quantitative magnetization transfer approaches. Neuroradiology. 2017;59:1251–1263.

122. van Zijl PCM, Yadav NN. Chemical exchange saturation transfer (CEST): what is in a name and what isn't? Magn Reson Med. 2011;65:927–948.

123. Li C, Peng S, Wang R, et al. Chemical exchange saturation transfer MR imaging of Parkinson's disease at 3 Tesla. Eur Radiol. 2014;24:2631–2639.

124. Li C, Chen M, Zhao X, et al. Chemical Exchange Saturation Transfer MRI Signal Loss of the Substantia Nigra as an Imaging Biomarker to Evaluate the Diagnosis and Severity of Parkinson's Disease. Front Neurosci. 2017;11:489.

125. Li C, Wang R, Chen H, et al. Chemical Exchange Saturation Transfer MR Imaging is Superior to Diffusion-Tensor Imaging in the Diagnosis and Severity Evaluation of Parkinson's Disease: A Study on Substantia Nigra and Striatum. Front Aging Neurosci. 2015;7:198.

126. Sasaki M, Shibata E, Tohyama K, et al. Neuromelanin magnetic resonance imaging of locus ceruleus and substantia nigra in Parkinson's disease. Neuroreport. 2006;17:1215–1218.

127. Martin-Bastida A, Pietracupa S, Piccini P. Neuromelanin in parkinsonian disorders: an update. Int J Neurosci. 2017;127:1116–1123.

128. Trujillo P, Summers PE, Ferrari E, et al. Contrast mechanisms associated with neuromelanin-MRI. Magn Reson Med. 2017;78:1790–1800.

129. Castellanos G, Fernández-Seara MA, Lorenzo-Betancor O, et al. Automated neuromelanin imaging as a diagnostic biomarker for Parkinson's disease. Mov Disord. 2015;30:945–952.

130. Kashihara K, Shinya T, Higaki F. Reduction of neuromelanin-positive nigral volume in patients with MSA, PSP and CBD. Intern Med. 2011;50:1683–1687.

131. Jansen JFA, Backes WH, Nicolay K, Kooi ME. 1H MR spectroscopy of the brain: absolute quantification of metabolites. Radiology. 2006;240:318–332.

132. Bertholdo D, Watcharakorn A, Castillo M. Brain proton magnetic resonance spectroscopy: introduction and overview. Neuroimaging Clin N Am. 2013;23:359–380.

133. Federico F, Simone IL, Lucivero V, et al. Proton magnetic resonance spectroscopy in Parkinson's disease and atypical parkinsonian disorders. Mov Disord. 1997;12:903–909.

134. Federico F, Simone IL, Lucivero V, et al. Usefulness of proton magnetic resonance spectroscopy in differentiating parkinsonian syndromes. Ital J Neurol Sci. 1999;20:223–229.

135. Abe K, Terakawa H, Takanashi M, et al. Proton magnetic resonance spectroscopy of patients with parkinsonism. Brain Res Bull. 2000;52:589–595.

136. Guevara CA, Blain CR, Stahl D, Lythgoe DJ, Leigh PN, Barker GJ. Quantitative magnetic resonance spectroscopic imaging in Parkinson's disease, progressive supranuclear palsy and multiple system atrophy. Eur J Neurol. 2010;17:1193–1202.

137. Zanigni S, Testa C, Calandra-Buonaura G, et al. The contribution of cerebellar proton magnetic resonance spectroscopy in the differential diagnosis among parkinsonian syndromes. Parkinsonism Relat Disord. 2015;21:929–937.

138. Cao H, Shi J, Cao B, Kang B, Zhang M, Qu Q. Evaluation of the Braak staging of brain pathology with 1H-MRS in patients with Parkinson's disease. Neurosci Lett. 2017;660:57–62.

139. Elmaki EEA, Gong T, Nkonika DM, Wang G. Examining alterations in GABA concentrations in the basal ganglia of patients with Parkinson's disease using MEGA-PRESS MRS. Jpn J Radiol. Epub 2017 Dec 26.

140. Lehéricy S, Bardinet E, Poupon C, Vidailhet M, François C. 7 Tesla magnetic resonance imaging: a closer look at substantia nigra anatomy in Parkinson's disease. Mov Disord. 2014;29:1574–1581.

141. Kwon D-H, Kim J-M, Oh S-H, et al. Seven-Tesla magnetic resonance images of the substantia nigra in Parkinson disease. Ann Neurol. 2012;71:267–277.

142. Kim J-M, Jeong H-J, Bae YJ, et al. Loss of substantia nigra hyperintensity on 7 Tesla MRI of Parkinson's disease, multiple system atrophy, and progressive supranuclear palsy. Parkinsonism Relat Disord. 2016;26:47–54.

143. Gramsch C, Reuter I, Kraff O, et al. Nigrosome 1 visibility at susceptibility weighted 7T MRI-A dependable diagnostic marker for Parkinson's disease or merely an inconsistent, age-dependent imaging finding? PLoS ONE. 2017;12:e0185489.

144. Schmidt MA, Engelhorn T, Marxreiter F, et al. Ultra high-field SWI of the substantia nigra at 7T: reliability and consistency of the swallow-tail sign. BMC Neurol. 2017;17:194.

145. Lehericy S, Vaillancourt DE, Seppi K, et al. The role of high-field magnetic resonance imaging in parkinsonian disorders: Pushing the boundaries forward. Mov Disord. 2017;32:510–525.

146. Pyatigorskaya N, Yahia-Cherif L, Gaurav R, et al. Multimodal Magnetic Resonance Imaging Quantification of Brain Changes in Progressive Supranuclear Palsy. Movement Disorders [online serial]. n/a. Accessed at: http://onlinelibrary.wiley.com/doi/abs/10.1002/mds.27877. Accessed November 21, 2019.

147. Plantinga BR, Temel Y, Duchin Y, et al. Individualized parcellation of the subthalamic nucleus in patients with Parkinson's disease with 7T MRI. Neuroimage. Epub 2016 Sep 26.

148. Lau JC, MacDougall KW, Arango MF, Peters TM, Parrent AG, Khan AR. Ultra-High Field Template-Assisted Target Selection for Deep Brain Stimulation Surgery. World Neurosurg. 2017;103:531–537.

149. Emir UE, Tuite PJ, Öz G. Elevated pontine and putamenal GABA levels in mild-moderate Parkinson disease detected by 7 tesla proton MRS. PLoS ONE. 2012;7:e30918.

150. Broski SM, Hunt CH, Johnson GB, Morreale RF, Lowe VJ, Peller PJ. Structural and functional imaging in parkinsonian syndromes. Radiographics. 2014;34:1273–1292.

151. Nichols KJ, Chen B, Tomas MB, Palestro CJ. Interpreting 123I-ioflupane dopamine transporter scans using hybrid scores. Eur J Hybrid Imaging. 2018;2:10.

152. Pagano G, Niccolini F, Politis M. Imaging in Parkinson's disease. Clin Med (Lond). 2016;16:371–375.

153. Smith SM. Fast robust automated brain extraction. Hum Brain Mapp. 2002;17:143–155.

154. Yushkevich PA, Piven J, Hazlett HC, et al. User-guided 3D active contour segmentation of anatomical structures: significantly improved efficiency and reliability. Neuroimage. 2006;31:1116–1128.

155. Patenaude B, Smith SM, Kennedy DN, Jenkinson M. A Bayesian model of shape and appearance for subcortical brain segmentation. Neuroimage. 2011;56:907–922.

156. Jenkinson M, Bannister P, Brady M, Smith S. Improved optimization for the robust and accurate linear registration and motion correction of brain images. Neuroimage. 2002;17:825–841.

157. Sjöström H, Surova Y, Nilsson M, et al. Mapping of apparent susceptibility yields promising diagnostic separation of progressive supranuclear palsy from other causes of parkinsonism. Sci Rep. 2019;9:6079.

158. Fischl B. FreeSurfer. Neuroimage. 2012;62:774–781.

159. Iglesias JE, Van Leemput K, Bhatt P, et al. Bayesian segmentation of brainstem structures in MRI. Neuroimage. 2015;113:184–195.

160. Ganzetti M, Wenderoth N, Mantini D. Whole brain myelin mapping using T1- and T2-weighted MR imaging data. Front Hum Neurosci. 2014;8:671.

161. Ganzetti M, Wenderoth N, Mantini D. Mapping pathological changes in brain structure by combining T1- and T2-weighted MR imaging data. Neuroradiology. 2015;57:917–928.

162. Friston KJ, Ashburner JT, Kiebel SJ, Nichols TE, Penny WD, Nichols TE. Statistical Parametric Mapping: The Analysis of Functional Brain Images. Elsevier Science; 9.

163. Avants BB, Epstein CL, Grossman M, Gee JC. Symmetric diffeomorphic image registration with cross-correlation: evaluating automated labeling of elderly and neurodegenerative brain. Med Image Anal. 2008;12:26–41.

164. Avants BB, Tustison NJ, Song G, Cook PA, Klein A, Gee JC. A reproducible evaluation of ANTs similarity metric performance in brain image registration. Neuroimage. 2011;54:2033–2044.

165. Benjamini Y, Hochberg Y. Controlling the False Discovery Rate - a Practical and Powerful Approach. J R Stat Soc Ser B-Methodol. 1995;57:289–300.

166. Ahmed Z, Asi YT, Sailer A, et al. The neuropathology, pathophysiology and genetics of multiple system atrophy. Neuropathol Appl Neurobiol. 2012;38:4–24.

167. Wang Y, Butros SR, Shuai X, et al. Different iron-deposition patterns of multiple system atrophy with predominant parkinsonism and idiopathetic Parkinson diseases demonstrated by phase-corrected susceptibility-weighted imaging. AJNR Am J Neuroradiol. 2012;33:266–273.

168. Murakami Y, Kakeda S, Watanabe K, et al. Usefulness of Quantitative Susceptibility Mapping for the Diagnosis of Parkinson Disease. AJNR Am J Neuroradiol. Epub 2015 Mar 12.

169. Gelb DJ, Oliver E, Gilman S. Diagnostic criteria for Parkinson disease. Arch Neurol. 1999;56:33–39.

170. Jin L, Wang J, Wang C, et al. Combined Visualization of Nigrosome-1 and Neuromelanin in the Substantia Nigra Using 3T MRI for the Differential Diagnosis of Essential Tremor and de novo Parkinson's Disease. Front Neurol. 2019;10:100.

171. Shahmaei V, Faeghi F, Mohammdbeigi A, Hashemi H, Ashrafi F. Evaluation of iron deposition in brain basal ganglia of patients with Parkinson's disease using quantitative susceptibility mapping. Eur J Radiol Open. 2019;6:169–174.

172. Li G, Zhai G, Zhao X, et al. 3D texture analyses within the substantia nigra of Parkinson's disease patients on quantitative susceptibility maps and R2∗ maps. Neuroimage. 2019;188:465–472.

173. Bergsland N, Zivadinov R, Schweser F, Hagemeier J, Lichter D, Guttuso T. Ventral posterior substantia nigra iron increases over 3 years in Parkinson's disease. Mov Disord. 2019;34:1006–1013.

174. Azuma M, Hirai T, Nakaura T, et al. Combining quantitative susceptibility mapping to the morphometric index in differentiating between progressive supranuclear palsy and Parkinson's disease. Journal of the Neurological Sciences. 2019;406:116443.

175. Mazzucchi S, Frosini D, Costagli M, et al. Quantitative susceptibility mapping in atypical Parkinsonisms. NeuroImage: Clinical. 2019;24:101999.

176. Pyatigorskaya N, Yahia-Cherif L, Gaurav R, et al. Multimodal Magnetic Resonance Imaging Quantification of Brain Changes in Progressive Supranuclear Palsy. Mov Disord. 2020;35:161–170.

177. Bocchetta M, Iglesias JE, Chelban V, et al. Automated Brainstem Segmentation Detects Differential Involvement in Atypical Parkinsonian Syndromes. J Mov Disord. Epub 2019 Sep 26.

178. Oba H, Yagishita A, Terada H, et al. New and reliable MRI diagnosis for progressive supranuclear palsy. Neurology. 2005;64:2050–2055.

179. Mangesius S, Hussl A, Krismer F, et al. MR planimetry in neurodegenerative parkinsonism yields high diagnostic accuracy for PSP. Parkinsonism Relat Disord. 2018;46:47–55.

180. Du G, Lewis MM, Sica C, Kong L, Huang X. Magnetic resonance T1w/T2w ratio: A parsimonious marker for Parkinson disease. Ann Neurol. 2019;85:96–104.

181. Fukutomi H, Glasser MF, Zhang H, et al. Neurite imaging reveals microstructural variations in human cerebral cortical gray matter. Neuroimage. 2018;182:488–499.